FACIES OF THE UPPER TRIASSIC VERTEBRATE-BEARING SCOTS BAY MEMBER AT WASSON BLUFF, NOVA SCOTIA

Colin Arthur Price

Submitted in Partial Fulfilment of the Requirements

for the Degree of Bachelor of Science, Honours

Dalhousie University, Halifax, Nova Scotia

March 2014

Distribution License

DalSpace requires agreement to this non-exclusive distribution license before your item can appear on DalSpace.

NON-EXCLUSIVE DISTRIBUTION LICENSE

You (the author(s) or copyright owner) grant to Dalhousie University the non-exclusive right to reproduce and distribute your submission worldwide in any medium.

You agree that Dalhousie University may, without changing the content, reformat the submission for the purpose of preservation.

You also agree that Dalhousie University may keep more than one copy of this submission for purposes of security, back-up and preservation.

You agree that the submission is your original work, and that you have the right to grant the rights contained in this license. You also agree that your submission does not, to the best of your knowledge, infringe upon anyone's copyright.

If the submission contains material for which you do not hold copyright, you agree that you have obtained the unrestricted permission of the copyright owner to grant Dalhousie University the rights required by this license, and that such third-party owned material is clearly identified and acknowledged within the text or content of the submission.

If the submission is based upon work that has been sponsored or supported by an agency or organization other than Dalhousie University, you assert that you have fulfilled any right of review or other obligations required by such contract or agreement.

Dalhousie University will clearly identify your name(s) as the author(s) or owner(s) of the submission, and will not make any alteration to the content of the files that you have submitted.

If you have questions regarding this license please contact the repository manager at dalspace@dal.ca.

Grant the distribution license by signing and dating below.

_____ _____

Name of signatory Date

Abstract

Sedimentological research on the Scots Bay Member of the McCoy Brook Formation at Wasson Bluff provides evidence of lacustrine facies that rest unconformably on the North Mountain Basalt. Since the first vertebrate fossils were found at Wasson Bluff in 1976 by Paul E. Olsen, the site has been the focus of extensive paleontological research. The Scots Bay Member extends as a series of micro-basin successions for several kilometres. Although attributed to a lacustrine or playa setting, a detailed sedimentological study is needed to constrain this interpretation.

The initial 10 m of strata above the basalt were measured in a trench on the beach. The basal 1.9 m corresponds to the Scots Bay Member, which fills the uneven topography on the basalt surface. The lowermost fine- to-medium-grained red-brown sandstone is overlain in turn by red mudstone, grey-green mottled siltstone, ostracode-rich biomicrite (5 cm and 12 cm beds) and further red mudstone. The member is overlain by red fluvial sandstone with dinosaur bone fragments.

In a cliff separated from the trenched area by faults are three lithofacies not observed in the trench: vertebrate-bearing purple-grey fine-grained sandstone, green sandstone, and nodular limestone (a single bed 12 cm thick). The purple-grey sandstone, draped over basalt clasts, contains abundant, densely packed semionotid fish material. The nodular limestone has a disrupted fabric with discontinuous concave-up laminae of varied colour, sediment-filled cracks, and minor continuous red-brown laminae. This lithofacies contains abundant pale nodules of sparry calcite that increase in proportion upwards and layers with matrix-supported ostracodes. Disrupted fabrics are present also in the grey-green mottled siltstone, red mudstone, and ostracode-rich biomicrite in the trenched section. Minor fish material is present in the mottled siltstone, red mudstone, and nodular limestone facies.

The sedimentology, sequence stratigraphy, and taphonomy of the Scots Bay Member imply an extensive shallow lake that ponded on the basalt in the earliest stages of basin subsidence after the eruption. Correlation of the measured sections suggests the initial filling of an ~2.5 m depression on the basalt surface in this area. The fish-rich sandstone marks a transgressive lag, and the ostracode-rich biomicrite marks the most offshore and probably deepest conditions. Disrupted fabrics indicate periodic drying up and the topmost red mudstone may represent a regressing shoreline. The green sandstone and nodular limestone facies represent isolated playa ponds on top of the basalt that developed during second-order transgressive-regressive cycles. Dinosaur fragments in the Scots Bay Member and overlying fluvial strata imply transport of bone into the lake and deposition in a shoreline facies.

Key words: Minas Basin, lower McCoy Brook Formation, North Mountain Basalt, playa, lake, *Semionotus*, taphonomy, sedimentology.

Table of Contents

Table of Figures

Table of Tables

Acknowledgements

I'd like to offer sincere thanks to my supervisors, Martin Gibling and Tim Fedak, for their insight and support throughout this process. We had to dodge a few rocks along the way, but made it through with fond memories. Thank you to Leigh Van Drecht for the stimulating brainstorming and occasional "Why is the structure so complicated?" support group sessions. Special thanks to my friends: Natasha Morrison, Colin MacAdam, Siobhan McGoldrick, Jeff Minichiello, Carla Dickson, and Ian Juby. Your support balanced a stressful year with more fun times than I can count. Last but certainly not least, I would like to thank my parents for giving me the opportunity to go to university and study this incredible subject that I enjoy.

1.0 Introduction

1.1 General statement

Wasson Bluff provides a remarkable field setting to study the interplay of sedimentation with igneous environments. The contact between the North Mountain Basalt and the Scots Bay Member of the latest Triassic lower McCoy Brook Formation is exposed along the sea-cliffs of the section. This contact represents a subaerial unconformity. The top of the basalt is an uneven, clast-dominated surface due to the nature of the flow during emplacement and significant weathering throughout a hiatus in deposition. The sedimentary infilling of the basalt's fissure-riddled surface is of particular scientific interest due to the abundance of disarticulated fish, shark, and terrestrial vertebrate fossils in the initial 1.9 m of strata that overlie the basalt.

The Scots Bay Member exposure at Wasson Bluff is so rich in fossiliferous material that it is known locally as the "fish bed." High on the cliff face a bed of vertebrate-bearing, purple-grey fine-grained sandstone is exposed. The bed contains so many *Semionotus* fish scales that it literally shimmers in the sunlight. Paleontologists have identified bone, scale, tooth, and spine material in this bed, derived from *Semionotus* and redfieldiforme fish, hybodont sharks, and tetrapod dinosaurs. Talus slope deposits of basalt breccia to the east of the study site are also prolific with fossil material (Olsen et al., 2005). Within the succeeding 50 m of strata articulated skeletons of theropod and the prosauropod dinosaurs *Clevosaurus biardi, Protosuchus micmac*, and *Pachygenelus sp.* have been found. These are the oldest

definitive vertebrate dinosaur remains discovered in Canada. The finds are also noteworthy because they are found within the disputed constraints of the Triassic-Jurassic boundary. The T/J boundary is formally defined by the Global Stratotype Section and Point (GSSP) in Kuhjoch, Austria, based on the first occurrence of the recovery taxa Psilocerus (Morton, 2012). The boundary therefore represents somewhat after the major Triassic-Jurassic extinction in which 43% of terrestrial vertebrate families became extinct (Olsen et al., 2005; Cirilli et al., 2009). Whether the taxa found at Wasson Bluff represent the population shortly before, during, or after the extinction event depends on the precise position of the boundary in the area, which remains unclear. Extensive paleontological research has been carried out on the site, but sedimentological studies have been regional and a detailed study of the Scots Bay Member at Wasson Bluff has not been completed. Wasson Bluff is a Special Protected Place of Nova Scotia and field work for this thesis was completed under the allowance of Permit#: P2013NS01.

1.2 Geographic setting

The field area of this thesis is located at Wasson Bluff, Nova Scotia. Wasson Bluff is on the northern shore of the Bay of Fundy approximately eight kilometers east of Parrsboro. UTM coordinates are: N5027359 E403212.9 Zone 20. Wasson Bluff is within the modern Minas Basin and the Mesozoic Fundy Basin (Fig. 1).

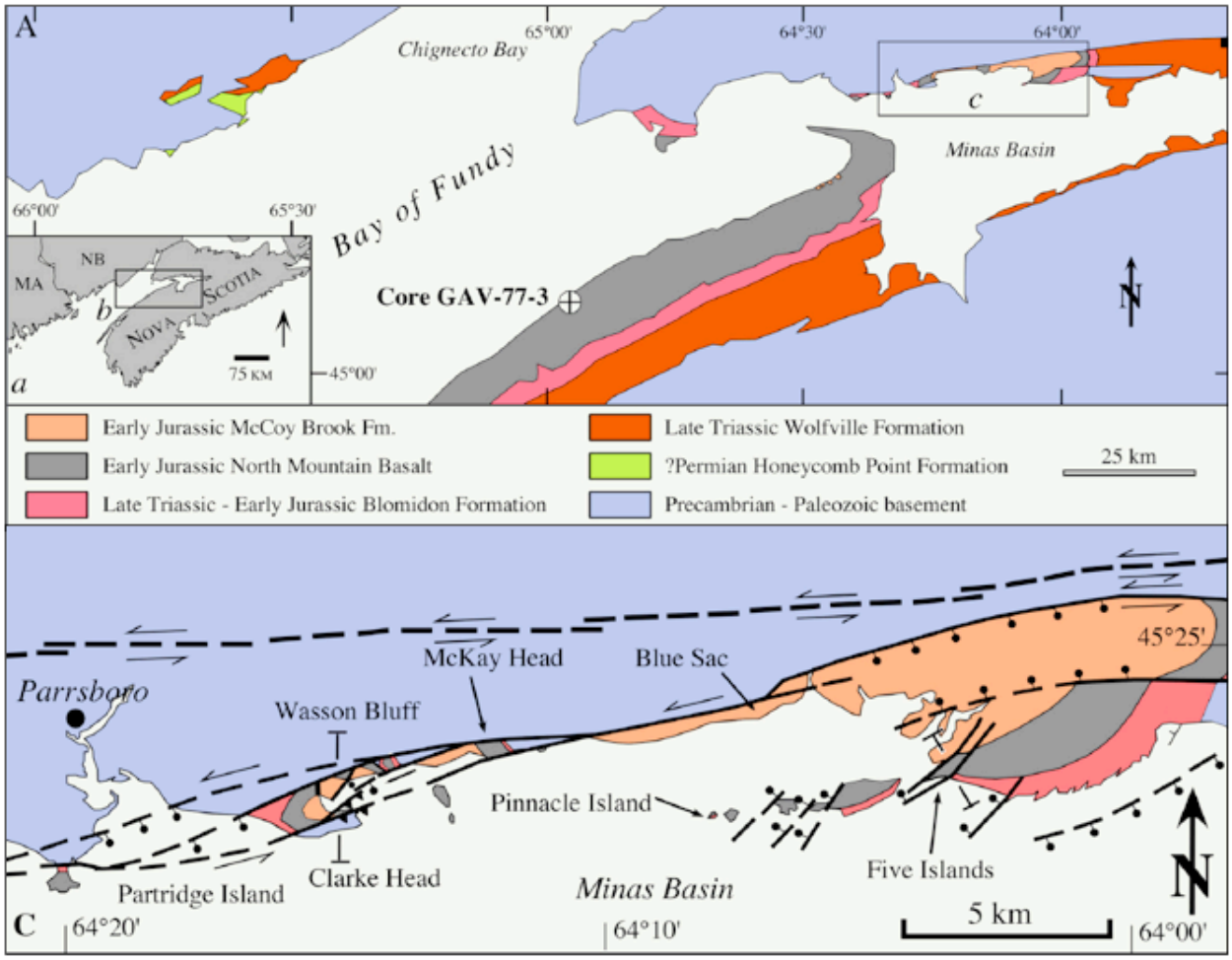

Figure 1: Map of the Fundy Basin (upper) highlighting the Minas Basin (lower) where Wasson Bluff is located (modified after Olsen et al., 2005).

The Fundy Basin is one of the northernmost basins that contain the Newark Supergroup a series of Triassic rift-valley basins formed during the breakup of Pangaea. The Minas Fault Zone, a transtensional fault zone that was reactivated as left-oblique slip during the Mesozoic, bounds the northern limit of the Minas Basin, and many significant faults in the area result in complex stratigraphic relationships. Two microbasins are exposed along the cliff-section at Wasson Bluff. This study is a sedimentological analysis of the Scots Bay Member that crops out in the southwestern microbasin (Fig. 2).

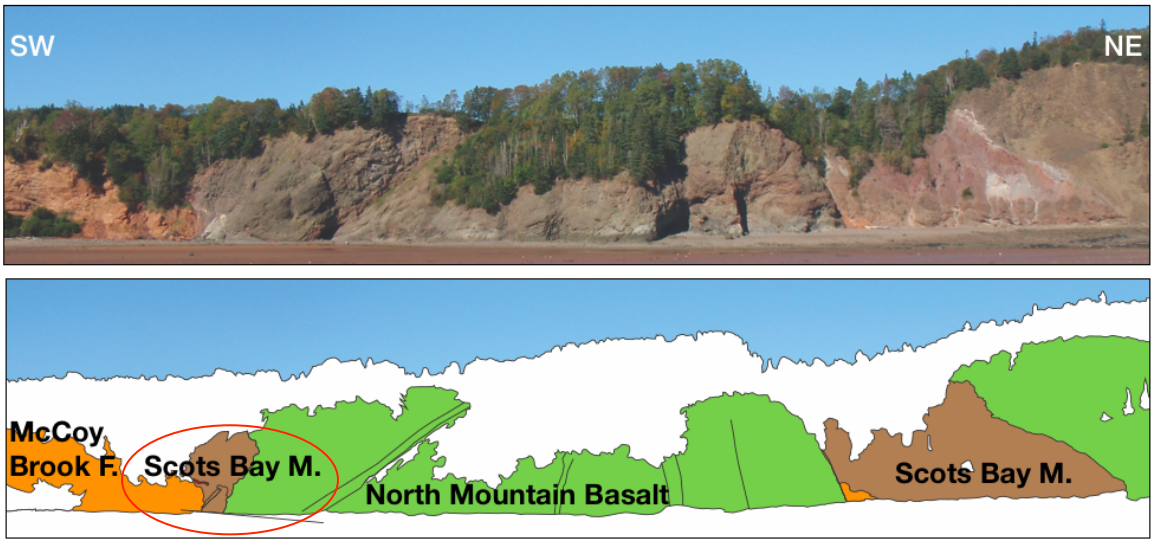

Figure 2: Study area at Wasson Bluff highlighted by a red circle. Black lines identify significant faults. Two exposures of the Scots Bay Member represent two micro-basins associated with fault-bounded depressions in the North Mountain Basalt.

1.3 Physiography and surficial geology

There are two types of exposure at Wasson Bluff: outcrop along the coastal cliff, and outcrop exposed along the beach. The coastal cliffs alternate between cliff-forming and slope-forming units. Units are cliff-forming where the lithology is relatively more consolidated. The best cliff-forming units are basalt with exposures >50 m in height, embayed at fault traces where the basalt has been fragmented. Sandstone units, while also cliff-forming locally, tend to yield lower cliffs ranging from 10-40 m in height. The bases of sandstone cliffs are deeply incised by the tide, which destabilizes the slope causing landslides. The fans of large, angular clasts grouped at the base of slopes are evidence of these slides. Rain, wind, and freeze-thaw processes also weather the outcrops, and rock-fall is common along the section. See Appendix A for recommendations on safety and access to the site.

Outcrops are common along the beach, but their locations vary because the gravel that covers the beach moves with every tide. Outcrop exposed along the

beach one day may be covered the next. Fortunately, this veneer of unconsolidated sediment is typically <0.5 m deep, and shallow trenches may be used to expose complete stratigraphic sections along the beach. Coarser grained sandstone units tend to crop out more readily along the beach section whereas finer grained, fissile layers are weathered flat and covered by sediment.

1.4 Scots Bay Member

The Scots Bay Member, formerly the Scots Bay formation, is defined as the "distinctive lacustrine facies" at the base of the McCoy Brook Formation (Tanner, 1996). The type section for the member is at East Broad Cove on the Blomidon Peninsula, 12 km to the southeast across the bay from Wasson Bluff. Exposures of the Scots Bay Member are also present along the southern coast of the Bay of Fundy and, although the strata occupy topographic lows in the surface of the North Mountain Basalt, the lithology of the member is quite diverse. Sandstone, siltstone, mudstone, chert, stromatolites, and carbonates have all been described in the Scots Bay Member along the Blomidon Peninsula.

Very little research of the Scots Bay Member along the north shore of the Minas Basin has been completed. Tanner and Hubert (1992) completed a regional study of the McCoy Brook Formation that generally outlines the member, but no stratigraphic column was presented. Tanner redefined the nomenclature of the member in 1996, and presented a stratigraphic column and general description of facies based on field observations, but no petrographic analysis was completed. Hassan (2000) completed petrographic analysis of microfossil assemblages on samples from the Scots Bay Member on the Blomidon Peninsula, but none from

Wasson Bluff. Given the abundance of taxa present within the Scots Bay Member at Wasson Bluff, the sedimentology of the area is now of great interest.

1.5 Objectives

The main objective of this thesis is to investigate the conditions under which the fossils of the "fish bed" accumulated in the Scots Bay Member at Wasson Bluff. Although it has been described in general terms as lacustrine or playa deposits, a detailed sedimentological study is needed to constrain this interpretation. These data will form a context for the extensive paleontological research in the area and possible regional correlation of the Scots Bay Member within the Fundy Basin.

2.0 Geological Setting and Previous Research

2.1 Geological setting

The sea-cliffs along the shore of the Bay of Fundy offer remarkable insight into Mesozoic geology. The Fundy Group, a subdivision of the Newark Supergroup, crops out over an area of 40 by 275 km around the bay (Hubert and Mertz, 1984). This succession of Late Triassic and Early Jurassic non-marine clastics and carbonates and tholeiitic basalt provides scientists with a nearly complete stratigraphic record of the transition period during the breakup of the supercontinent Pangaea. The Triassic-Jurassic boundary, one of the key extinction events of the Phanerozoic, is represented in this area.

The supercontinent Pangaea began to break up during the later Permian and Triassic. In the early stages of this breakup a long series of rift valleys formed in what is now North America, Europe, and Africa. Along the eastern coast of North America this series of rift valleys stretches from Nova Scotia to North Carolina. The infilling strata of these rift valleys is designated as the Newark Supergroup: a genetically related group of formations that crop out within Mesozoic basins that share close lithological and structural similarities (Luttrell, 1989). Part of the Newark Supergroup is found in the Fundy Basin that underlies and borders the Bay of Fundy, Nova Scotia.

The Fundy Basin is a sedimentary depocentre that has been active since the Early Mesozoic. The basin was named by Bell (1958) and is bounded at its northern limit by the Cobequid Mountains and at its southern limit by Grand Manan and Brier

islands (Luttrell, 1989). The Fundy Basin comprises three sub-basins: the Fundy, Minas, and Chignecto basins (Olsen et al., 2005). The total thickness of sediment in the Fundy Basin ranges from 6-12 km, and the rock units are stratigraphically constrained as Anisian to Hettangian (Middle Triassic to Lower Jurassic) (Leleu et al., 2010). The Wasson Bluff site is located in the Minas Basin.

The Minas Fault Zone, a continental transform fault zone that separates the Meguma and Avalon terranes, bounds the northern limit of the Minas Basin (Olsen and Schlische, 1990; Schlische and Ackermann, 1994). This fault underwent dextral slip during the Paleozoic and was subsequently reactivated as a left-oblique slip fault zone during the Mesozoic (Schlische and Ackermann, 1994). This reactivation was the product of the northwest-southeast extension that resulted in the rifting of Pangaea and the opening of the Atlantic Ocean. Active tectonics during the Mesozoic exerted a control on sedimentation in the Fundy Basin and its sub-basins, and can complicate sedimentological study by causing abrupt variations in formation thickness. The Minas Fault Zone created a series of synsedimentary microbasins within the Minas Basin (Olsen and Schlische, 1990).

The Minas Basin is the most structurally complex region in the Mesozoic Fundy Basin. During the reactivation of the Minas Fault Zone, a lattice of older structures acted as planes of weakness for fractures and faults to develop at orientations related to the overall regional stress regime (Olsen and Schlische, 1990). Thus, there are many faults with varied orientations in the Mesozoic strata. Due to deformation and fragmentation along the northern edge of the Minas Basin, the overall geometry of the basin cannot be constrained using seismic studies (Leleu

et al., 2010; Schlische and Ackermann, 1994). Wasson Bluff is an excellent field site to examine the penecontemporous faulting caused by the Minas Fault Zone. Two microbasins are exposed along the section with clear fault-traces visible due to the competency of the basalt.

Four formations of the Mesozoic Fundy Group crop out in the Minas Basin. From oldest to youngest, these formations are the Wolfville Formation, the Blomidon Formation, the North Mountain Basalt, and the McCoy Brook Formation (Hubert and Mertz, 1984; Schlische and Ackermann, 1994; Luttrell, 1989; Olsen et al., 2005) (Fig. 3).

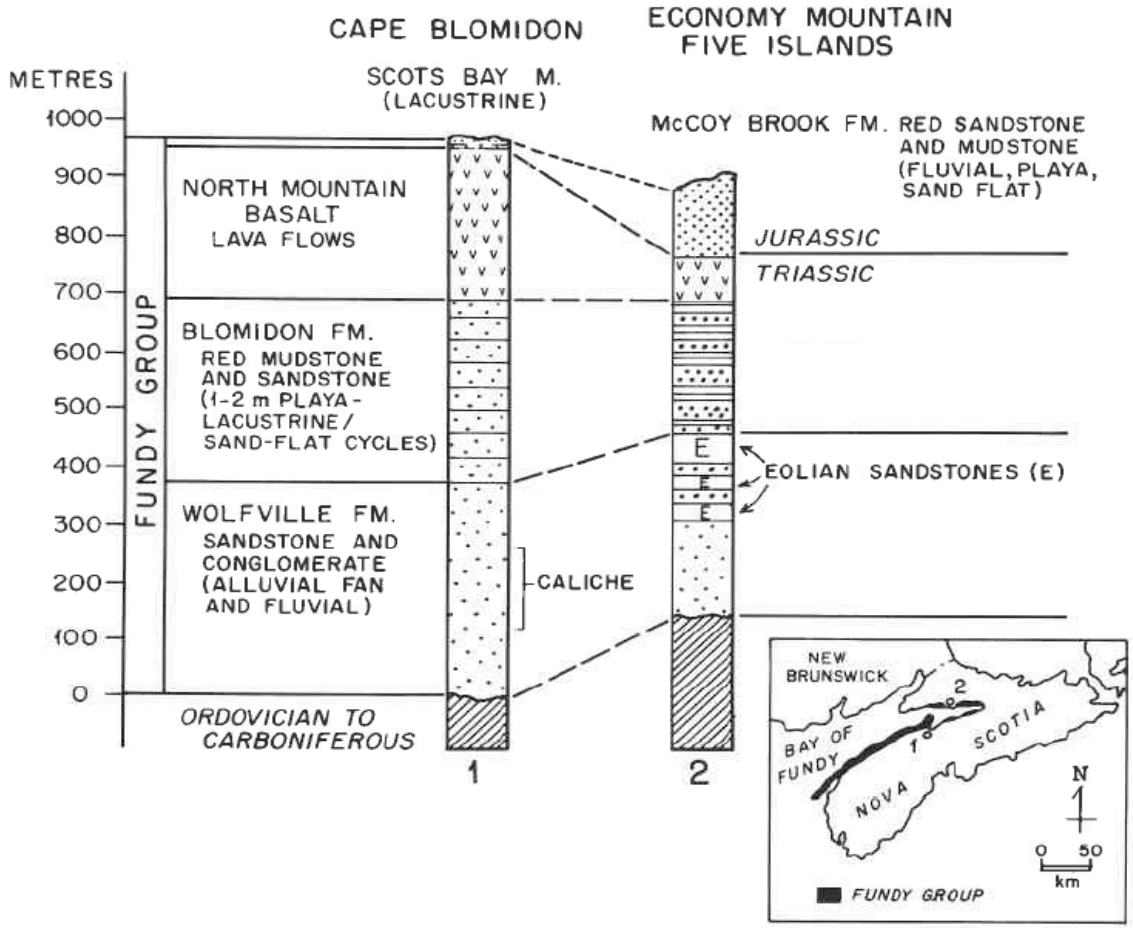

Figure 3: Stratigraphy of the Fundy Basin focusing on sections from (1) Cape Blomidon and (2) Economy Mountain (modified from Mertz and Hubert, 1990).

The Wolfville Formation is early Late Triassic in age and composed of fluvial sandstones with minor lacustrine mudstones (Leleu et al., 2010). The Blomidon Formation is Late Triassic in age and composed of interbedded lacustrine siltstone and gypsiferous playa mudstone with fluvial sandstone in stacked-channel successions (Hubert and Mertz, 1984; Olsen et al., 2005; Leleu et al, 2010; Cirilli et al., 2009). The Minas Basin contains the thinnest Mesozoic succession in the Fundy Basin, 1050 m in total with <800 m of Wolfville Formation, <250 m of Blomidon Formation, and >230 m of McCoy Brook Formation (Tanner, 1996; Leleu et al., 2010). The exact stratigraphic location of the Triassic-Jurassic boundary is still in dispute, however it may be constrained to the lowermost McCoy Brook Formation. A recent study of the Scots Bay Member at Scots Bay yielded a palynological assemblage dominated by Triassic bisaccate and *Patinasporites densus* pollen (Cirilli et al., 2009). Before this study, the palynomorph assemblage 30 cm below the basalt in the Blomidon Formation at Patridge Island was the last appearance of Triassic taxa and defined the boundary (Olsen et al., 2005). The discovery of *P. densus* palynomorphs in the Scots Bay Member is controversial since it indicates that the Triassic-Jurassic boundary is above the North Mountain Basalt, and that the Scots Bay Member represents uppermost Triassic strata.

The North Mountain Basalt is a tholeiitic flood basalt that has been dated using zircon U-Pb geochronology to establish an age of 201.564 ±0.15 m.y. (Blackburn et al., 2013). The basalt has columnar cooling joints that have been subjected to rotational stresses due to regional tectonics. In plan view, pentagonal

neptunian dikes have formed at the top of the basalt as a result of sedimentary infilling of fractures along the cooling joints (Schlische and Ackermann, 1994).

McCoy Brook Formation is formally recognized as the designation for all post-North Mountain Basalt sedimentary strata cropping out in the Minas Basin (Tanner, 1996). The basal unit, the Scots Bay Member, is composed of lacustrine deposits, whereas the upper sections of the McCoy Brook Formation consist of interbedded eolian and fluvial redbeds (Olsen et al., 2005).

The formations of the Fundy Group consist of non-marine clastics and minor carbonates or extrusive igneous rocks, implying a land-locked continental basin. There is no paleontological or sedimentological evidence that the Fundy Group was influenced by marine base-level changes. At the time, Nova Scotia was at 25˚ paleolatitude (Hubert and Mertz, 1984; Olsen et al., 2005; Leleu et al., 2010). There is controversy over the exact nature of the climate at the time, but a consensus is that the Fundy Basin was arid to semiarid (Olsen, 1981; Hubert and Mertz, 1980). Due to the aridity of the climate, playa lakes with a strongly seasonal water budget were probable landscape components.

2.2 Previous Research

Wasson Bluff has drawn a lot of attention from the scientific community due to the diversity and abundance of vertebrate fossils found at the site (Table 1).

Table 1: Site-specific faunal list for the McCoy Brook Formation. Sites listed are (W) Wasson Bluff, (B) Blue Sac, (M) McCoy Head, and (F) Five Islands (T. Fedak, personal commun., 2014).

	W	B	M	F
Arthropoda, Ostracoda				
Darwinula sp.	■			
Elasmobanchii, Hybotondiae				
Hybodus sp.	■			
Actinopterygii				
Redfieldiidae ?				
skull bones and scales	■			
Semionotidae				
Semionotus sp.	■			■
Synapsida				
Trithelodontidae				
Pachygenelus sp.	■			
Reptilia				
Sphenodontidae				
Clevosaurus bairdi	■			
Protosuchidae				
Protosuchus micmac	■			
Batrachopus spp.	■	■		■
Dinosauria				
Prosauropoda				
new genus	■			
Otozoum moodii	■	■		
Theropoda				
cf. Syntarsus sp.	■			
Grallator (Grallator) spp.		■	■	■
Grallator (Anchisauripus) spp.	■	■	■	■
Grallator (Eubrontes) sp.				■
"Fabrosauridae"				
cf. Scutellosaurus sp.	■			

Paul E. Olsen discovered the first fossils at Wasson Bluff on August 11th, 1976 (Olsen et al., 2005). Olsen was on a trip from Princeton University with colleagues Donald Baird and John Horner who assisted in the recovery of more fossils over the following days. The "Princeton Quarry" remains the richest site to date. In 1986 Neil Shubin, Hans-Dieter Sues and Bill Amaral discovered small postcranial elements, perhaps of a Protosuchus, in the fluvial successions near the vertebrate-bearing sandstone that marks the top of the Scots Bay Member (Olsen et al., 2005; Fedak, 2006). This was followed in 1988 by the discovery of more dinosaur bone fragments by a 9th grade student on a field trip. The next significant find was made in 1992 by Bob Grantham who found several small fragments of bone at the Princeton Quarry, which prompted the discovery of a nearly complete and fully articulated sauropodomorph dinosaur skeleton over the following years (Olsen et al., 2005). In 1997 Tim Fedak began working on preparation and study of the Grantham find and subsequently made significant discoveries of his own. Three more articulated specimens were collected between 1998 and 2004. The bone bed exposed at the Princeton Quarry of Wasson Bluff, containing at least five nearly complete and fully articulated vertebrate fossil specimens, is the richest site in North America for basal sauropodomorph dinosaurs (T. Fedak, personal commun. 2013).

Paul E. Olsen has been a key contributor to the study of the Newark Supergroup. Olsen has carried out research on the orbital theory of climate change and its effects on the periodicity of lacustrine stacking patterns, the morphology of Early Jurassic fish species, paleoclimate, sedimentary controls, and the tectonic

mechanisms that created the Fundy Basin (Olsen, 1981; Olsen et al., 1982; Olsen, 1986; Olsen and Gore, 1989; Olsen and Schlische, 1990; Olsen and McCune, 1991). The bulk of this research has been completed on a broad scale to answer questions relevant to the Fundy Group and Fundy Basin as a whole.

Lawrence Tanner and John Hubert have done extensive work on the Upper Triassic-Lower Jurassic strata of the Minas sub-basin, including studies of the eolian redbeds of the Blomidon Formation and the paleoclimatic setting (Hubert and Mertz, 1984; Mertz and Hubert 1990). Tanner studied the post-North Mountain Basalt strata of the Minas sub-basin. He has published on the distribution of clay minerals in the McCoy Brook Formation (Tanner, 1994) and redefined the formal nomenclature of the formation to include the Scots Bay Member, formerly defined as a separate formation (Tanner, 1996). In his 1996 paper Tanner presented a stratigraphic column of the cliff exposure of the Scots Bay Member at Wasson Bluff. For a thorough discussion of the location and significance of this stratigraphic column see Chapter 4.

3.0 Methods

3.1 Introduction - Research methods

This thesis is primarily a field-based study. Fieldwork was completed between late August and mid-November 2013. Detailed field notes were taken of large-scale sedimentological and kinematic structures in the area. General descriptions of lithology and facies relationships along the section were recorded, as well as three detailed measured sections of the Scots Bay Member.

Consistent research methods were applied to both the collection of data in the field and laboratory analysis of samples. The key methods used in the field were: photography, tracings, detailed measured sections, and sample collection for petrographic analysis. Twelve thin sections - nine at 2.5 x 5 cm, three at 5 x 7.5 cm - were produced from collected samples for petrographic analysis. Two polished thin sections were produced for electron-microprobe analysis. Unfortunately, microprobe analysis was not completed due to time constraints, but the polished sections are available for future work. One sample of nodular limestone was slabbed and polished for inspection of small-scale sedimentary structures and laminae. The objective of microscope analysis was to determine the mineralogy, grain size, sorting, roundness, matrix content, cement, and fossil content of the samples. Other research tools used were software packages (Adobe Illustrator, Microsoft Office) to generate or refine maps and figures.

3.2 Photography and tracing

Photographs and tracings were used as tools for both observation and interpretation. Panoramic photos of the section were taken from the intertidal sandbar, approximately 500 m from the outcrop, during low tide. This wide-frame perspective offers an uncommon view of the section at Wasson Bluff and provides context to the specific study area. Over 150 additional photos were taken of points of interest on the outcrop. Adobe Illustrator was used to indicate specific features of interest on the photos including sedimentary infill of cracks in the basalt, channel scours, and structural features to communicate observations from the field area. This tracing method was adapted from Dennar (2012).

3.3 Measured section

Three stratigraphic columns (A, B and C) were created from measured sections recorded in the field. Section A comprises two measured sections taken along the beach using a 30 m measuring tape set perpendicular to strike, and linked by a datum of fine-grained sandstone. The first section measured 17.85 m horizontally, and the second section measured 17.4 m. Joining the two sections generated a complete stratigraphic column. The corrected thickness of the complete stratigraphic column is 10.45 m using an average dip of 38˚, based on three dip measurements along the section (beds 6A, 9A, and 19A). The majority of the section was trenched by hand, and the gravel overlying the outcrop ranged from 0.1-0.4 m thick. Once the outcrop was fully exposed, markers were placed at lithological contacts and surfaces of interest. A customized rubric was then used to make detailed notes of each bed. For the full table of bed-by-bed information see Appendix

B. Samples were collected along the section for further analysis. For a full inventory of samples and microscope sections see Table 2 and Appendix C.

Sections B and C comprise measured sections along the cliff exposure at Wasson Bluff. Sections were measured perpendicular to the strike of beds using a tape measure. Samples were collected from each lithofacies for laboratory analysis (Appendix C).

3.4 Microscope analysis

Microscope analysis was carried out using binocular and petrographic microscopes. Hand samples were inspected under low magnification using a binocular microscope to verify the accuracy of composition, grain size, sorting, and roundness observations recorded in the field. Twelve thin sections and two polished sections were prepared by Gordon Brown at the Dalhousie Earth Sciences Thin Section Laboratory. Preliminary qualitative petrographic observations were conducted to determine the mineralogy of grains, matrix content, and cement, as well as textural information. Quantitative petrographic analysis of seven thin sections was carried out using point-counting equipment at St. Mary's University to determine the modal composition of the samples. Photographs of thin sections were taken at Dalhousie University using a Nikon DS-Fi1 petrographic microscope camera. Carbonates were classified using the Folk classification scheme (Folk, 1959). Sandstones were classified using the Dott classification scheme (Dott, 1964).

Table 2: List of thin sections and polished sections.

Bed #	Lithofacies	Thin section # *5x7.5cm size	Polished section #	Analysis
00	Basalt	CP-01-00		Qualitative analysis
2A	Basal Sandstone	CP-01-02		400 point-count + qualitative analysis
6A	Ostracode-rich biomicrite	CP-01-03-04	CP-01-03-04	800 point-count + qualitative analysis
9A	Ostracode-rich biomicrite	CP-01-03-07	CP-01-03-07	800 point-count + qualitative analysis
10A	Red mudstone	CP-01-03-08		Qualitative analysis
16A	Red sandstone	CP-01-06*		400 point-count + qualitative analysis
1B	Basal sandstone	CP-02-01		Qualitative analysis
2B	Green sandstone	CP-02-02		400 point-count + qualitative analysis
3B	Nodular limestone	CP-02-03*		Qualitative analysis
1C	Basal Sandstone	CP-03-01		Qualitative analysis
2C	Vertebrate-bearing sandstone	CP-03-03*		400 point-count + qualitative analysis
5C	Mottled siltstone	CP-03-02		Qualitative analysis

3.5 Point-counting analysis

Point-counting was carried out on seven thin-sections (Table 2). Modal composition of sandstones was determined using 400 counts per sample. The original detrital composition of the sandstones was quantified using the Gazzi-Dickinson method wherein discrete minerals within detrital grains are counted as individual grains rather than placing them in the category of the larger fragment (Ingersoll et al., 1984). For instance, if the cross-hairs of the point-counter settled on a large feldspar grain within a rock fragment, grain the point would be counted as

feldspar. Inclusions were counted as discrete grains if they constituted >50% of the center of the cross-hairs using the 10X lens. Modal composition of biomicrites was determined using 800 counts per sample. The high point-count density allowed for a more accurate quantification of ostracode shell fragments and sparite cement within the slides.

Matrix and cement was defined during point-counting as terrigenous, calcareous, pseudo-terrigenous, or pseudo-calcareous based on the presence or absence of clay minerals and calcite cement. Terrigenous matrix comprises moderate-birefringence clays. Since the point-counting system did not have an option to classify the groundmass as cement, "calcareous matrix" was used to define zones of sparry calcite cement. Pseudo-terrigenous matrix is >70% clay minerals with minor patches of intergranular, low-birefringence carbonate. Pseudo-calcareous matrix is >30% carbonate material associated with a typically clast-supported matrix of clay or silt grains. Pseudo-calcareous matrix is the point-counting classification equivalent to micrite of the Folk classification scheme.

Monocrystalline quartz was differentiated from polycrystalline quartz based on the absence of discrete grain boundaries dividing the grain. Microcline was differentiated from plagioclase based on its cross-hatched twinning. Textural features, including visible growth rings in cross-polarized light and delaminating edges, helped identify bone and fish scale material. Fish scales have different optical properties at their edge due to the enamel-like ganoid coating. For a complete table of point-counting data see Appendix D.

4.0 Stratigraphic column

4.1 Overview of study area

Two fault-bounded micro-basin successions of the McCoy Brook Formation are exposed along the cliff section at Wasson Bluff (Fig. 2). The section is continuously exposed, but many faults in the area complicate the stratigraphy. Five principal faults cut the North Mountain Basalt, and weathering has embayed the cliff where the basalt has been significantly faulted. The section is latest Triassic in age and youngs to the southwest (Cirilli et al., 2009). The focus of this study is the southwestern micro-basin that has the best exposure of the Scots Bay Member.

4.2 Stratigraphic columns

Three sections of Scots Bay Member strata, isolated from one another by faults, were studied in detail (Fig. 4b). Figures 5 and 6 are stratigraphic logs of the three sections.

Section A is a trenched section 35.25 m long which combines two measured sections correlated along an outcropping bed of red-orange sandstone (Fig. 4a). Beds on the beach dip uniformly at 38˚ and strike at 112˚. Correcting for dip, the trench represents 10.45 m of strata. Outcrop exposure is partial on the beach, but section A is a complete representation since the covered parts were trenched. Exposed beds can be traced laterally for approximately 20 m. The Scots Bay Member is represented by the basal 1.9 m of section A.

Sections B and C are separated from section A by a large fault that runs parallel to the cliff line. Both sections are completely exposed along the cliff section

(Fig. 4c). Section B is a 1.92 m measured section of pale green sandstone and nodular limestone. The hard-bed of nodular limestone dips 42˚ and strikes 120˚. Section C is a 0.45 m measured section of vertebrate-bearing sandstone draped over basalt clasts. Section C is separated from section B by a series of small faults that dramatically rotate the block of basalt that it overlies; the vertebrate-bearing sandstone dips 80˚ and strikes 093˚.

From these three sections and small exposures, nine facies were established using field observations and petrographic analysis. Thorough descriptions of these facies are provided in Chapter 5.

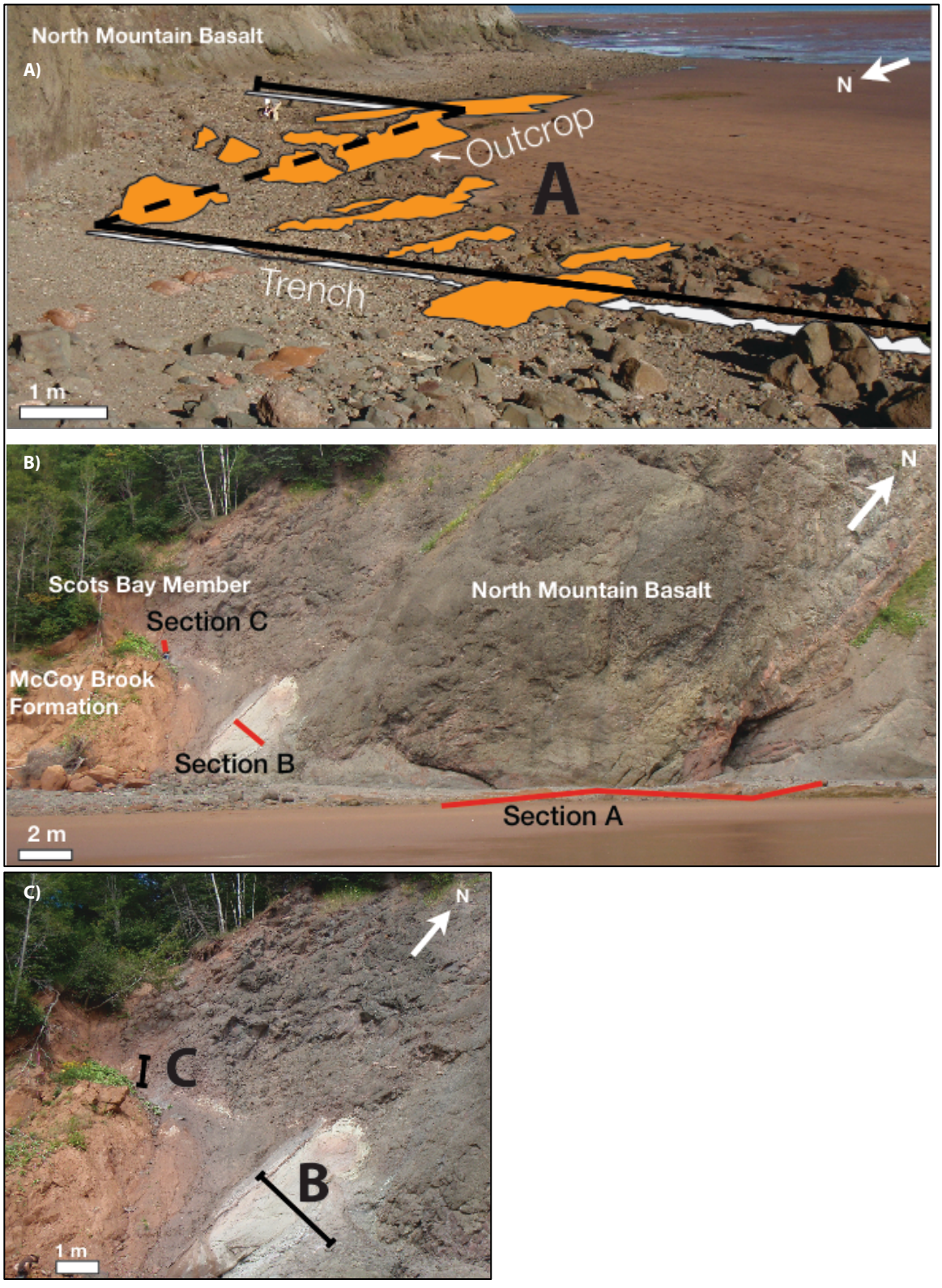

Figure 4: a) Section A comprises two trenched sections (white) and a series of small exposures (orange). The trenched sections are tied together using bed 19A; b) Relative locations of three measured sections at Wasson Bluff. Solid lines represent the approximate location of sections, dashed lines indicate correlation between sections along exposed outcrop; c) Section B is at the base of the cliff, separated from section C by a series of small faults.

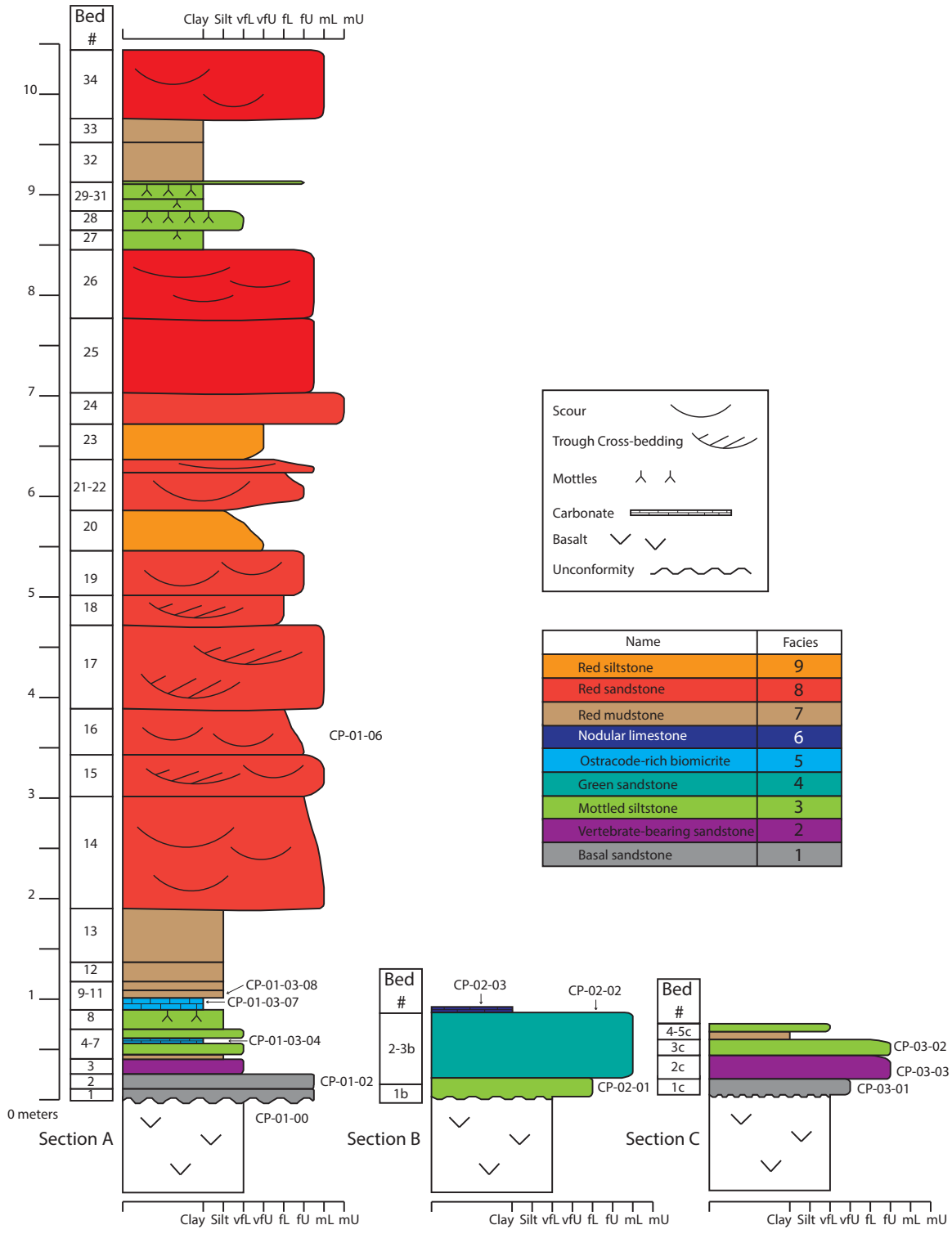

Figure 5: Stratigraphic columns of sections A-C. Sample numbers correspond to thin-sections.

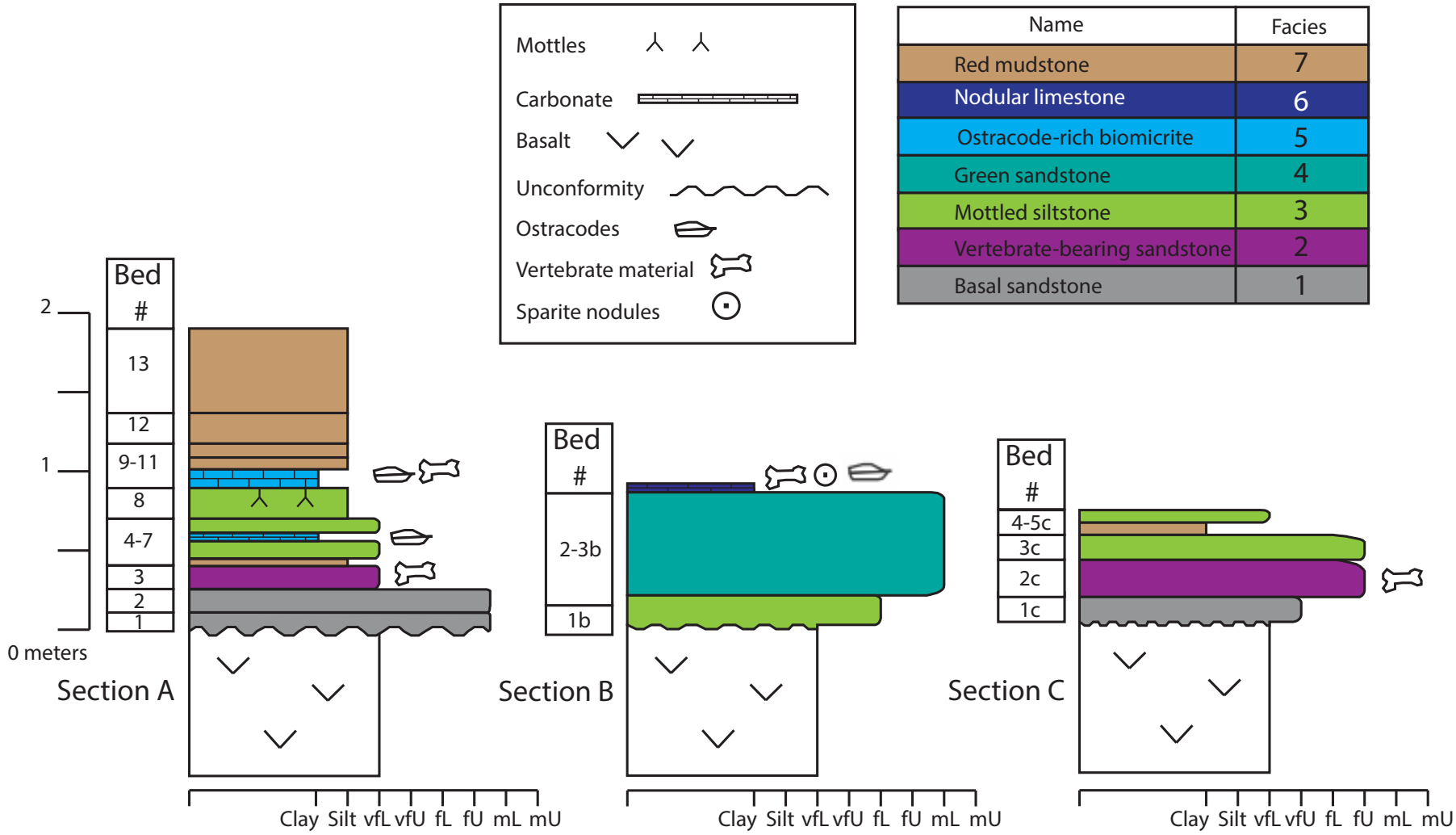

Figure 6: Lower 1.9 m of strata, comprising the Scots Bay Member.

4.3 Previous stratigraphic columns

Stratigraphic columns have been generated for the "fish bed" (Scots Bay Member) at Wasson Bluff by Lawrence Tanner (1996) and Tim Fedak (2006). The stratigraphic column of Fedak (2006) comprises measured sections taken from the intertidal zone (Fig. 7) and cliff exposures. The primary focus of this study was the eolian and fluvial successions of the McCoy Brook Formation that succeed the "fish bed" interval. The Scots Bay Member in this representation comprises ~2.8 m of limestone, and minor sandstone and mudstone (Fig. 8).

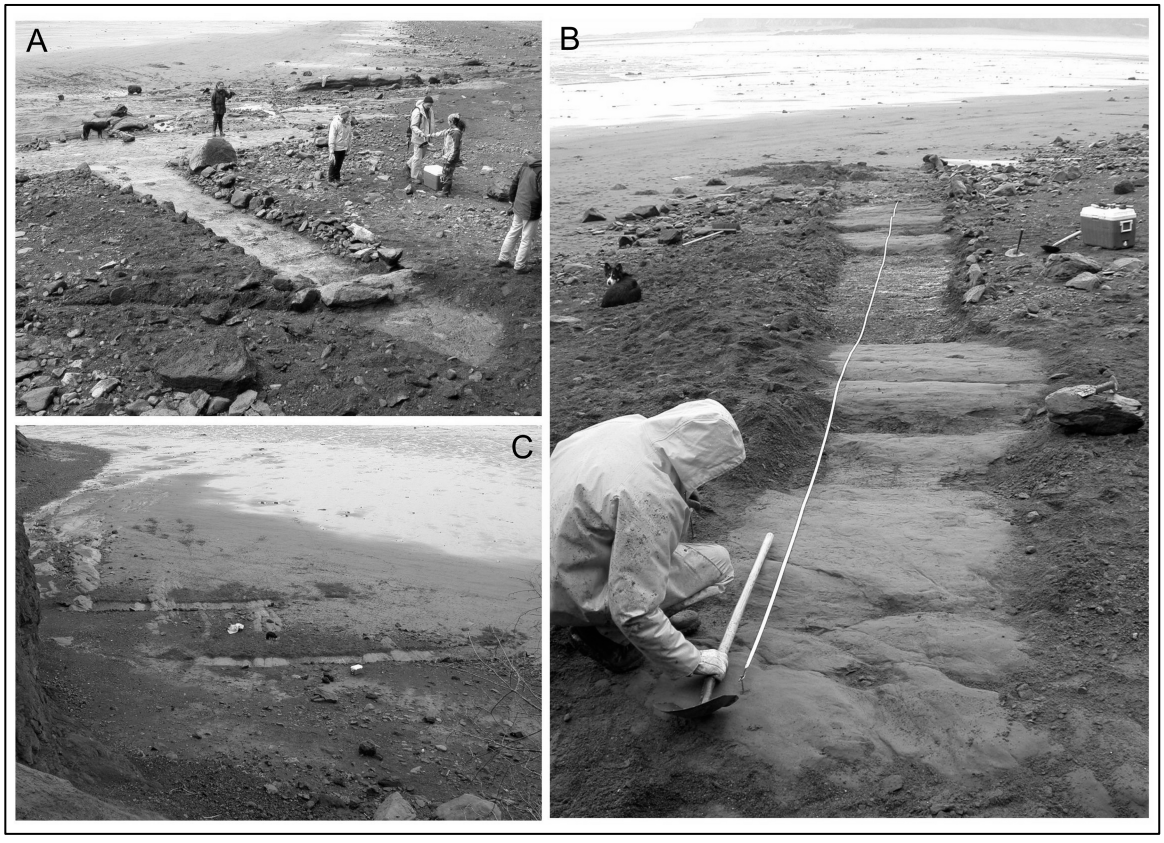

Figure 7: Trenching of the intertidal exposures of the lower McCoy Brook Formation; a) lowermost section includes the "fish bed"; b) upper portion of redbed sandstones; c) bird's eye view of the section (Fedak, 2006).

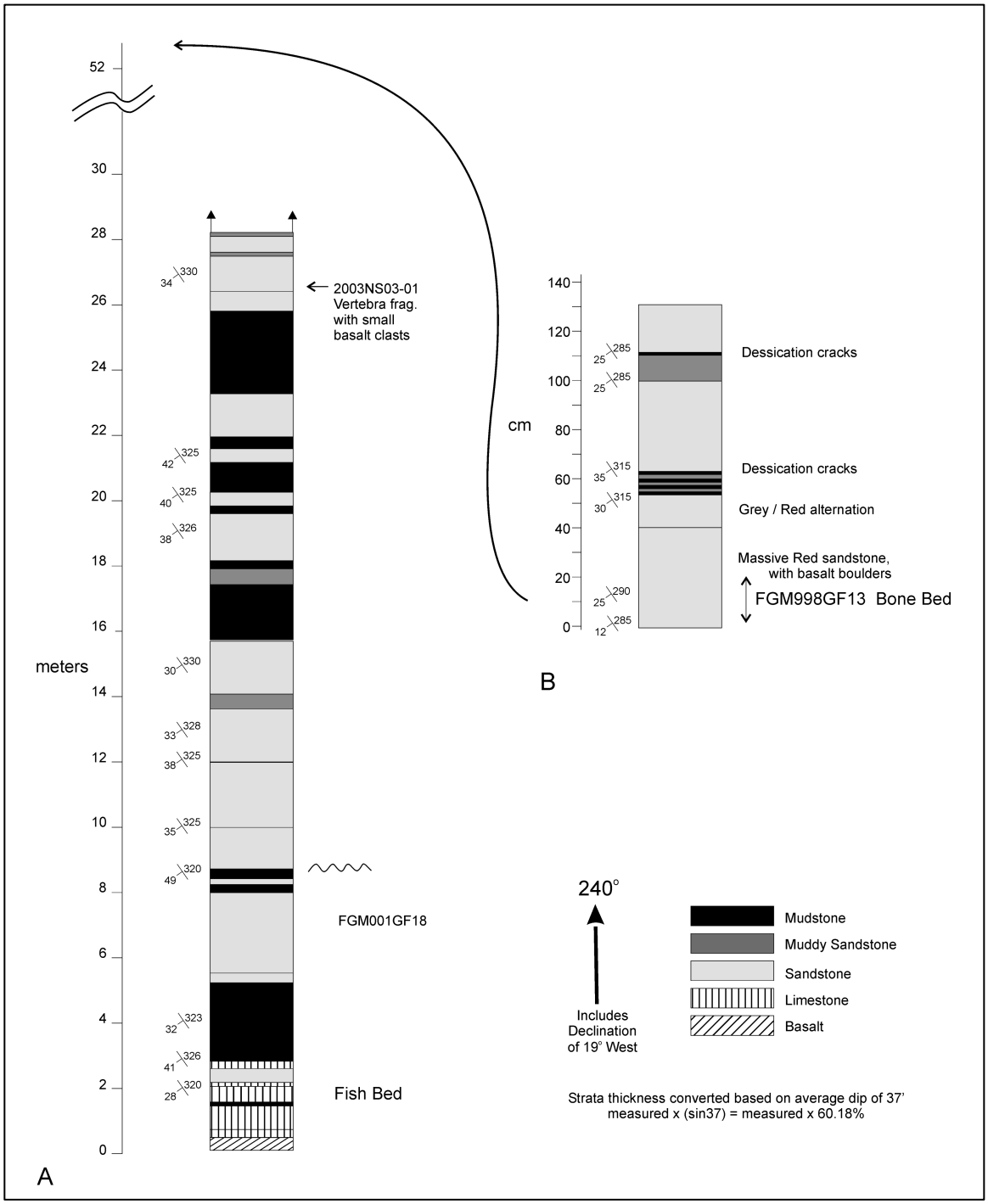

Figure 8: Stratigraphic column of the lower McCoy Brook Formation at Wasson Bluff showing the location of dinosaur bone beds and the "fish bed" Scots Bay Member (Fedak, 2006).

In 1996 Tanner published a measured section of the Scots Bay Member which onlaps the North Mountain Basalt at Wasson Bluff in his paper redefining the nomenclature of the strata (Fig. 9). The measured section shows the cliff exposure as a continuous unit. In the outcrop as presently visible, this section would be truncated between the 3 and 4 m marks by a fault. Comparing photos of the site when Tanner measured his sections in 1996 and the site photos taken in August 2013 it is clear that the cliff scarp has been significantly weathered (Fig.10). The section Tanner measured may not have been faulted, and the cliff may since have been weathered back to expose the fault scarp. The fact that Tanner's section does not obviously correlate well to the findings of this thesis is an indication of the dramatic local variation in the morphology of the Scots Bay Member at Wasson Bluff. For further discussion see Chapter 7.

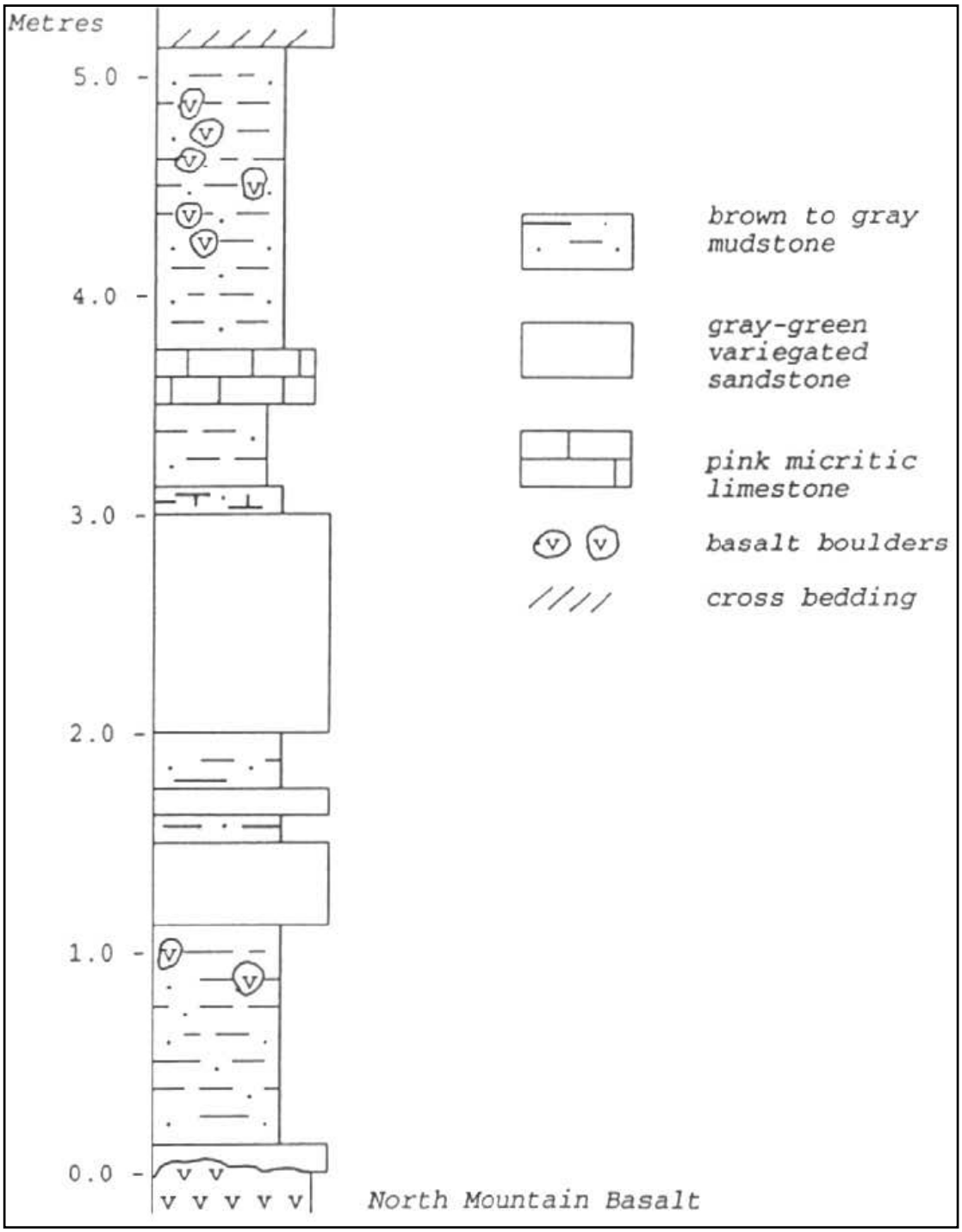

Figure 9: Representative measured section of lacustrine Scots Bay Member at Wasson Bluff. Thick gray-green variegated sandstone corresponds to bed 2B of section B (Fig.6). Right arrow in Figure 10 corresponds to base of section; left arrow corresponds to top of section (Tanner, 1996).

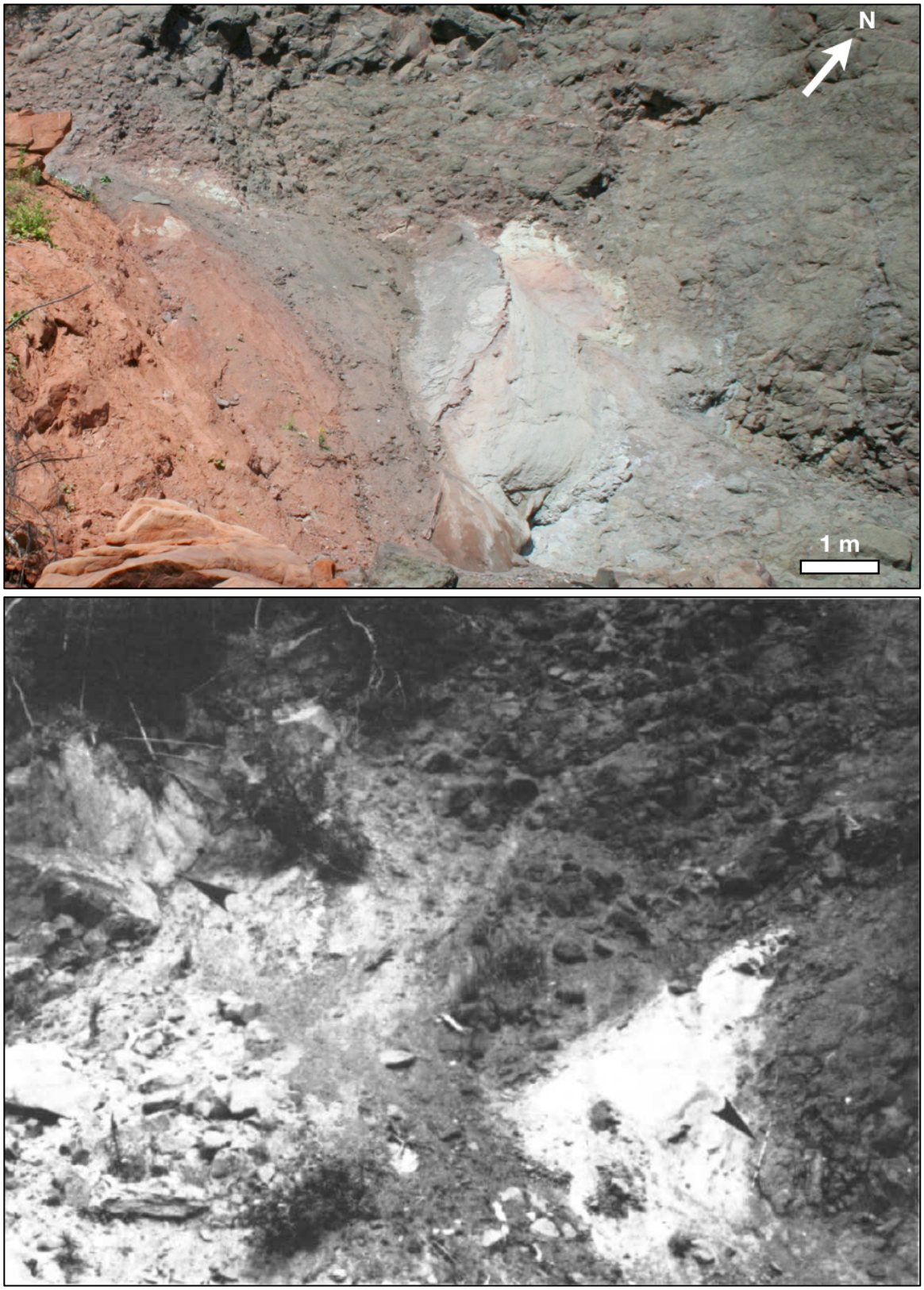

Figure 10: Outcrop photos of Scots Bay Member at Wasson Bluff: (upper) August 2013 and (lower) 1996. The arrow at the lower right indicates a 1.5 m staff at the contact of lacustrine strata with the basalt (Tanner, 1996).

5.0 Sedimentology

5.1 Overview

Nine facies were established based on field observations and petrographic analysis. Table 3 summarizes the general characteristics of these facies. The distribution of the facies is quantified in Figures 11 and 12, and discussed in context of general facies associations in section 5.3 later in this chapter.

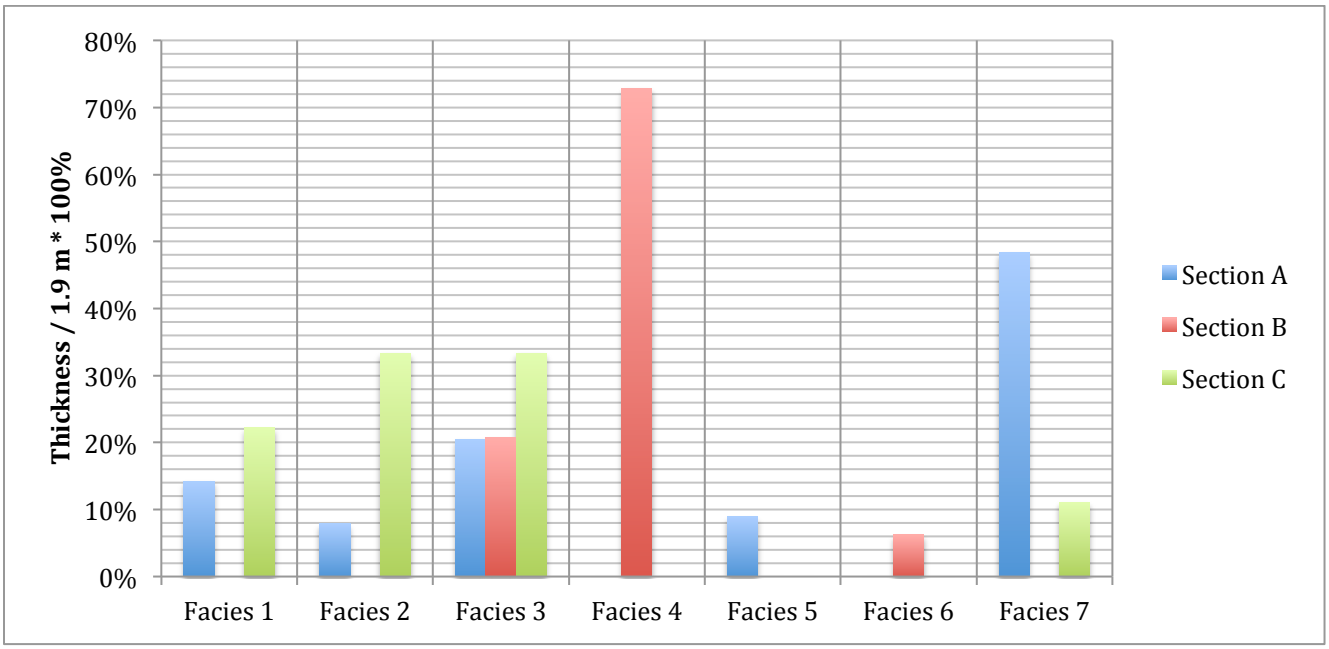

Figure 11: Relative proportions of each facies in the measured sections. Note that percentages were calculated exclusively for the Scots Bay Member and are based on the initial 1.9 m of strata. Facies 8 and 9 are not present in this interval.

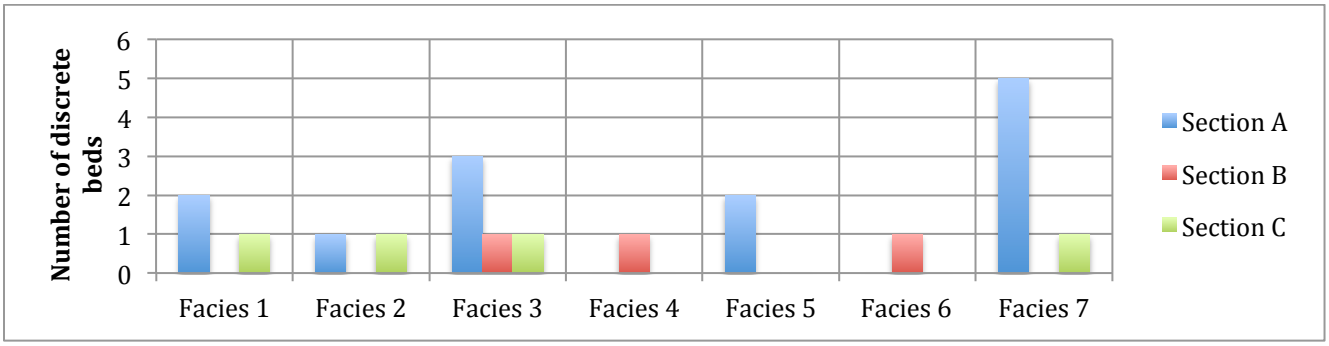

Figure 12: Histogram of number of discrete beds of each facies defined by abrupt contacts in each measured section of the Scots Bay Member.

Table 3: General characteristics of facies.

#	Facies	Grain Size	Fresh Color	Sedimentary Structures	Notes
1	Basal Sandstone	Very fine- to medium-grained sand	Red-orange, grey		Infills cracks in basalt
2	Vertebrate-bearing Sandstone	Fine-grained sand	Purple-grey, abundant fish material	*Semionotus* scales concentrate around basalt clasts, diffuse laminae	*Semionotus* fish, hybodont shark, and tetrapod fossils, friable
3	Mottled Siltstone	Clay to fine-grained sand	Grey-blue, buff green, red, red-brown, grey-green	~0.02 cm diffuse laminae	Fissile
4	Green Sandstone	Medium-grained sand	Pale green	Diffuse laminae at 20-30 cm intervals	
5	Ostracode-rich Biomicrite	Silt or sparry calcite cement	Green, pale green, red	Diffuse laminae	Ostracodes common in thin sections
6	Nodular Limestone	Micrite with very fine-grained sand	Purple-grey	Disrupted fabrics, 0.5-2 cm diffuse laminae	Rich in white calcite nodules
7	Red Mudstone	Clay to very fine- grained sand	Red-brown or red-orange-brown with green or grey patches	< 0.02 cm laminae	Fissile
8	Red Sandstone	Fine- to medium-grained sand	Red-orange, orange-brown	20-30 cm wide scours, massive or 2-10 cm beds, cross-bedding, parallel lamination	Dinosaur bones
9	Red Siltstone	Silt to very fine sand	Red-orange	<0.5 cm laminae	Fissile

5.2 Facies

5.2.1 Facies 1: Basal Sandstone

Field description: This grey to red-brown facies overlies the North Mountain Basalt infilling cracks and fissures in its uneven surface. The beds range from 0.1-0.25 m thick and make up approximately 2 % of section A, and 22 % of section C (Fig. 11). The facies is very fine- to medium-grained sandstone. Grains are moderately to well sorted and well rounded. Beds are massive.

Petrological description: This facies is a grain-supported assemblage of monocrystalline quartz (47.5 %), polycrystalline quartz (3.75 %), altered igneous lithic grains <1mm in diameter (5 %) (Fig. 15a), and minor plagioclase, microcline, zircon, and muscovite. A small proportion of poikilotopic calcite cement is present (Fig. 15b), enclosing grains that are more widely separated than in the rest of the rock. The matrix comprises clay minerals (23.25 %), with greenish patches that may indicate the presence of chlorite, and many grains have ferruginous pellicles. Laminae are <2mm thick and graded. Diffuse red-brown oxides vary in proportion throughout the sample. Zones of more intense oxidation are parallel to the bedding planes. There are abundant zircon inclusions within monocrystalline quartz grains. A single sub-rounded scale fragment was observed.

Interpretation: The basal sandstone of the Scots Bay Member signifies initial deposition of sediment on the North Mountain Basalt. Fine grains infilling fissures in the basalt surface may reflect minor eolian or water-laid deposition. The presence of

one fish scale suggests the presence of standing water and, although the evidence is sparse, this bed may represent the initial development of the Scots Bay Lake (see Chapter 7). The separation of grains in calcite-cemented areas implies early cementation, prior to significant compaction.

5.2.2 Facies 2: Vertebrate-bearing Sandstone

Field Description: This facies is the most fossiliferous. The beds range from 0.1-0.3 m thick, average 0.15 m, and make up approximately 33 % of section C and 8 % of section A (Fig. 11). Grains are moderately sorted and well-rounded with subangular to angular lithics and vertebrate fossils. This facies is purple-grey, with minor patches of reduction (Fig. 14d), and shows a distinctive reflection of light from the abundant fish scales, teeth, and bone fragments of semionotid fish (Fig. 13). For a full treatment of the fossil material see Chapter 6 on taphonomy. The bed is locally so rich in fossils that it crumbles to the touch. Fossils are concentrated around subrounded basalt clasts on the uneven surface of the underlying basalt, giving beds a hummocky appearance (Fig.14b). The sediment is deeply weathered in the outcrop and the hummocks have a wide range of shapes and sizes depending on their exposure, ranging from 0.2-1.5 m in diameter.

Figure 13: Purple-gray vertebrate-bearing sandstone with abundant teeth, bone, and scale fragments.

Petrological description: The vertebrate-bearing sandstone is variably grain- and matrix-supported. It comprises monocrystalline quartz (19 %), vertebrate fragments (19 %), polycrystalline quartz (2 %), and minor augite, biotite, muscovite, detrital igneous lithics, microcline, plagioclase, and zircon. Clay-rich matrix (38.5 %) and oxidized matrix (12.5 %) make up the rest of the sample, with small patches of calcite cement. Fragments of vertebrate material range from 0.5–3 mm long and are typically subround in shape (Fig. 15b-c). The vertebrate materials have two characteristic internal textures: linear fabrics that truncate at the end of the vertebrate fragment or radial growth-ring textures. The vertebrate material is concentrated together in clast-supported laminae 2–10 mm thick with abundant void space and oxidized matrix. Planar bedding is observed in continuous laminae of

very fine-grained quartz that are 0.5-2 mm thick. Laminae are typically matrix-supported and are not graded.

Interpretation: The vertebrate-bearing sandstone represents a catastrophic fish kill or condensed section of fish material. Facies 2 is only found within 0.25 m of the surface of the basalt. The highest concentration of fossils is found surrounding basalt clasts, implying that the trapping effect of the uneven surface of the basalt governed the distribution of fossil material. The fine-grained grade of sediment and disarticulation of vertebrate material indicate a medium-energy, proximal environment. A proximal setting is further supported by the presence of terrestrial vertebrate teeth within the fossil assemblage, which suggests interaction of terrestrial scavengers with the fish material. The disarticulated nature of the vertebrate material may, therefore, be the result of both transport and in-situ disruption by scavengers.

In order to be preserved the fish material had to be buried in a low-energy environment where the fossils would not be disturbed. Due to the proximity of these beds to the basalt and the taphonomic mechanisms necessary for the disarticulation and burial of the fish material, Facies 2 is provisionally interpreted as a transgressive lag deposit. During this interval, water deepening prevented sediment from getting into the lake area, allowing vertebrate material to build up over time and spread across the surface. Vertebrate material was concentrated around basalt clasts on the bottom (Fig. 14c). Lag deposits are known for concentrating bone fragments, but typically in conglomeratic facies (Arp et al., 2005). The uneven

surface of the basalt provides an uncommon sedimentological control for the distribution of the vertebrate material.

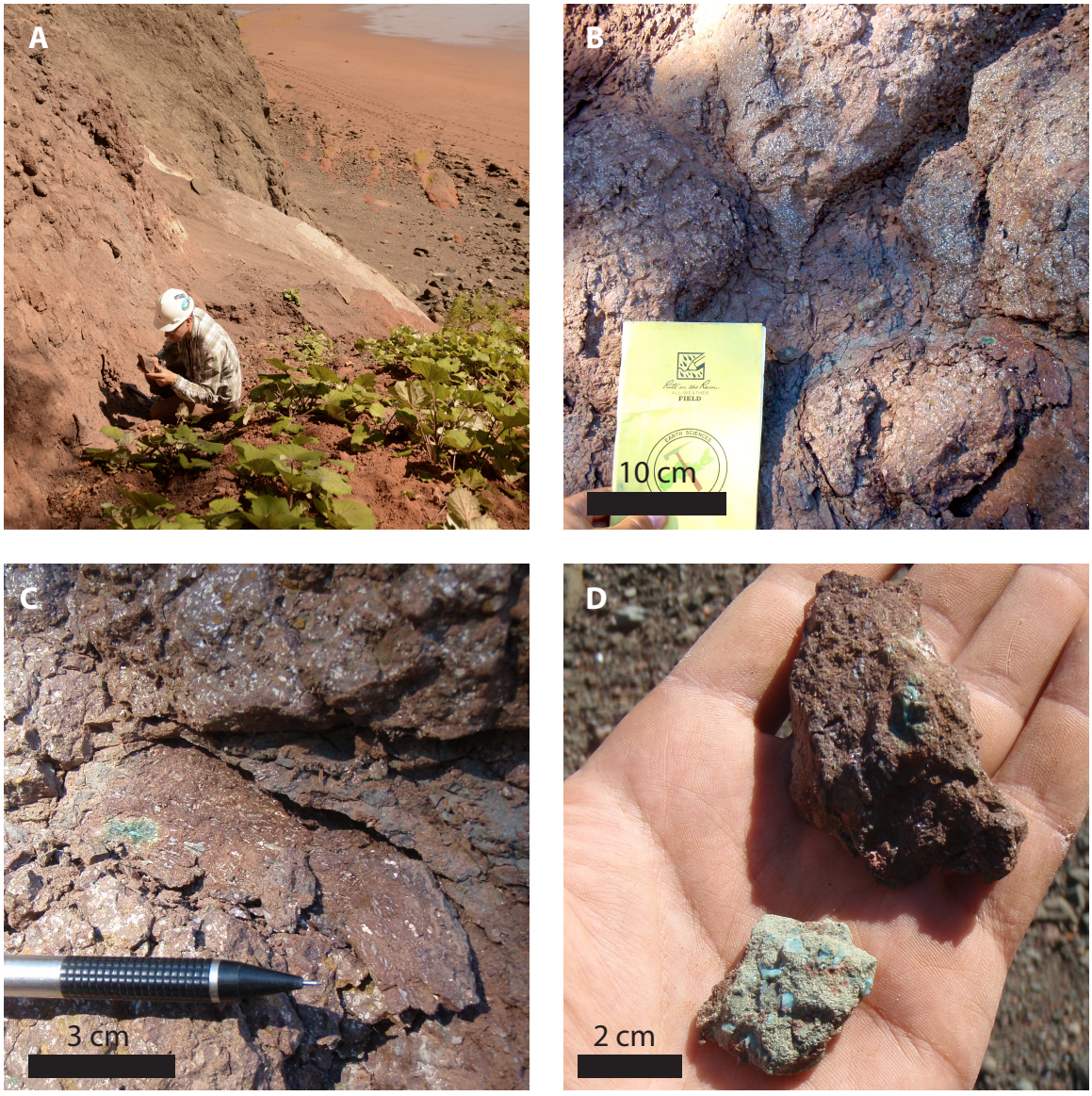

Figure 14: Facies 2 at outcrop. a) Facies 2 in outcrop (forming steeply dipping face to left of person) high on the cliff at Wasson Bluff; b) shimmery scale and bone material concentrated around the hummocks that represent the uneven surface of sediment draped over basalt clasts; c) oriented scale and bone fragments with long axes parallel to the side of the basalt hummock; d) fragments of vertebrate-bearing sandstone with purple-grey color and minor green patches.

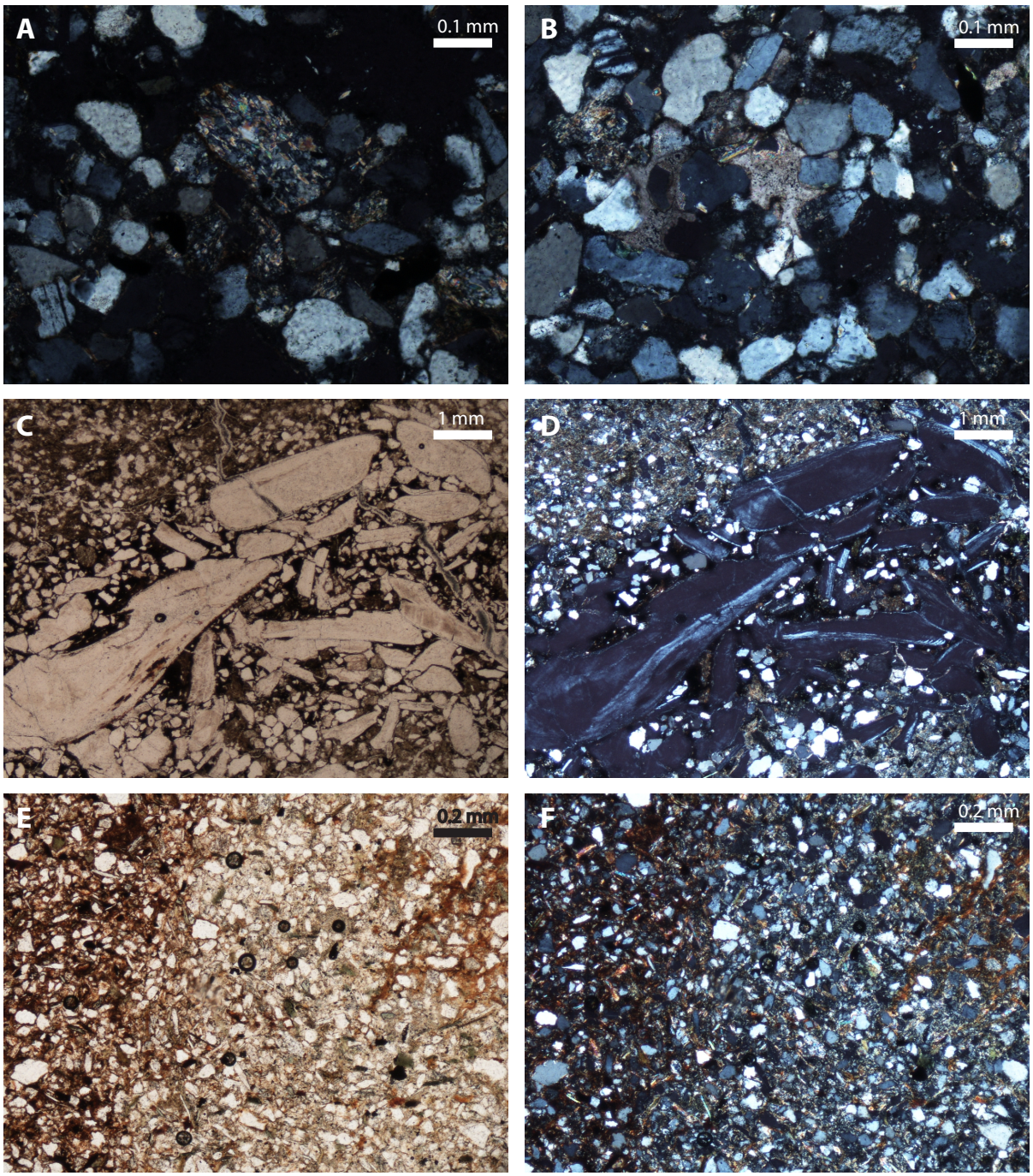

Figure 15: A) Igneous lithic in basal sandstone (xpl, 10x mag); B) patch of carbonate cement in basal sandstone (xpl, 10x mag); C) fish scale and bone material in vertebrate-bearing sandstone (ppl, 2x mag); D) fish scale and bone material in vertebrate-bearing sandstone (xpl, 2x mag); E) mottled siltstone (ppl, 5x mag); F) mottled siltstone (xpl, 5x mag).

5.2.3 Facies 3: Mottled Siltstone

Field description: This facies is predominantly red and characterized by green, grey, and grey-blue oblate mottles, roughly 2-10 cm in size (Fig. 16). It occurs in units that are 0.03-0.19 m thick, averaging 0.12 m, and makes up 12 % of section A, 21 % of section B, and 33 % of section C (Fig. 11). There are nine discrete beds in section A, one bed in section B, and two beds in section C (Fig. 12). Zones of mottles are discontinuous and are not accompanied by any apparent change in grain size, roundness, or sorting. Grain size for this facies ranges from clay to lower-very-fine sand with one lens of upper-fine quartz-rich sandstone in section A. The grains are well sorted and well rounded, and the beds display a blocky weathering habit. Fractures are common along boundaries between red-brown matrix and green patches of discontinuous alteration.

Petrographic description: The mottled siltstone is grain-supported with drab and red patches, and abundant flakes of chlorite, biotite, and muscovite; chlorite is especially abundant and locally forms "matrix" patches (Fig. 15e-f). Approximately 55 % of the sample comprises silt-sized grains of monocrystalline quartz, with 20 % mica, 10 % lithics, 15 % feldspar, and 40 % variegated chlorite-rich clay matrix.

Interpretation: Tentative interpretation is that the mottled siltstone of the Scots Bay Member represents a period of shallow ponding, allowing variable redox conditions that promote mottle formation due to gleying. The discontinuous fabrics and fine-grained nature imply a low energy environment, and a variable degree of oxidation

would be due to varied water saturation and aeration. A shallow lacustrine environment prone to seasonal variation in water depth and chemistry fits this profile. Alternatively, mottles may represent diagenesis during shallow burial of siltstone deposited in a stable low-energy environment. Although mottling is common in paleosols, the beds are weakly stratified and no indications of soil textures were noted in thin section.

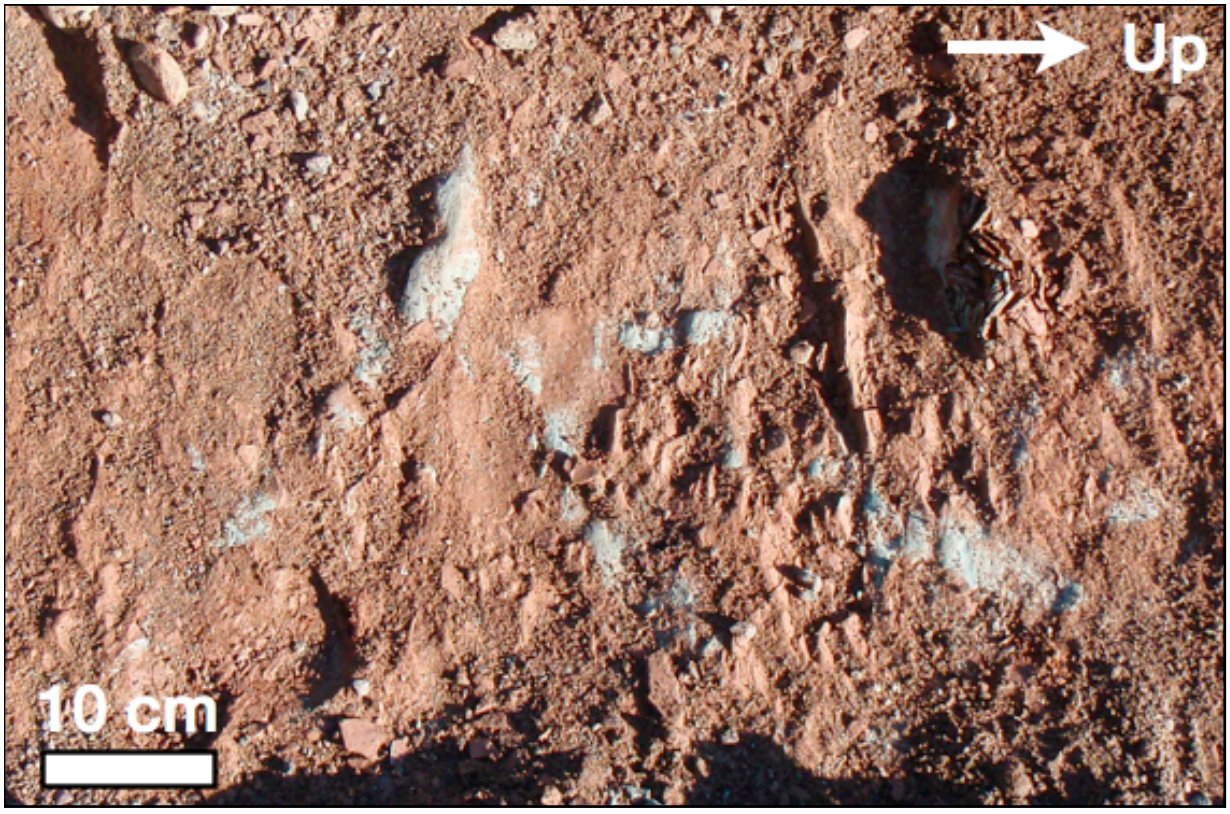

Figure 16: Mottled siltstone exposed in trench of section A.

5.2.4 Facies 4: Green Sandstone

Field description: This facies is exclusive to section B where it forms a 1.4 m bed of pale green medium-grained sandstone with minor mica visible (Fig. 17). Grains are well sorted and subrounded to subangular. The top 30 cm has a purplish hue and thin, diffuse red lenses. Diffuse stratification defines bedding thickness of

approximately 20-30 cm. The bed is lensoid, occupying a hollow in the underlying basalt.

Petrological description: The green sandstone is grain-supported and comprises monocrystalline quartz (44 %), polycrystalline quartz (3.75 %), and minor vertebrate material (<1 %), potassium feldspar, biotite, muscovite, chlorite, igneous and metamorphic lithic grains, microcline, plagioclase, and zircon. Clay-rich matrix (25 %) (Fig. 19a), poikilotopic calcite cement with isolated grains (9.75 %) (Fig. 19b) and oxidized matrix (4.75 %) infill pore spaces between the clasts. There is no indication of stratification in the thin-section and grains are typically well rounded. Sorting is good except for <1 mm subangular lithic grains.

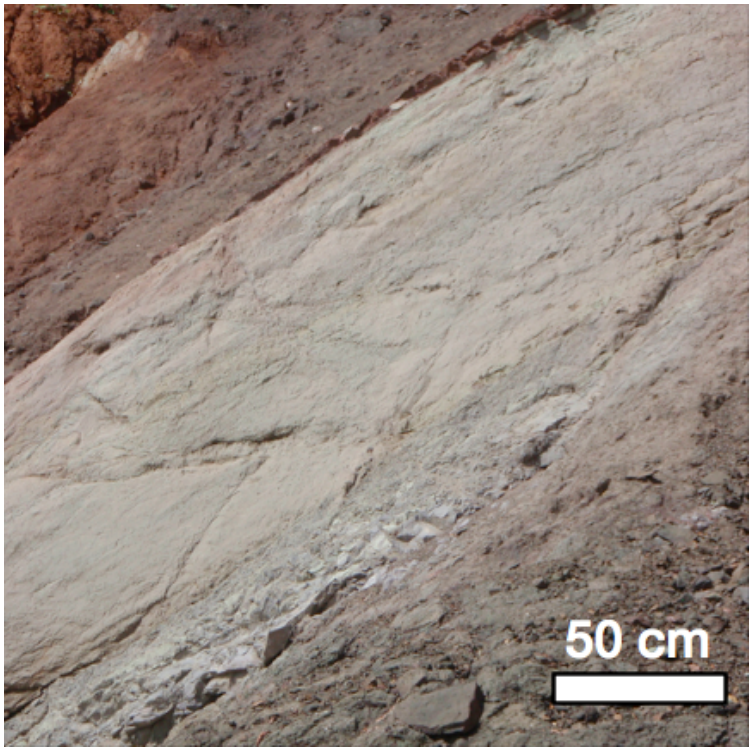

Figure 17: Green sandstone outcrop at Wasson Bluff. Bed is 1.4 m thick.

Interpretation: The green sandstone with relatively coarse grains represents an interval of high-energy deposition within the Scots Bay Member. The drab colour implies a low degree of oxidation, perhaps due to water saturation, lack of ferruginous material, or reduction after deposition. The lens shape of the bed is consistent with infilling of a hollow in the surface of the basalt. Facies 4, therefore, represents the preferential infilling of anomalous low-points in the surface of the basalt during the initial deposition of sediment over the North Mountain Basalt. The drab colour may be the result of increased, prolonged water saturation in the hollow after it was filled with sand. The presence of fish material supports this theory of subaqueous deposition in a nearshore or isolated pond setting.

5.2.5 Facies 5: Ostracode-rich Biomicrite

Field description: This facies is found in two thin units, 0.05 m and 0.12 m thick. It makes up only 2 % of section A (Fig. 11). The beds are tougher than the surrounding siltstones, and react moderately to HCl. Diffuse red-brown laminae are visible. Beds are green with diffuse red bands that penetrate along cracks.

Petrographic description: The ostracode-rich biomicrite is a micrite matrix-supported assemblage of ostracode fossils and detrital grains. The ostracodes are dispersed in the matrix, indicating that the fine carbonate must originally have been a detrital matrix to support the fossils. Sample CP-01-03-04 from bed 6A comprises quartz (3.25 %), ostracodes (6.25 %), sparite cement matrix (17.75 %), biomicrite matrix (68.5 %), oxides (3.6 %), and minor muscovite and chlorite-rich lithic grains. Patches of sparite are associated with void spaces within (Fig. 19c) and around

articulated shells where the original detrital matrix did not penetrate. Occasional large patches of sparite fill cracks in the section, and are not apparently associated with shells. Abundant disarticulated ostracode shells are commonly oriented concave-down. In places, disarticulated shells are stacked on top of one another, implying some degree of current sorting. Intact articulated ostracodes tend to be solitary, but groupings of three or more are observed (Fig. 19d). Red, oxidized laminae are associated with cracks and layers of ostracodes in the matrix. Patches of the most intense oxidation are located along bedding planes of laminae composed of detrital quartz grains. Some red seams are also near vertical, implying potential desiccation cracks. Sample CP-01-03-07 from bed 9A comprises quartz (2.5 %), ostracodes (7.5 %), sparite cement (4 %), biomicrite (84.6 %), and minor muscovite, biotite and oxides. Micas are elongate and oriented parallel to the bedding plane of laminae. A single fish scale was observed.

Interpretation: The ostracode-rich biomicrite represents an interval of low energy sedimentation, on the basis of the very fine grade micrite matrix and silt grade detrital grains. Episodes of higher-energy deposition are the concave-down current-stable position of concentrated shells fragments, and diffuse matrix-supported laminae of quartz grains. Storms, high-wind events, active water flows, or anomalous wave activity may have caused an influx of silt-grade sediment to the system and locally concentrated it by this means. Cracks with red seams at both horizontal and near vertical orientations are evidence of drying or disruption during the bed's early history. The absence of other invertebrate fossils potentially

indicates a harsh environment; ostracodes are tolerant organisms that can survive a wide range of depth and salinity conditions. The presence of a fish scale in the facies suggests that the population that generated the condensed section of vertebrate-bearing sandstone in Facies 2 was still present in the lake at the time Facies 5 was deposited. However, it is possible that the grain was reworked into the sediment from elsewhere.

5.2.6 Facies 6: Nodular Limestone

Field description: Commonly known as the "hard-bed", this facies crops out at Wasson Bluff in a single 0.12 m thick unit with uniform thickness across the outcrop. This bed is laterally continuous for ~8 m overlying the green sandstone in section B, but was not observed in trenched sections along the beach. It is significantly harder than other beds and weathers to large tabular blocks. In polished cross-section, the hard-bed comprises discontinuous concave-up laminae of red, red-brown, and cream sediment with minor continuous red-brown laminae (Fig. 18). This facies contains abundant off-white nodules that increase in proportion higher in the bed. The hard-bed reacts strongly with HCl and contains macroscopic bone and tooth fossils (T. Fedak, personal commun., 2013). The majority of beds are discontinuous and many segments are concave-up, resembling dish structures. Two continuous laminae of red-brown siltstone divide the sample into lower, middle, and upper sections. The lower section is a homogeneous cream color with few nodules and some thin red lenses. The middle section is more heterogeneous with many small white nodules (<0.5 cm in diameter). Red lenses are thicker in the middle section and angular bone fragments are visible. The upper

section is heterogeneous with a red matrix and many large nodules of varied size, composed of white calcareous material. Nodules tend to be near-spherical through the lower and middle parts of the section, and irregular and flattened in the upper part of the section. Vertical red fills are observed at varied levels in the slab, implying multiple desiccation cracking events. Fragments of bone material, white with a red reaction rim, 1 mm in diameter were also identified in the slabbed hand sample (Fig. 18).

Petrographic description: Held to light the large thin-section of nodular limestone is red, brown, and pale to transparent. Bedding is clearly visible but discontinuous and very-fine grains are visible. Color becomes darker red-brown moving up-section (sample orientation is known). The nodular limestone comprises approximately 25 % detrital grains of monocrystalline quartz, biotite, muscovite, and lithics, and 75 % micrite matrix. The micrite matrix is slightly coarser than that of the ostracode-rich biomicrite of Facies 5. Oxidation is concentrated along predominantly clast-supported laminae of detrital clasts. Lithic grains are composed of chlorite-rich altered basalt. Horizontal red seams are associated with the clast-supported layers of detrital clasts. Nodules of sparry calcite 0.2 – 40 mm in diameter punctuate the micrite matrix (Fig. 19f). Detrital grains are not found inside these nodules except where they have invaded the nodule via cracks along its abrupt edges. Chalcedony sheaves are observed inside one nodule. Ostracodes and some sparite patches associated with hollow shells are present in the section (Fig. 19e). Shells are matrix-

supported and typically oriented concave-down. A single scale fragment was found in the thin-section.

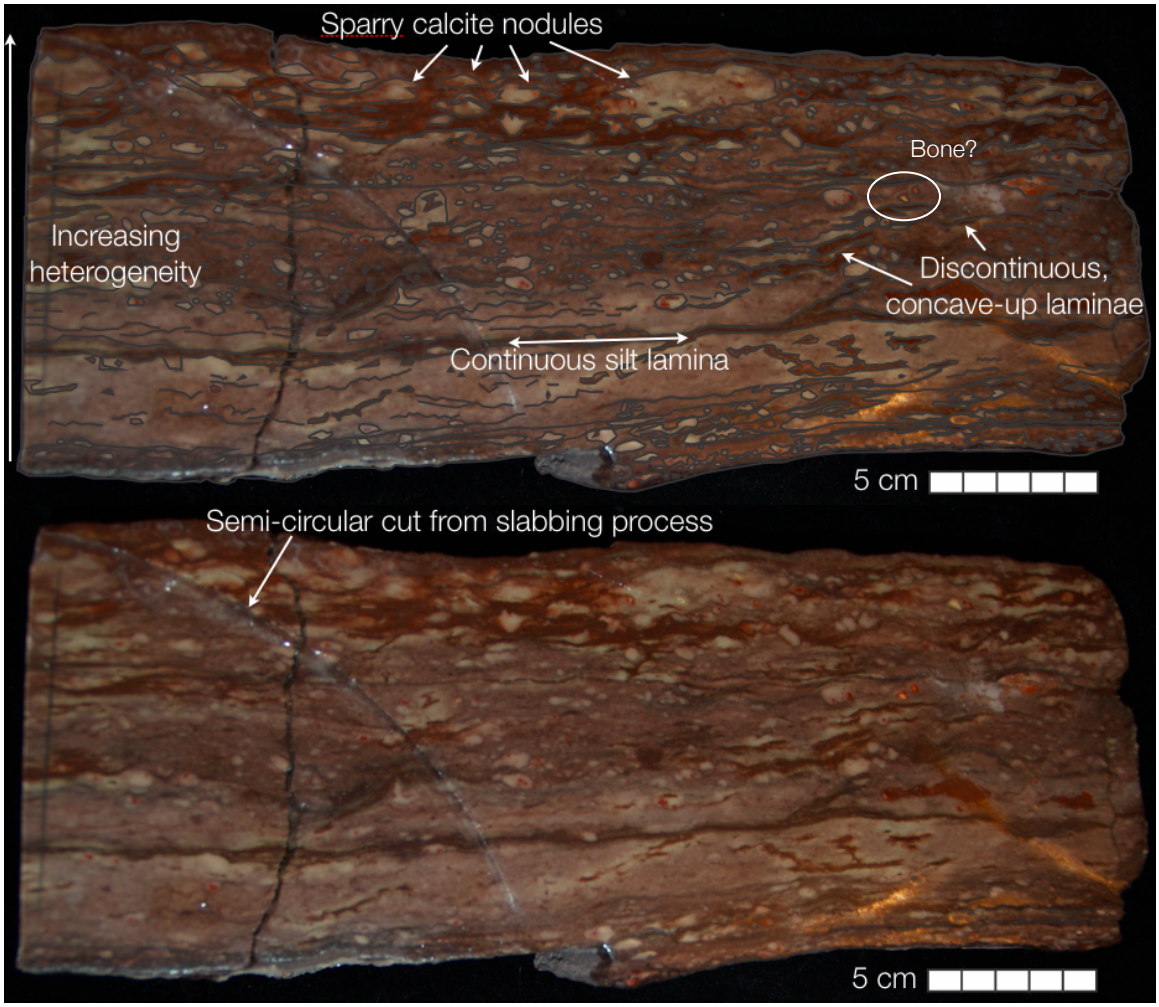

Figure 18: Annotated (upper) and original (lower) photos of polished slab of nodular limestone. Note that semi-circular cut on left is relict of sample preparation.

Interpretation: The bed of nodular limestone represents the final drying phases of an isolated pond filling a small, anomalous hollow in the basalt. The nodular limestone at Wasson Bluff is not observed in section A below the beach, ~20 m distant, and it may be assumed that the ~8 m wide cliff exposure represents a near-complete profile of the bed. The lensoid shape of the green sandstone underlying the nodular limestone supports the hypothesis that the beds of section B infill a hollow

in the surface of the basalt. Periodic wetting and drying cycles of the uppermost portion of this infill succession created a dense, nodule-rich layer with discontinuous, concave-up fabrics. The nodular texture is indicative of precipitation of carbonate material, and is analogous to the nodular facies that commonly develop in the shallow soils of poorly drained swamps in the Atchafalaya Basin near the Mississippi Delta (Coleman, 1966). The increased size and abundance of nodules close to the top of the nodular limestone bed at Wasson Bluff indicate that these nodules formed close to the surface. The concave-up laminar remnants in the nodular limestone and vertical red seams are evidence of desiccation cracking, however polygonal patterns were not observed on the bedding surface. The frequency of desiccation events was much higher in the nodular limestone (Facies 6) than the mottled siltstone (Facies 3), judging by the relative abundance of macroscopic vertical red seams in Facies 6. The upcurling of edges observed is analogous to the desiccation fabrics of the Trentishoe Formation where fragile desiccation fabrics were preserved by rapid low energy burial possibly by eolian deposition (Tunbridge, 1984). Eolian transport of fine-grained particles may have been a contributing factor in the deposition of the nodular limestone bed. The majority of the bed is a biomicrite matrix with matrix-supported ostracode-rich lenses. The fish scale and bone material may have been deposited in situ, however the very small quantity and fragmented nature of the vertebrate material implies that these particles were transported some distance prior to deposition.

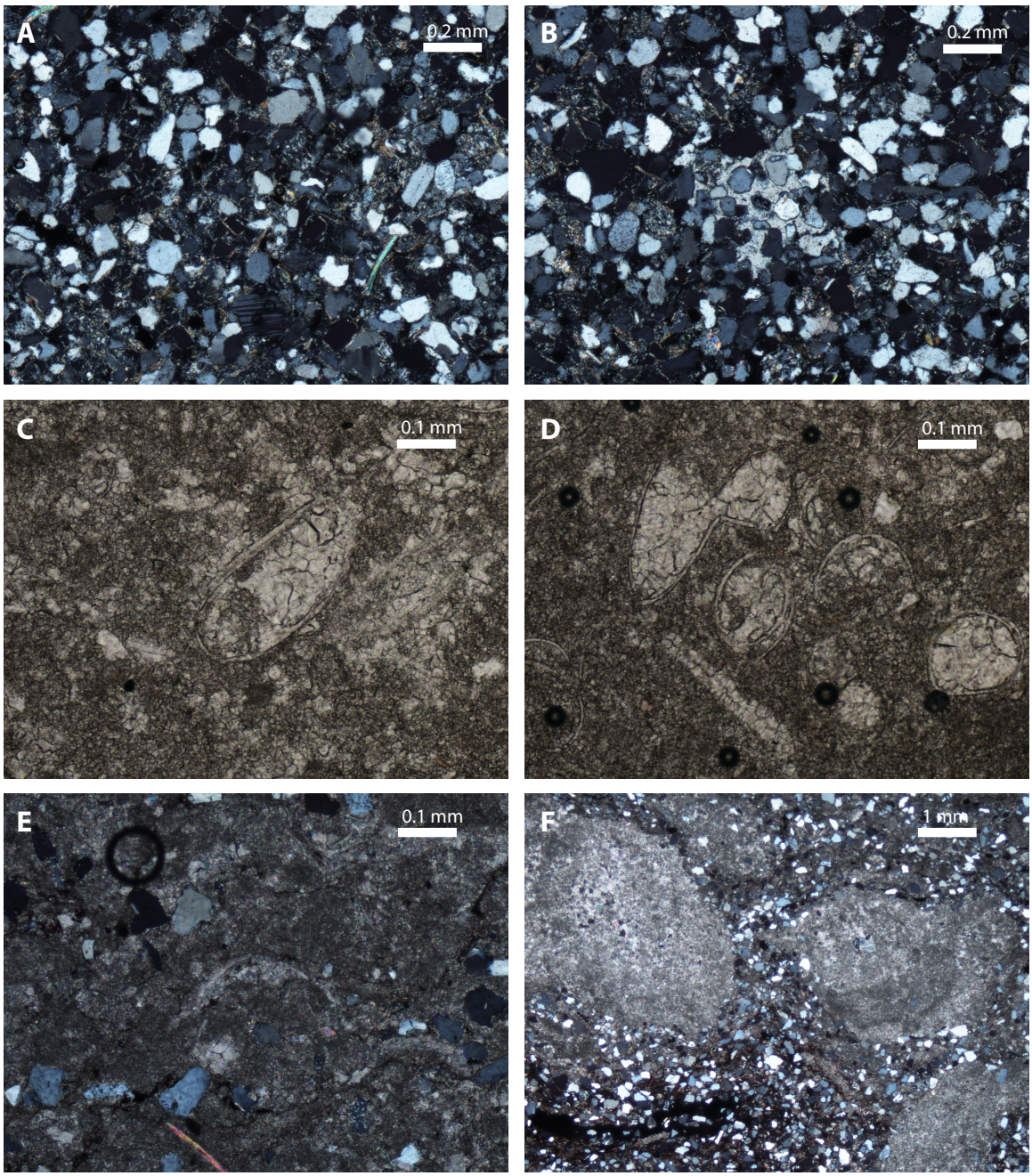

Figure 19: A) Clay filling pore space of green sandstone (xpl, 5x mag); B) patch of carbonate cement in green sandstone; C) ostracode-rich biomicrite with sparite cement filling void space in shell cavity (ppl, 10x mag); D) group of articulated ostracode shells in ostracode-rich biomicrite (ppl, 10x mag); E) matrix-supported ostracodes in nodular limestone (xpl, 10x mag); F) sparite nodules in nodular limestone (xpl, 2x mag).

5.2.7 Facies 7: Red Mudstone

Field description: These strata form tabular units 0.04-0.53 m thick, averaging 0.25 m, and make up 14 % of section A and 11 % of section C (Fig. 11). There are seven discrete beds of Facies 7 in section A and one bed in section C (Fig. 12). Beds are composed of laminae of silt and clay that break with a fissile habit (Fig. 20). Individual laminae are less than 2 mm thick. This facies is typically red-brown or red-orange-brown with a few green or grey patches.

Petrographic description: This facies is a matrix-supported assemblage of detrital grains. Thin laminae of very-fine grained sand are discontinuous and show gradients of oxidation: redder in the center of laminae, pale at the margins. Round reduction spots of drab matrix ~3 mm in diameter are present. This change of colour is associated with finer grained matrix, but there is no change in grain-size, sorting, roundness, or mineralogy of detrital grains. Two small fish scales were observed in the sample: one in pale laminae at the base of the section (Fig. 21a), and another amongst quartz-dominated laminae. Approximately 40 % of the sample comprises grains of monocrystalline quartz and minor microcline, biotite, and lithics. Muscovite is abundant and defines the lamination. The remaining 60 % of the sample is oxidized clays with some silty lenses, with minor pale zones of chlorite-rich clay (Fig. 21b).

Interpretation: The red mudstone represents an oxygenated low-energy environment. Minor pale reduction spots may represent localized microchemical

environments around small organic components on the lake-bottom, although no organic material was observed. A shallow lake environment meets these criteria, and is supported by the presence of fish scales within the thin-section. Thin lamination causing the fissile habit may be the result of parallel lamination deposited by fine-particle settling from particle suspension in the water column.

Figure 20: Fissile mudstone exposed along the trench in section A.

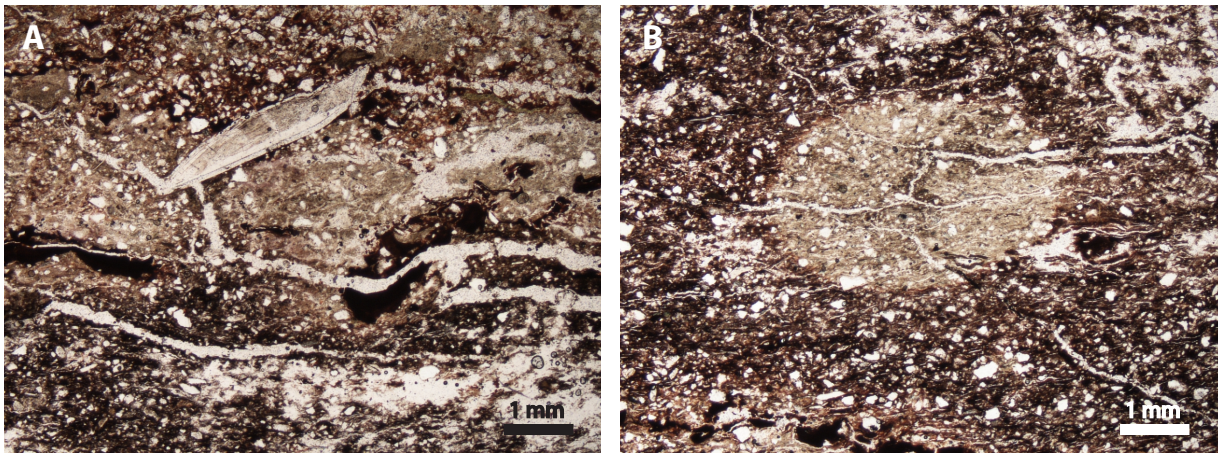

Figure 21: A) Fish scale in thin section (ppl, 2x mag); B) patch of alteration in thin section (ppl, 2x mag)

5.2.8 Facies 8: Red Sandstone

Field description: These sandstones form units 0.12-1.1 m thick, averaging 0.48 m, and make up 65 % of section A and 22 % of section C (Fig.11). There are 14 discrete beds of Facies 8 in section A and a single bed in section C (Fig.12). Beds comprise fine- to medium-grained quartz-rich sandstone with variable quantities of mica. The sand is well rounded, and medium-well to well sorted. Cross-stratification, planar lamination and scours are common (Fig. 22). Fine laminae above scour features have micas parallel to bedding. Thicker beds tend to be more resistant and crop out along the beach.

Figure 22: Trough cross-bedding in red sandstone of Facies 8 at Wasson Bluff.

Petrographic description: The red sandstone comprises monocrystalline quartz (38.75 %), polycrystalline quartz (9.25 %), microcline (4 %), plagioclase (2.5 %), undifferentiated feldspar minerals (3.75 %) lithics (8 %), terrigenous matrix (5.75 %), oxides (4 %), and minor augite, garnet, zircon, biotite, muscovite, and alkali

feldspar. Porosity is 21 % for the sample. Most detrital grains are surrounded by pellicles of red oxides. No bedding structures were observed in thin-section.

Interpretation: The red sandstone represents a variable energy environment, judging by grain size and sedimentary structures of the sandstone. The abundant scour-and-fill structures in the red sandstone imply scour erosion by currents followed by backfilling as the current velocity decreased. Beds with trough cross-bedding indicate that some scours migrated laterally and formed elongate structures of curved foreset laminae. Both of these sedimentary structures are evidence of an active, variable current flow. The ungraded, medium-grained, planar-laminated beds of red sandstone may represent short periods of high flow velocity. These parallel laminae are too coarse-grained to have formed from settling of grains from particle suspension. Eolian processes can form parallel laminae, however wind-formed parallel laminae are not common (Boggs, 1966). This facies has significantly more polycrystalline quartz and unaltered feldspars than other sandstones of the Scots Bay Member (Fig. 23-24). The increase in polycrystalline quartz may indicate a change of provenance. The difference in feldspar alteration is likely due to a difference in water saturation since the red sandstone was deposited in a more oxygenated environment as suggested by the abundance of ferrous oxide pellicles surrounding detrital grains.

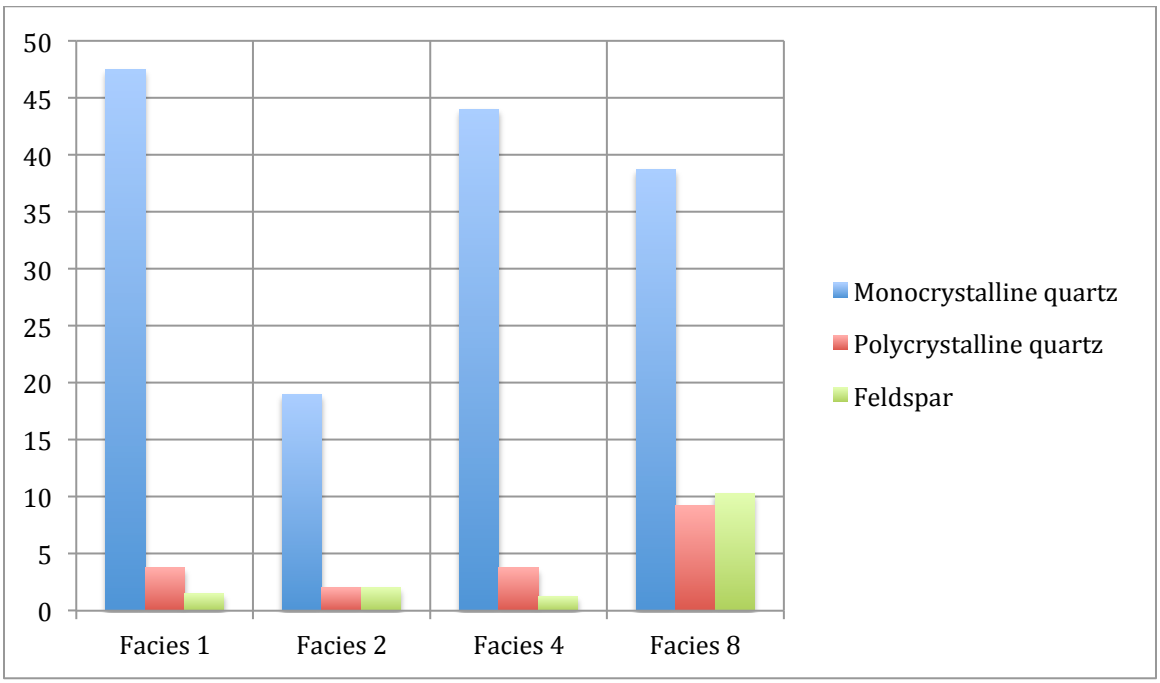

Figure 23: Histogram comparing the modal percent of monocrystalline quartz and polycrystalline quartz in the basal sandstone, vertebrate-bearing sandstone, green sandstone (Facies 1, 2 and 4), and red sandstone (Facies 8) of the Scots Bay Member at Wasson Bluff.

5.2.9 Facies 9: Red Siltstone

Field description: This facies is found interbedded with Facies 8 sandstone in two units 0.35-0.40 m thick that make up 7 % of section A (Fig. 11). It comprises red-orange beds of siltstone with minor very-fine-grained sand that is well sorted and well rounded. Beds are less than 0.5 cm thick and have a fissile weathering habit. Individual beds tend to fine upwards from very-fine sand grade detrital grains at their base to silt at the top. Fine mica-rich laminae are foliated parallel to bedding. Red siltstone intervals are interbedded within thicker beds of red sandstone from Facies 8, and may represent fining-up cycles of the same overall facies regime.

Petrographic description: No thin-section available.

Interpretation: The red siltstone of the McCoy Brook Formation represents a period of lower energy deposition as part of fluvial cycles. The top of red siltstone beds is abruptly truncated by medium-grained red sandstone. The two intervals of red siltstone may represent flooding events. During a period of higher than average flow, the river spilled its banks and fine-grained overbank deposits were laid down. The red sandstones of Facies 8 subsequently covered these fining-upwards sequences of low energy deposits. Alternatively, the red siltstone is a subset of the red sandstones of Facies 8, representing the very fine-grained tops of graded scour-and-fill successions.

5.3 Facies associations

There are two general facies associations at the "fish bed" of Wasson Bluff, interpreted here as lacustrine and fluvial. The general characteristics of each facies are summarized in Table 4.

Table 4: General characteristics of facies associations.

Facies association	Grain Size	Sedimentary Structures	Taxa
Lacustrine	Clay to fine-grained sand, micrite, or sparry cement	Diffuse lamination (< 0.02 –2 cm), disrupted fabrics, sparite nodules, desiccation cracks	Ostracodes, aquatic vertebrates (*Semionotus* fish and hybodont sharks), and terrestrial vertebrates (tetrapod teeth)
Fluvial	Fine- to medium-grained sand, minor silt to very-fine sand	Erosional scours, trough cross-bedding, parallel lamination	Terrestrial vertebrates (Table 1)

The lacustrine facies of the Scots Bay Member at Wasson Bluff are characterized by very fine-grained sediment, carbonate cement, fissile weathering habit, parallel laminations, disrupted fabrics, and aquatic fauna. The absence of ripple lamination or any other indications of current imply a low-energy environment where fine-grained sediment settled out of suspension to form beds of thin parallel laminae. The presence of both aquatic and terrestrial fauna, and disrupted fabrics such as desiccation-cracks suggest a transitory environment with periodic wetting and drying phases. A lacustrine shoreline meets these criteria. Since Wasson Bluff was landlocked at the center of Pangaea during the uppermost Triassic, and no marine evidence has been found, it is assumed that these low-energy facies are of fully non-marine origin.

The lacustrine facies association comprises the basal 1.9 m of sections A-C. The Scots Bay Member at Wasson Bluff is characterized by basal sandstone overlain by a vertebrate-bearing transgressive lag sandstone, succeeded by interbedded mottled siltstone, ostracode-rich biomicrite, and red mudstone, with green sandstone and nodular limestone (section B) representing the fill of a hollow apparently distinct from facies in the closely adjoining sections (A and C). The lacustrine facies of the Scots Bay Member constitutes Facies 1-7 (Fig. 5-6).

Fluvial facies overlie the Scots Bay Member. Fluvial facies are characterized by fine- to medium-grained sediment with sedimentary structures that imply current flow. Compositionally, the red sandstone is classified as subfeldspathic arenite (Fig. 24). The red sandstone and red siltstone of Facies 8 and 9 represent an oxygenated moderate- to high-energy flow environment with periods of low energy.

This is consistent with a fluvial channel system with periodic overbank floodplain deposits. Trough cross-bedding and scours indicate intermittent to permanent flow regimes of variable moderate to low energy that would generate backfilled erosional structures. Beds of planar laminations infer sheet-like high-energy ephemeral flows. Variable flow regimes are expected during the latest Triassic and Early Jurassic due to the semi-arid climate (Olsen, 1981; Hubert and Mertz, 1980). Fluvial and eolian facies are characteristic of the lower McCoy Brook Formation. The bone beds rich in dinosaur material found 50 m stratigraphically up-section are within fluvial facies (Olsen et al., 2005). These beds measured in this study of the "fish bed" at Wasson Bluff may represent the precursor to the channel system that entombed the prosauropod dinosaurs.

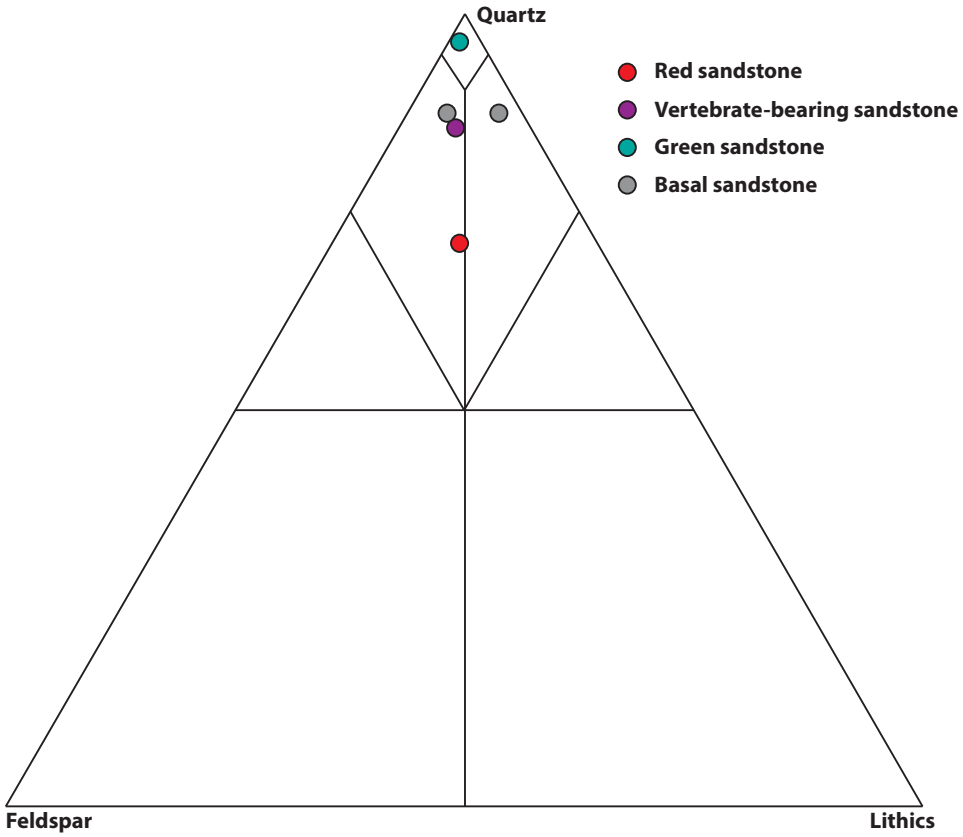

Figure 24: Compositional classification scheme (Dott, 1964).

6.0 Taxonomy and taphonomy

6.1 Quantitative analysis of fossil material from Facies 2

The fossils found in the Scots Bay Member at Wasson Bluff represent a wide variety of vertebrate and invertebrate fauna. Prescott (2010) quantified the fossil content of 16 samples from Facies 2 of section C collected in 2008 (Fedak, NS Permit P2008NS02; Fig. 25). Five morphological categories were defined: scales, spines, teeth, bone, and coprolite. These morphological categories were further subdivided into four taxonomic groups: hybodont shark, semionotid fish, tetrapod, and unidentifiable (Tables 5-7, Figs. 26-7). Cumulatively, the fossil material extracted from the very fine-grained sand matrix accounted for 17.13 % of the 3339.69 g of sediment studied. Scales are the dominant component, comprising 7.61 % (254.3 g) of the sample. Due to the effects of weathering the majority of scales were unidentifiable, but small quantities of semionotid fish scales were identified. Bone

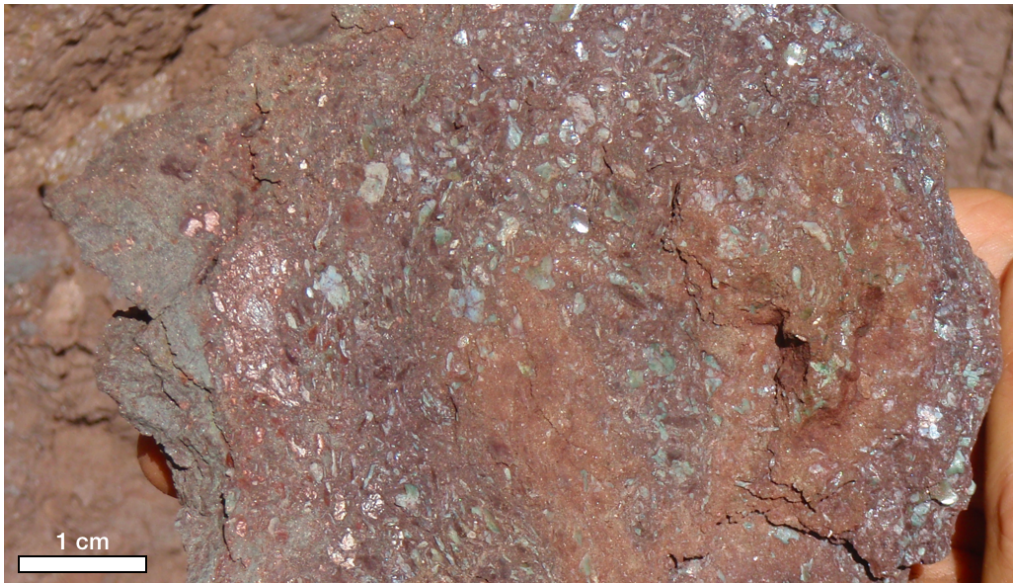

Figure 25: Small disarticulated fossils of scale, bone, teeth, spine, and coprolite fragments in Facies 2, section C of the Scots Bay Member.

fragments, teeth, spines, and coprolites constitute the remainder (Tables 5-7). Several other larger elements including a dinosaurian cervical vertebra, a large theropod tooth, and a tritylodont (mammal-like reptile) dentary and tooth were also located in the samples but are described elsewhere (Fedak et al., 2014).

The competency of the teeth, scale, and bone material facilitate their preservation in the rock record. Geological processes can concentrate this material into condensed sections. Such accumulations of material lack complete skeletons of individual specimens but permit studies of the local population since they gather a large volume of sample material into a single location. From Prescott's study of the fossils at Wasson Bluff the population of aquatic fauna that inhabited the lake shortly after the initial deposition of sediment can be established.

Table 5: Weight of fossil material recovered from 3339.69 g of unsorted material from vertebrate-bearing sandstone of Facies 2 and relative percent of each component recovered (Prescott, 2010).

Morphology	Scales	Spines	Teeth	Bone	Coprolite
Weight	254.3 g	6.16 g	11.26 g	29.99 g	4.86 g
Relative %	82.95 %	2.01 %	3.67 %	9.78 %	1.59 %

Table 6: Scales sorted into taxonomic groupings. "Unidentifiable Scales" were too damaged to classify. There are approximately 15-20 scales per gram (Prescott, 2010).

Taxonomy	Fish Scales	Shark Scales	Unidentifiable Scales
Weight	0.23 g	0.23 g	253.83 g
Relative % of scales	0.09 %	0.09 %	99.82 %
Approx. number of scales	3 to 5 scales	3 to 5 scales	3807 to 5077 scales

Table 7: Teeth sorted into taxonomic groupings. "Unidentifiable Teeth" were too damaged to classify. Teeth varied from 1 to 10 fragmented or whole teeth per gram (Prescott, 2010).

Taxonomy	Fish Teeth	Shark Teeth	Tetrapod Teeth	Unidentifiable Teeth
Weight of sample	1.15 g	2.87 g	2.3 g	4.94 g
Relative % of teeth	10.21%	25.49%	20.43%	43.87%

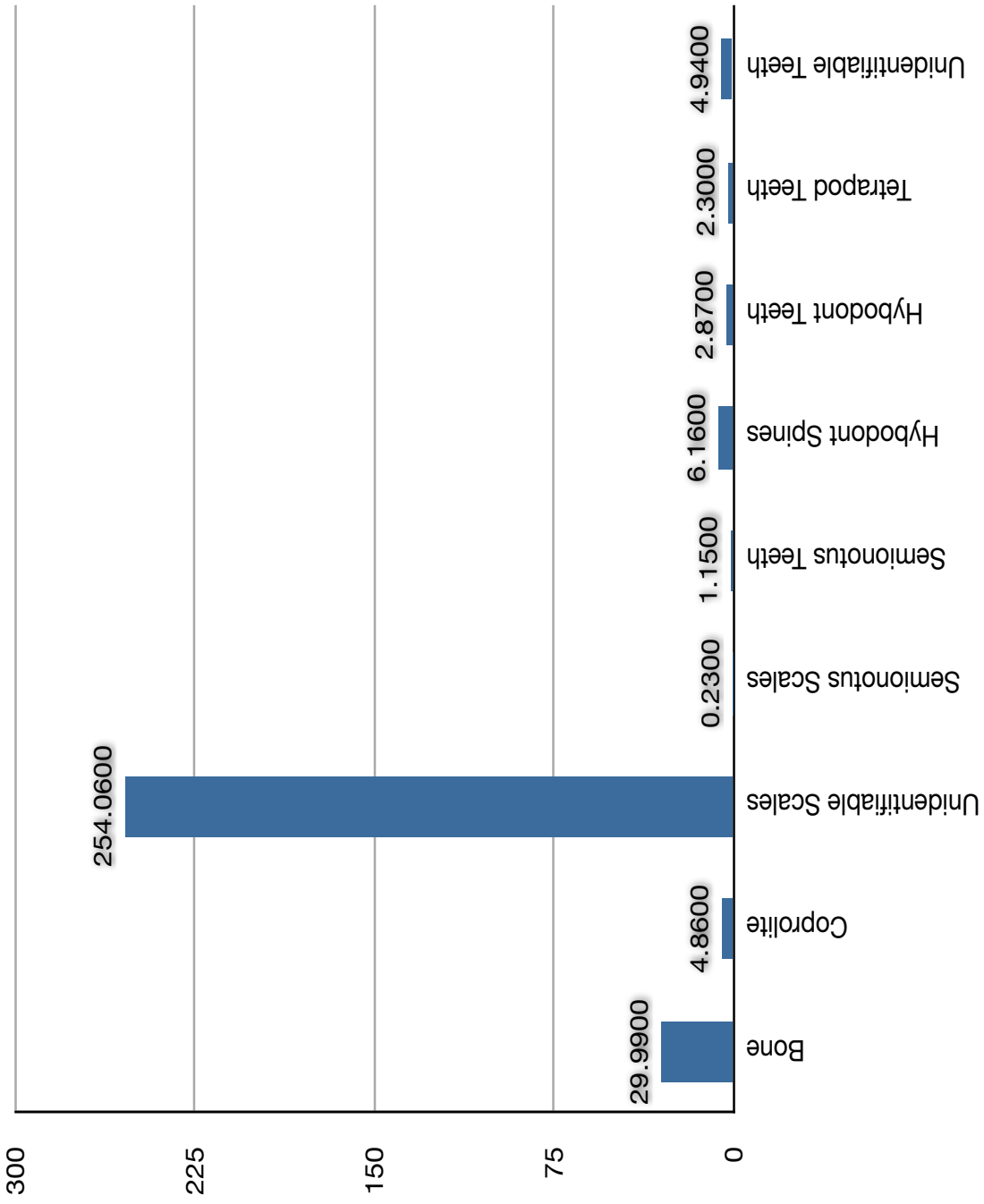

Figure 26: Weight of fossil material recovered from 3339.69 g of vertebrate-bearing sandstone from Facies 2 of Scots Bay Member (Prescott, 2010).

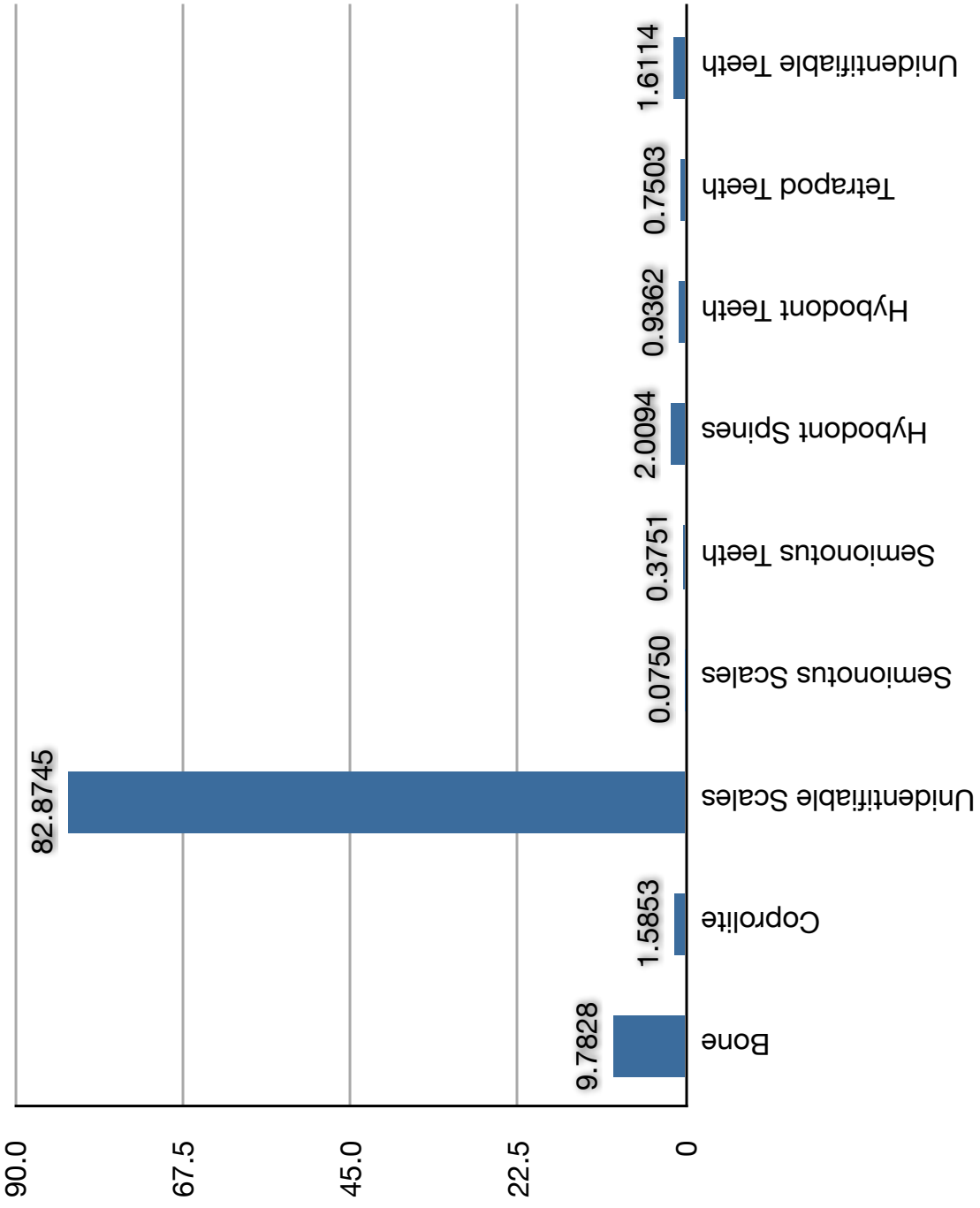

Figure 27: Weight percent of fossil taxa relative to total (306.56 g) fossil material recovered (Prescott, 2010).

6.2 Taxonomy

The most common fossils in the Newark Supergroup are osteichthyan fish. Superclass Osteichthyes comprises bony fish, both freshwater and marine. Osteichthyes are the most successful of all aquatic vertebrates, arising in the late Silurian (Fig. 28) and totaling over 20,000 living species (Kotpal, 2010).

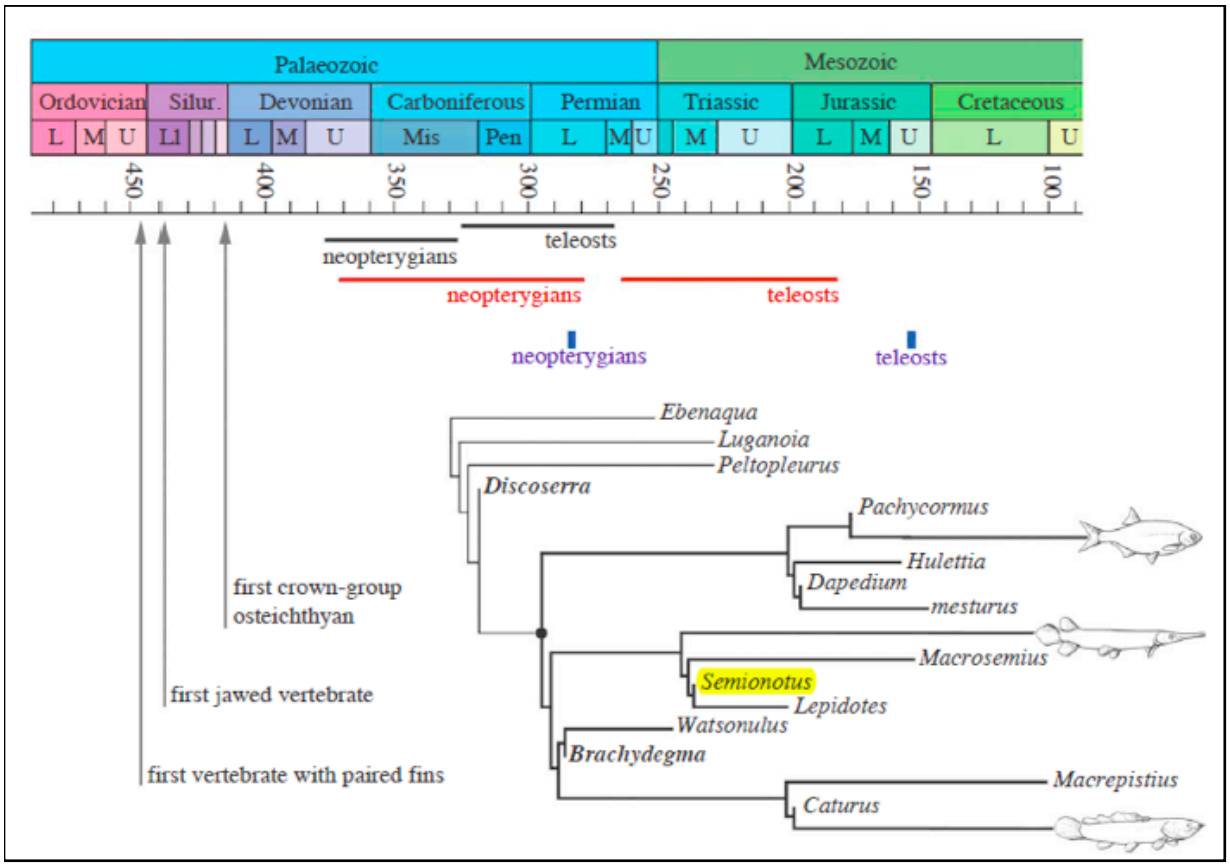

Figure 28: Evolutionary time-ranges of actinopterygian fish (modified from Hurley et al., 2007).

The morphology of osteichthyan fish varies greatly, but they all have a spindle-shaped body covered by dermal scales, a bony endoskeleton, swim using fins, and breathe using gills. Actinopterygii, a subclass of Osteichthyes, are ray-finned fish. These fish have particular morphological and histological characteristics that aid identification: an acrodine cap on teeth in addition to enamel, a single dorsal fin,

large maxilla, ganoin-coated scales, fulcral scales on the leading edge of the tail, and nasal notches for nostrils (Janvier, 1996). The acrodine-capped teeth and ganoin scales are particularly useful tools for identifying the disarticulated actinopterygians at Wasson Bluff. Ganoin is a hard enamel-like substance that forms the outer layer of scales of certain fish. It is ganoin that gives the Scots Bay Member scales their shiny luster. Acrodine is a transparent cap of hypermineralized tissue on the tip of teeth (Janvier, 1996). Since the acrodine is harder than the enamel at the base of the tooth, it forms a crown that may be observed with a hand-lens or binocular microscope.

Taxonomic identification for the vertebrate-bearing sandstone of Facies 2 is difficult due to the disarticulation of fossil material and severely damaged quality of the samples. Two types of actinopterygians have been confirmed at Wasson Bluff: semionotiformes and redfieldiiformes.

Semionotiformes are thick-scaled, primarily freshwater fish that lived in Triassic to Early Jurassic lakes. Although found worldwide, their distribution in North America is limited to the Newark Supergroup of the eastern seaboard. There are over 20 genera of semionotiformes, but only six are well known: *Semionotus, Lepidotes, Dapedium, Tetragonolepis, Heterostropheus,* and *Acentrophorus*. *Semionotus* is the most common genus found north of the Newark Basin (Fig. 29). The deep rift-valley lakes hosted populations of at least four distinct species of *Semionotus* during the Late Triassic and Early Jurassic: *Semionotus braunii*, *Semionotus tenuice*, *Semionotus micropt*, and *Semionotus elegans* (Fig. 30).

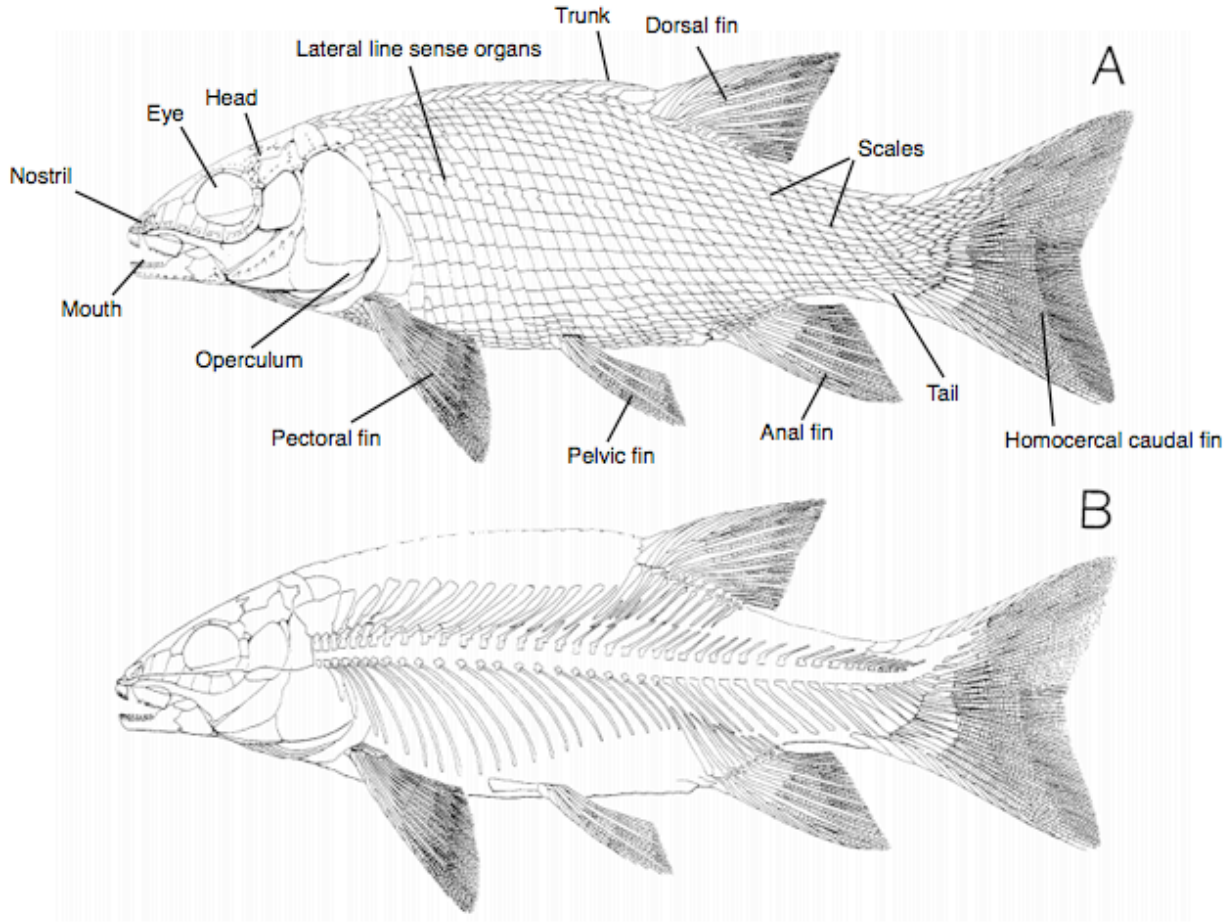

Figure 29: Reconstruction of complete individual of the *Semionotus elegans* group; a) external view of dermal scales; b) endoskeleton based on specimens from the Lockatong Formation, New Jersey (modified from Olsen and McCune, 1991).

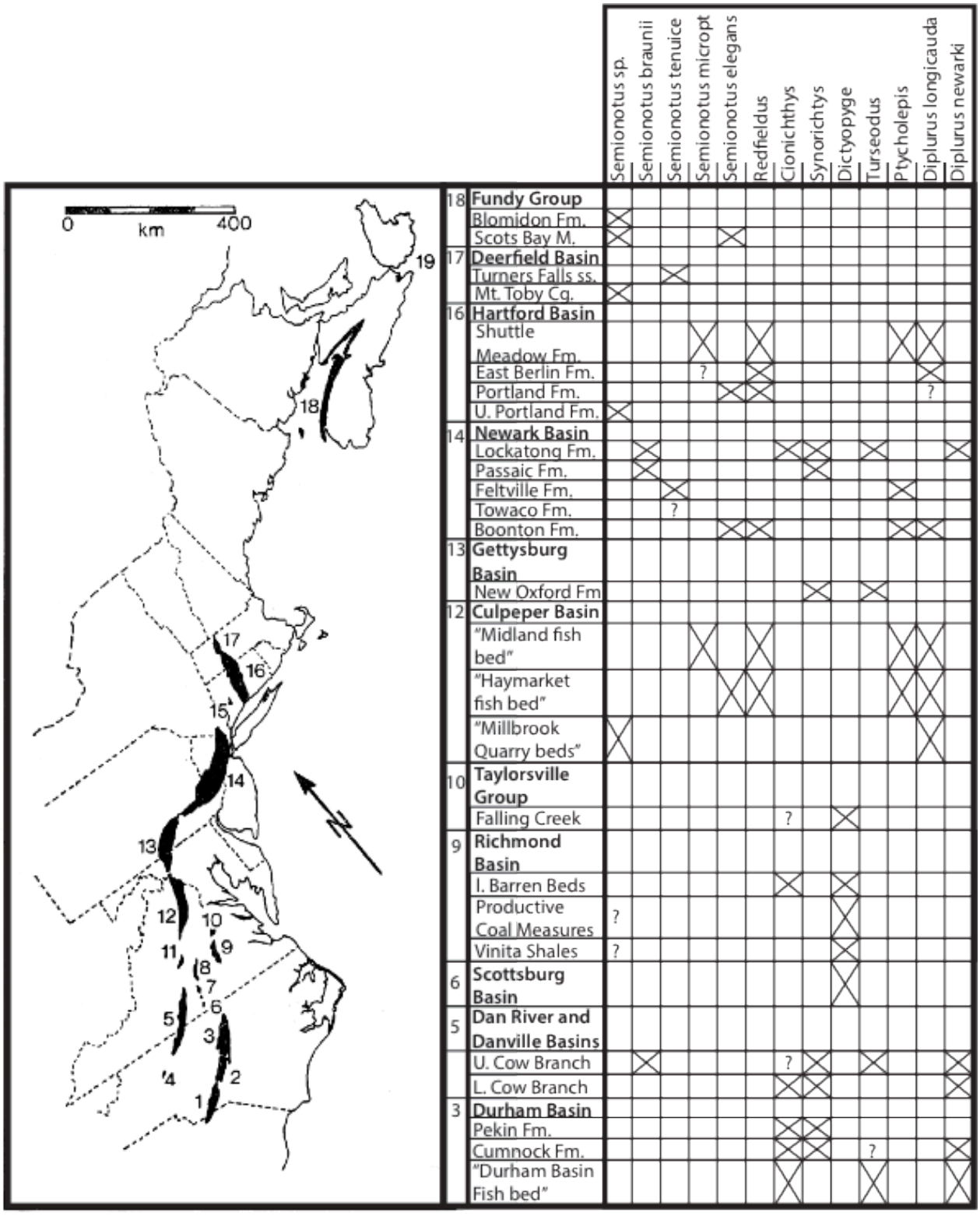

Figure 30: Distribution of actinopterygians in the Newark Supergroup. Numbers correspond to basin locations. No recorded discoveries in (1) Wadesboro Basin, (2) Sanford Basin, (4) Davie County Basin, (7) South Farmville Basins, (8) Farmville Basin, (11) Scottsville Basin, (15) Pomperaug Basin, and (19) Chedabucto Basin (modified from Olsen et al., 1982; Olsen et al., 2005).

The morphological characteristics used to classify *Semionotus* species are: skull-bone proportion, scale and skull ornamentation, and meristic characteristics (Olsen el al., 1982). Since overlap of specific characteristics is common among species, complete or near-complete skeletons are required to confidently identify individuals. The *Semionotus* remains found in the Scots Bay Member at Wasson Bluff are not complete. The assemblages of scale, teeth, and bone fragments (Figs.26-27) have not yet yielded any articulated fish remains. However, articulated *Semionotus* specimens were found in the McCoy Brook Formation at Five Islands (Olsen et al., 2005). The lack of full skeletons prevents accurate classification beyond genus level at Wasson Bluff.

Redfieldiiformes are the second order of ray-fin fish found at Wasson Bluff. J.H. Redfield of Connecticut defined the original genera of redfieldiiformes in the early 1800s (Janvier, 1996). These freshwater fish have since been found in Triassic and Early Jurassic strata of Australia, South Africa, Zambia, Morocco, and North America. The most primitive forms are found in South Africa and Australia, whereas more advanced genera are found in Morocco and North America (Maisey, 1996). The distribution of redfieldiiforme discoveries is similar to many other ancient freshwater fish, but most genera of redfieldiiformes became extinct in the Late Carboniferous or Permian so little is known about them. The Scots Bay Member has yielded scales and skull bones from undetermined redfieldiid fish (Olsen et al., 2005). These redfieldiiformes would represent the latest surviving genera.

Hybodont, or “hump-tooth”, sharks were the most common marine and freshwater sharks during the Triassic, Jurassic, and Cretaceous periods (Maisey,

1996). Although primarily marine, some freshwater lineages diverged during the Triassic. Teeth and spines of freshwater hybodont sharks have been found at Wasson Bluff (Olsen et al., 2005; Prescott, 2010). Hybodont teeth are distinguished by their sinuous ridges, numerous nutrient canals, and elongated, often low profile (Fig. 31) (Janvier, 1996).

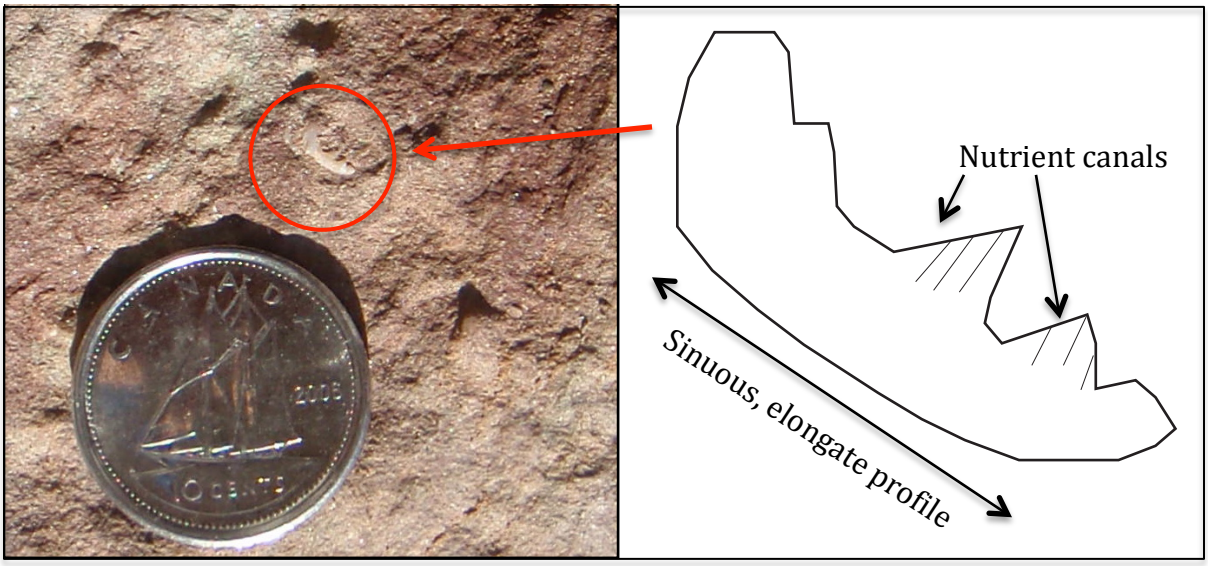

Figure 31: Hybodont shark tooth from bed 3B of the Scots Bay Member, highlighted by red circle.

Fin spines are also characteristic of hybodont sharks. Spines are rounded in section and are ornamented by smooth ridges of dentine (Janvier, 1996). The size, ornamentation, and morphology of fin spines can facilitate identification of specific genera of hybodont. The teeth and fin spines recovered from the Scots Bay Member at Wasson Bluff are close to those of *Hybodus*, a late hybodontiforme. Late hybodontiforms have non-growing, placoid-type scales (Janvier, 1996). Placoid scales do not have a ganoin layer and thus lack the characteristic shine of actinopterygian fish scales. Furthermore, since the scales are non-growing, hybodont scales may be differentiated from actinopterygian scales in thin section by

their lack of growth rings. The global distribution and wide range of tolerance of hybodont sharks make them a poor environmental indicator.

Invertebrate fossils are common within the Scots Bay Member along the Blomidon Peninsula (Hassan, 2010), but only brief mention has been made of ostracode fossils within the Scots Bay Member along the Wasson Bluff section (Olsen and Gore, 1989; Tanner and Hubert, 1994). Ostracodes are small bivalved crustaceans that range in size from 0.5 mm to 4 mm and live in both freshwater and marine environments (Moore et al., 1952). The shell consists of two ovate valves that are generally different sizes. Shell composition is calcium carbonate. The valves articulate along their dorsal edge, one valve with hinge teeth and the other accommodating movement with sockets or ridges. Shells may overlap. Ostracodes live on the bottom or attached to the base of plants, and many kinds dig burrows. The classification criteria defined by Moore et al. (1952) is: "(1) general shape, size, and convexity of valves, and the position of greatest thickness; (2) position and amount of overlap of the valves; (3) presence of spines, frills, lobes, sulci, and pits on the valves; (4) hinge characteristics, such as reticulations; and (5) structures due to sex differences, such as brood pouches."

The ostracodes observed in beds 6A and 9A at Wasson Bluff in this study were noted only in thin section making identification difficult. Further work needs to be done to extract fossils in order to establish the genus. For a thorough study of ostracodes in the Scots Bay Member along the southern shore of the Bay of Fundy, see Hassan (2010). The majority of ostracodes observed by Hassan in the Scots Bay

Member belong to the freshwater genus *Darwinula*. *Metacypris, Timiriasevia,* and *Megawoodworthia* were also noted, but in smaller quantities.

Remains of terrestrial vertebrates are surprisingly common in the Scots Bay Member at Wasson Bluff. Disarticulated tetrapod bones and teeth have been found, although no particular taxon is dominant (Olsen et al., 2005). Finds include protosuchid girdle elements and osteodems, small theropod dinosaur teeth similar to those of *Syntarsus* or *Coelophysis*, small ornithischian teeth, vertebrae, limb elements, and trithelodont postcranial elements (Olsen et al., 2005). The presence of terrestrial vertebrate fossils implies close proximity to the shoreline during deposition.

6.3 Taphonomy

Fossil material is concentrated near the base of the Scots Bay Member at Wasson Bluff, as seen in sections A and C (Fig. 6). Fossil material has not been found to date in the sandstones filling the cracks in the surface of the basalt, where former fissures 20-30 cm wide are filled with red-brown, fine-grained sandstone. However, fossil material is concentrated around the basalt clasts in beds overlying the basalt. Aquatic fossil material is significantly more rare in strata above this bed. Thus, the peak preservation potential of aquatic fauna was shortly after the initial deposition of sediment on the basalt during the early phases of transgression of the lake.

Dinosaur bone beds are found within the fluvial redbed successions that overlie the Scots Bay Member. Within the lower McCoy Brook Formation the general statement may be made that fluvial facies are more favorable for preservation than

eolian facies. For a thorough discussion of the taphonomy of dinosaur material within the redbeds of the lower McCoy Brook Formation see van Drecht (2014).

7.0 Discussion

7.1 Sequence stratigraphy

Figure 32 presents a lake-level curve for the lake that deposited the Scots Bay Member: the Scots Bay Lake (termed by Hassan, 2010).

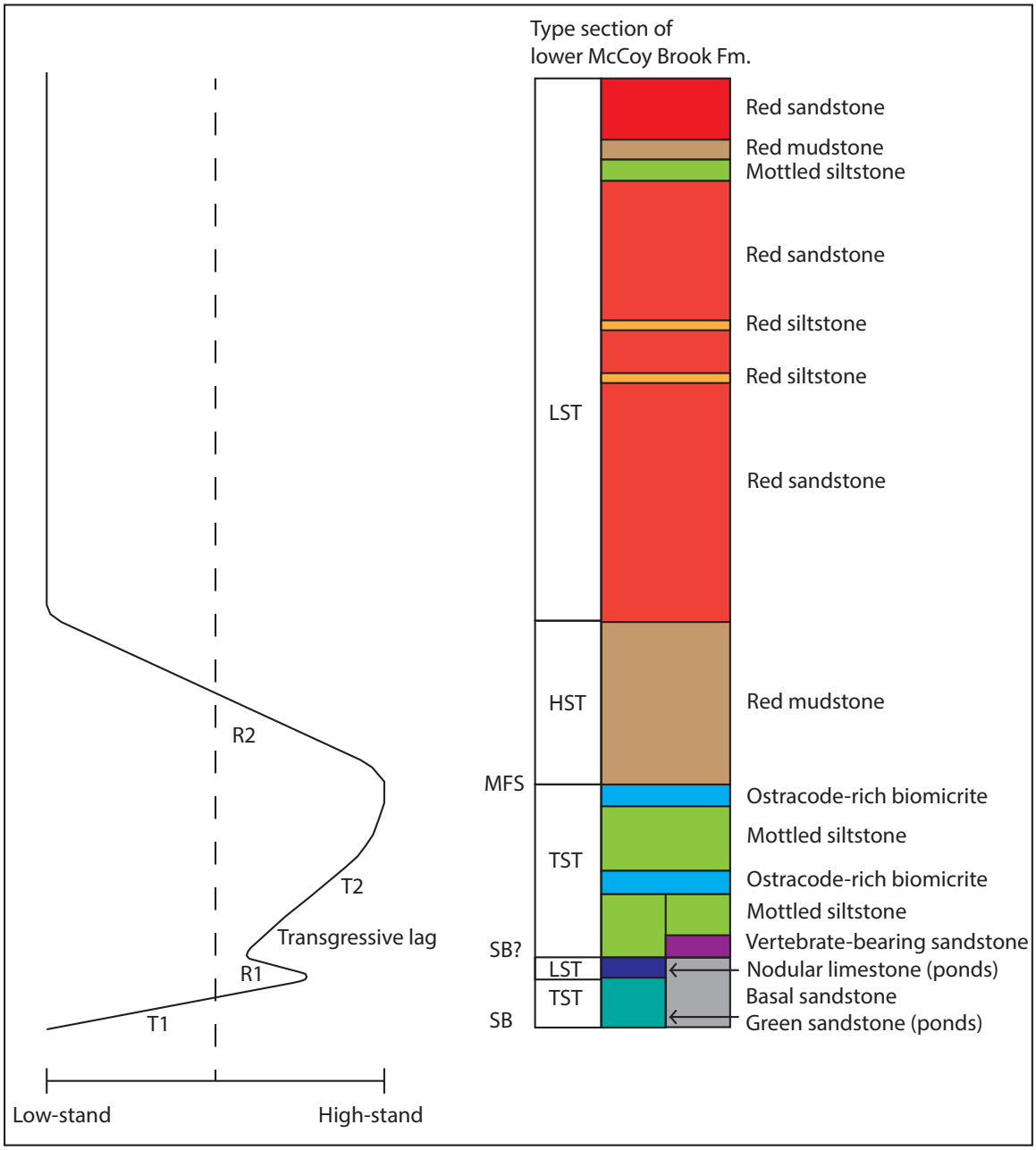

Figure 32: Proposed lake-level curve for the Scots Bay Lake.

The terminology used in this discussion is adopted from Catuneanu et al. (2009) based on a consensus on sequence stratigraphic terminology for fully non-marine settings. Sequence concepts can be applied to successions of non-marine origin by considering how fluvial accommodation is created and destroyed by: (1) tectonic movement between basin and source area, and (2) cycles in climate that control water supply (Catuneanu at al., 2009). These are considered "upstream controls" based on fluvial processes as opposed to "downstream controls" based on changes in maritime base-level. In systems governed by upstream controls, subaerial unconformities may be used to define sequence boundaries. The terms "transgression" and "regression" are used to describe the movement of a coeval shoreline, in this case the shoreline of the Scots Bay Lake. Likewise, "highstand" and "lowstand" refer to lake-level, not maritime base-level. Table 8 provides a general summary of sequence stratigraphic terminology.

Table 8: Summary of sequence stratigraphic terminology (Catuneanu et al., 2009).

Term	Abbreviation	Event
Sequence boundary	SB	Bounding surfaces defined by significant erosional unconformities and their correlative conformities.
Transgression	T	Landward shift of lacustrine system as base-level rises at rates higher than sedimentation rates at the shoreline.
Maximum flooding surface	MFS	The surface that marks the change in shoreline trajectory from transgression to highstand.
Highstand	H	Basinward shift of lacustrine system as sedimentation outpaces accommodation.
Lowstand	L	The base-level stillstand following regression of the shoreline.
Systems tract	ST (TST, HST, LST)	A linkage of contemporaneous depositional systems.

The lake-level curve for the Scots Bay Lake, constructed based on sections A-C, reveals an overall transgressive-regressive pattern. The basal sandstone and green sandstone of Facies 1 and 4 were deposited during a moderate-energy period and attributed to the transgressive systems tract. This was the initial flooding event over the North Mountain Basalt. The top of the basalt represents a subaerial sequence boundary. Medium-grained sand filled cracks and hollows in the basalt as the shoreline prograded landward. The presence of nodular limestone (Facies 6) with disrupted fabrics, a relic of multiple desiccation events, indicates that this initial transgression (T1) was followed by a regression (R1) and lowstand during which playa facies developed in localized pond settings (Fig. 36). The mottled siltstone of Facies 3 represents a low-energy environment, and is inferred to mark a second deepening cycle of the lake (T2). Vertebrate-bearing sandstone (Facies 2) was deposited as a transgressive lag deposit during the second transgressive systems tract. Facies 2 is found draped around basalt hummocks that likely acted as traps for fossil material. The smooth top of the nodular limestone does not have any trapping mechanisms to collect fossil material; therefore the minor fish material found in the nodular limestone is likely not from the same taphonomic event as the fish material in the vertebrate-bearing sandstone.

The maximum flooding event of the Scots Bay Lake is defined in the rock record by beds of ostracode-rich biomicrite. The two beds of ostracode-rich biomicrite in section A comprise micrite and minor terrigenous silt with abundant ostracodes. The mottled siltstone that separates the two beds may represent a second-order regressive cycle prior to the maximum flooding surface (MFS) (Fig. 6),

or might represent a short-lived influx of terrigenous sediment. The uppermost bed of ostracode-rich biomicrite, bed 9A, has been interpreted as the maximum flooding surface because: (1) carbonate muds are characteristic of low energy and distal environments, commonly in the deepest settings, where terrigenous material is sparse and skeletal remains concentrated; (2) the bed is overlain abruptly by a thick bed of red mudstone that represents sustained terrigenous supply and is attributed to the highstand systems tract, with readvance of marginal systems. The red mudstone is inferred to represent low-energy lake-margin deposits that mark the final regressive phase of the Scots Bay Lake (R2). The presence of fish material in the red mudstone facies supports this interpretation. Fine- to medium-grained sandstone fluvial facies were deposited during the subsequent lowstand. The interbedded red siltstone, red mudstone, and mottled siltstone facies within the lowstand fluvial facies have been interpreted as floodplain deposits that represent intrinsic channel-forming events rather than changes in lake level.

General statements that can be made regarding this stacking pattern are:

1. Basal sandstone, green sandstone, vertebrate-bearing sandstone and mottled siltstone facies are associated with the transgressive systems tract.
2. The top of the ostracode-rich biomicrite defines the maximum flooding surface and end of the transgressive systems tract.
3. Red mudstone is associated with the highstand systems tract and regression.
4. Nodular limestone and fluvial facies are associated with the lowstand.
5. The Scots Bay Lake underwent one first-order transgressive-regressive cycle and multiple second-order transgressive-regressive cycles.

7.2 Local correlation

Although the top of the North Mountain Basalt is the intuitive choice of datum for correlating the section, this is not a consistent surface. A regional stratigraphic datum is located at the consistent topographic baseline established after first-order accommodation – cracks, fissures, and depressions in the surface of the basalt – was filled (Fig. 33).

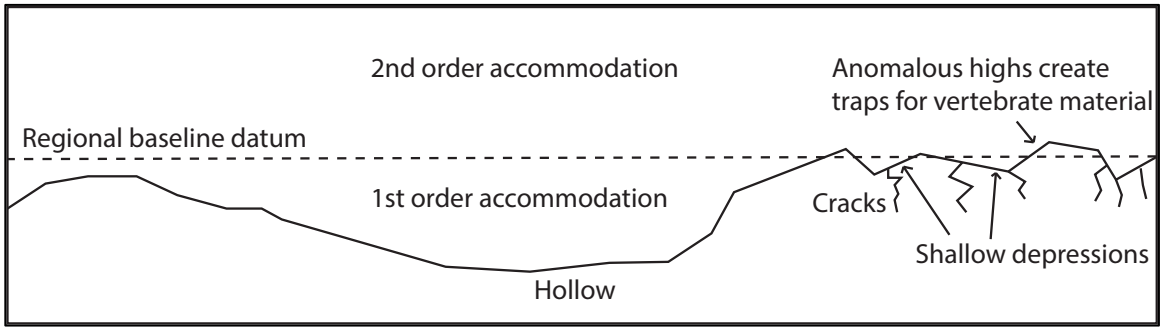

Figure 33: Regional baseline datum represents the boundary between 1st order (local) and 2nd order (regional) accommodation.

The regional baseline datum probably corresponds to the contact between the basal sandstone and vertebrate-bearing sandstone, as well as the top of the nodular limestone (Fig. 34).

Correlation of the measured sections recorded in fall 2013 and Tanner's section from 1996 reveals that both record a localized depression ~2.5 m deep in the surface of the basalt filled by green sandstone and mudstone, based particularly on correlation of limestone beds (Fig. 35). The topography of the basalt is important to consider because shallow ponds would have developed within hollows on the uneven surface. Since these ponds are local features, they would have formed components at various stages of both regional depositional models presented later in this chapter.

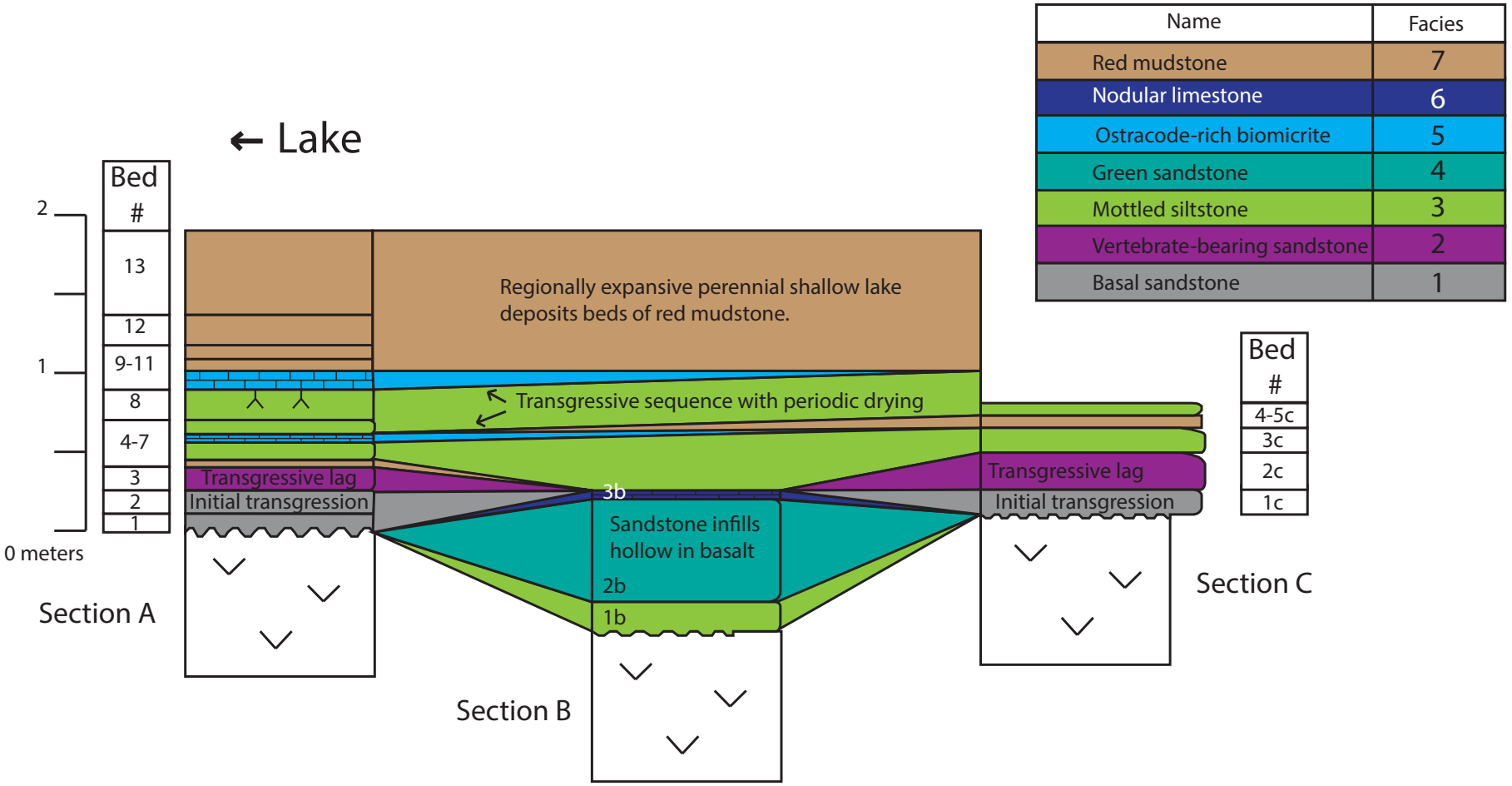

Figure 34: Correlation of sections A-C of the Scots Bay Member at Wasson Bluff.

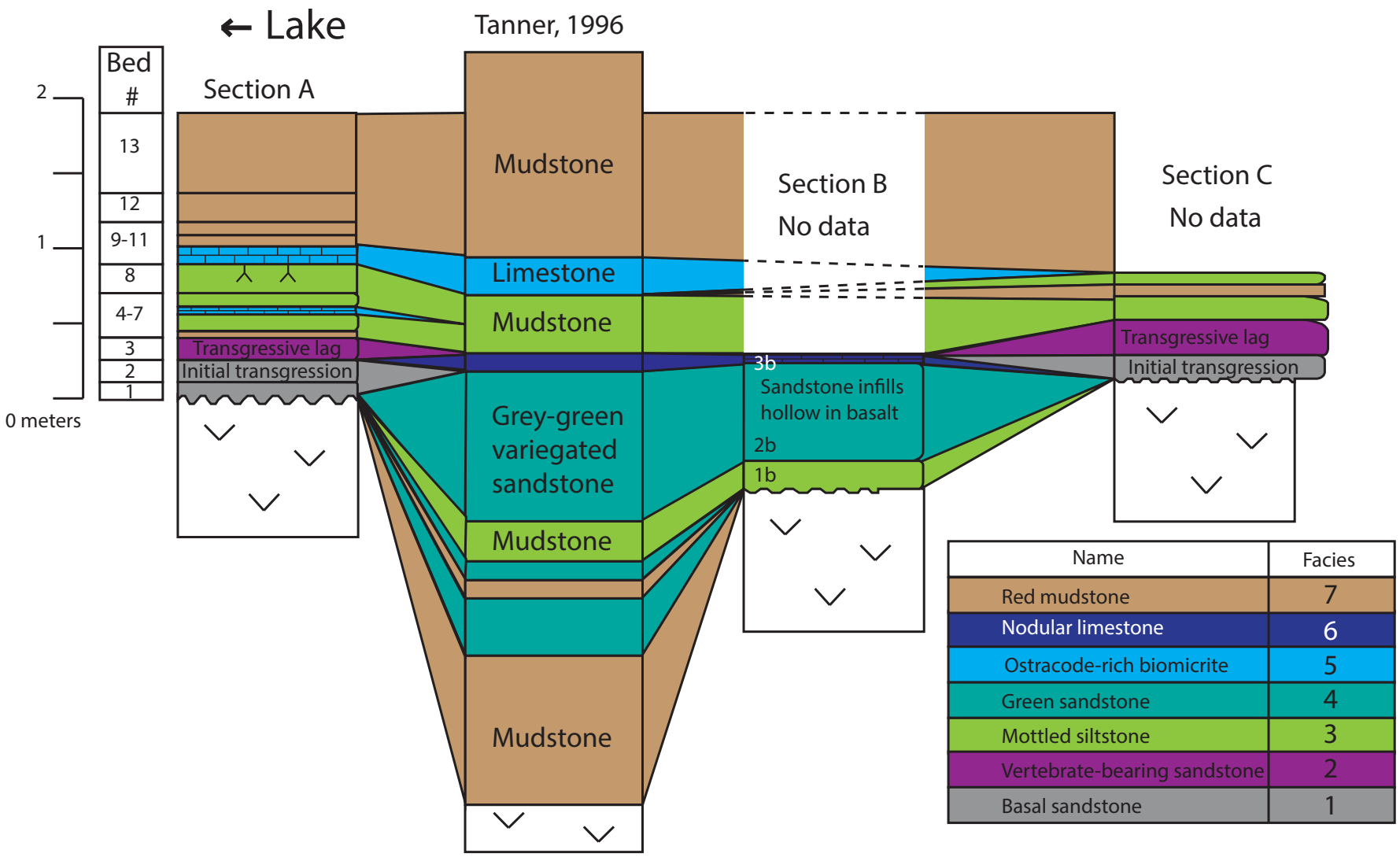

Figure 35: Correlation of sections A-C and modified section from Tanner, 1996.

Hollows and the cracks and fissures in the surface of the basalt would have been the first accommodation to be filled with sediment during lacustrine transgression. It may be assumed that the ponds that filled hollows in the basalt would have been poorly drained due to the low permeability of the crystalline basalt. During regression, the sediment filling the hollows would have remained saturated with water longer than the average basal sandstone atop the basalt (Fig. 36). Prolonged water saturation in the relatively arid, evaporative setting of the Fundy Basin might have raised the level of dissolved solids in the brackish water in the hollow. In the final drying phases of the isolated ponds, playa environments would have formed. Nodular limestone facies with desiccation fabrics generated in the playa environment would have developed. These lithologies and their stacking pattern are consistent with the findings of this study at Wasson Bluff: the green sandstone of Facies 6 is overlain by nodular limestone of Facies 7 (Fig. 5-6). The green sandstone and basal sandstone are both medium-grained sandstone and were likely deposited during the same transgressive event. However, it is possible that the very fine-grained sand at the base of cracks in the basal sandstone is of eolian origin (Table 3).

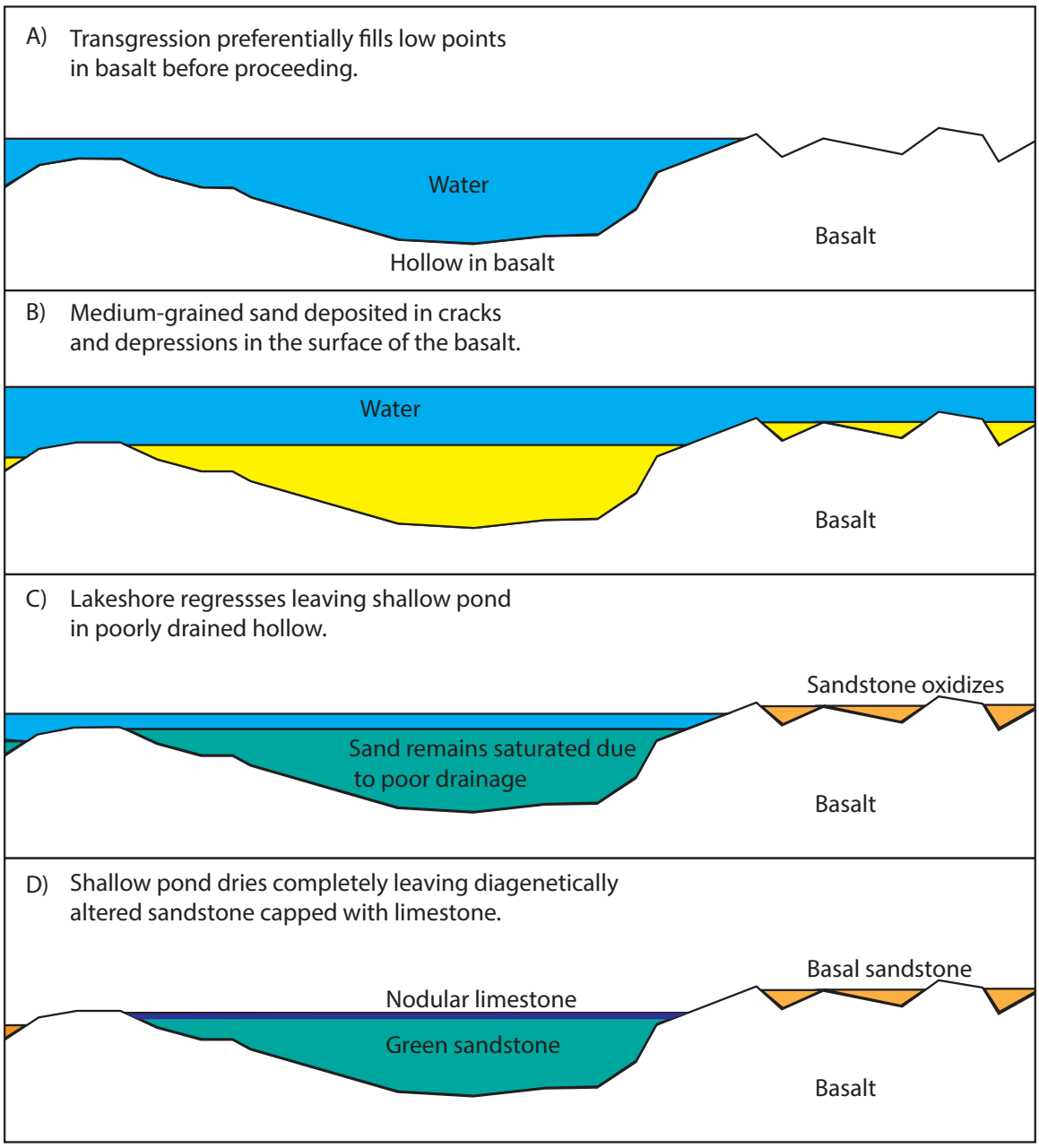

Figure 36: Simplified schematic model of ponding in hollows along the surface of the basalt.

A modern analogue for localized ponding within poorly drained basalt hollows is the isolated ponding along the shore of Lake Turkana in modern Kenya. Lake Turkana is a rift-valley lake that has formed on a sequence of basalts. The Kenyan Rift Valley that hosts Lake Turkana has a hot and dry climate with a strongly seasonal water budget. Turkana is the world's largest desert lake. The connectivity

of the small ponds dotted across the volcanic terrace close to the shoreline is a function of the regional water budget. In years with more water the ponds grow and join together to form larger water bodies. In years with less water the connectivity of the ponds decreases. During prolonged lowstands, smaller ponds dry up completely and leave a patch of evaporites in their hollow (Fig. 37-38).

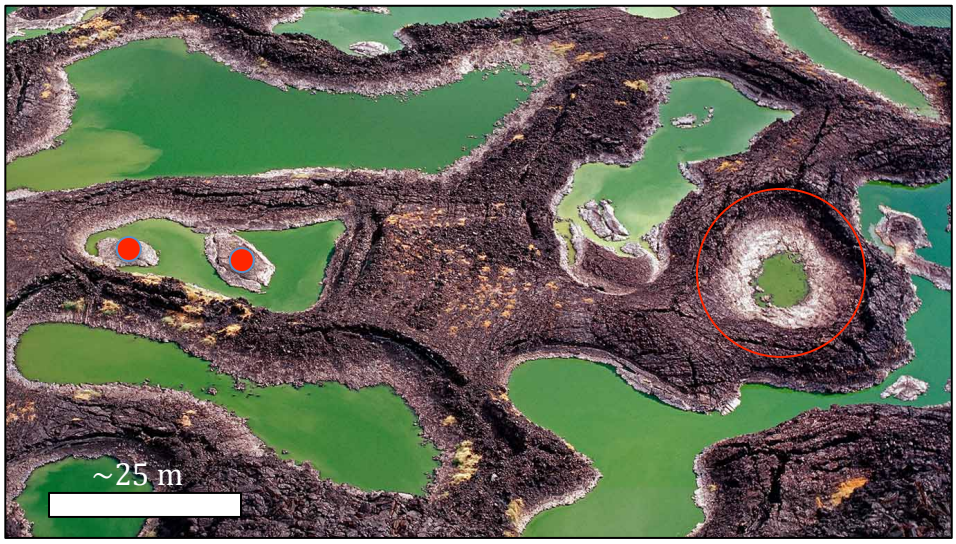

Figure 37: Isolated ponds infilling depressions in the surface of basalt near Lake Turkana, Africa. Photo taken in September 2013 (Wikipedia, 2013).

Figure 38: Satellite photo of same ponds as Figure 37, image taken in 2014 (Google Earth, 2014).

Figures 37 and 38 are photos of the same area of isolated ponds infilling depressions in the surface of the basalt along the south coast of Lake Turkana. The islands of the boot-shaped pool (highlighted by red dots) provide reference points for comparison of the two images. The photos were taken approximately a year apart, judging by the photographer's credit and satellite date (Wikipedia, 2013; Google Earth, 2014). Over that time a pool ~5 m wide dried completely, leaving a white deposit of likely evaporite-rich sediment (red circle on Fig. 37-38). With mean potential evaporation of ~3000 mm/yr and mean annual precipitation reaching only ~200 mm/yr, the drying of shoreline pools is observed annually along the south coast of Lake Turkana (Garcin et al., 2012). The same would have been true when the lowermost Scots Bay Member was deposited. The anomalous 1.4 m lensoid bed of green sandstone capped by nodular limestone in section B is likely the product of local ponding and desiccation.

7.3 Attempted regional correlation

A regionally consistent datum is the maximum flooding surface of the Scots Bay Lake that corresponds to the top of the uppermost ostracode-bearing layer. This surface is laterally consistent over a broad area, possibly the entire basin. The maximum flooding surface was used to correlate the sections from the Blomidon Peninsula recorded by Hassan (2010) with the sections from Wasson Bluff (Fig. 39). The correlation among Hassan's sections is the same as the correlation he published in his thesis, Figure 39 simply links his work with that of this study. Detailed lithological information summarizing Hassan's findings is provided in the annotated regional correlation in Figure 40. Flattened on the maximum flooding surface, the section deepens towards the center of the basin with the ostracode-bearing layer thinning towards the sides. This is consistent with the expected morphology of a large lake body.

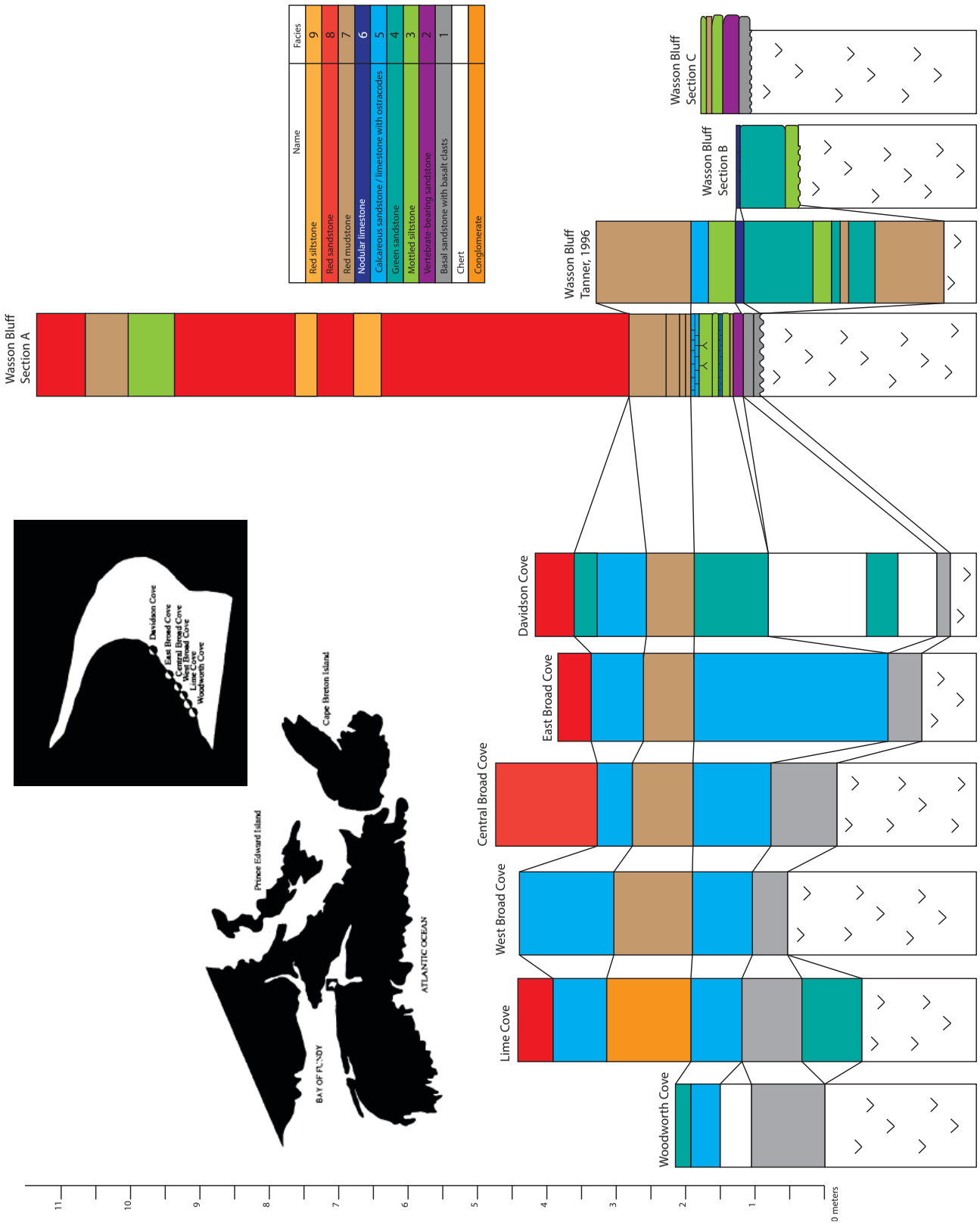

Figure 39: Attempted regional correlation conjoining correlation of Hassan (2010) with sections A-C.

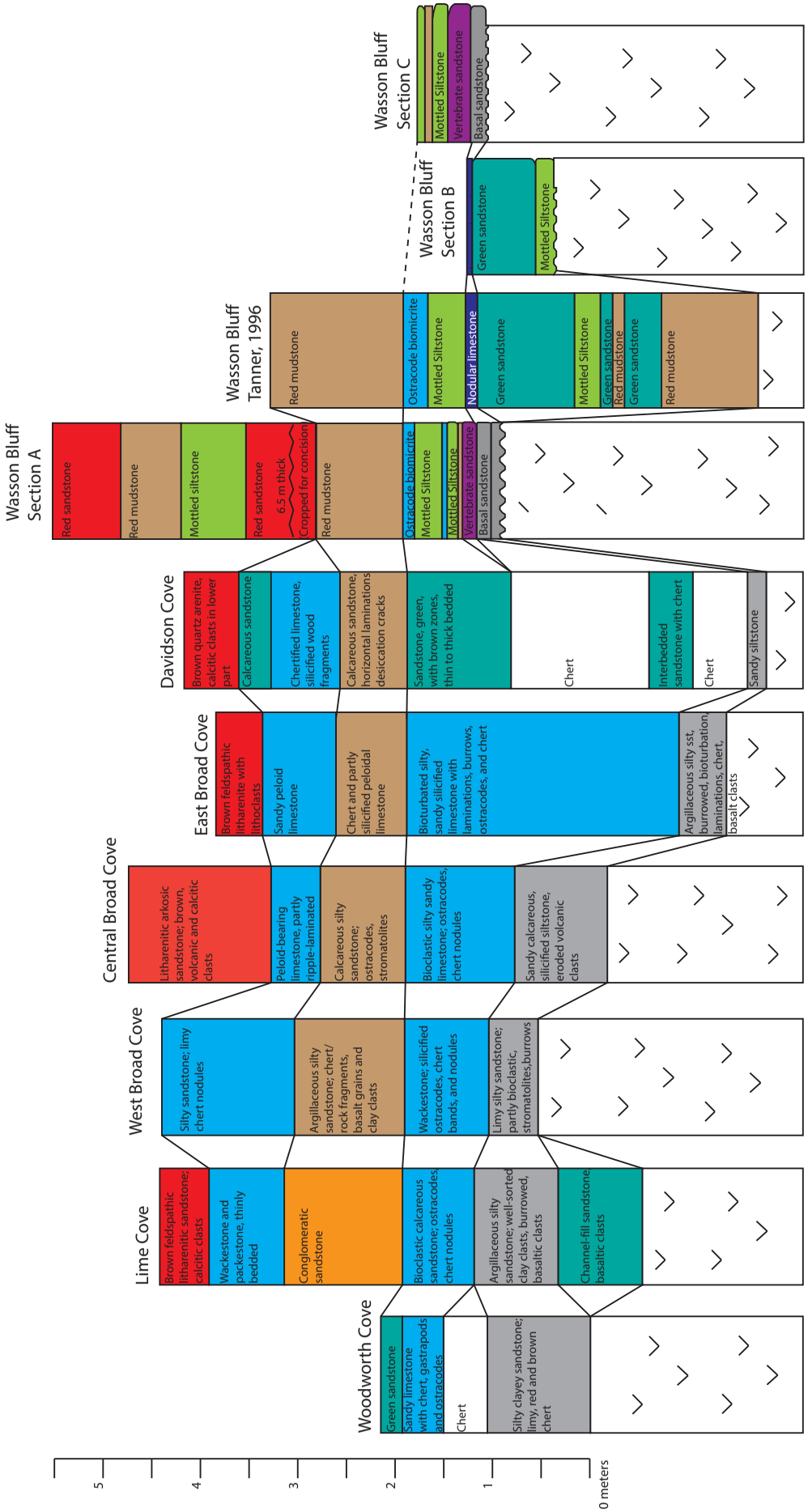

Figure 40: Attempted regional correlation with summary of outcrop lithology (modified from Hassan, 2010).

7.4 Shallow lake model

A shallow lake model proposes that the Scots Bay Member was deposited in a broad shallow lake that covered the base of the rift valley. In the early stages of rifting of the Fundy Basin half-graben, the rift valley would have been a long and narrow regional low that formed the outlet of the regional watershed. If enough water was available, a broad, shallow lake may have promoted an aquatic fauna that prospered in this nutrient-rich environment. Rocky, irregular coastlines provide shelter and habitat for a variety of fish, and it is possible that fish were exceptionally abundant in the area of the rocky shore at Wasson Bluff, contributing to the abundance of bone material found (Ferreira et al., 2001). A condensed section of disarticulated bone and scale material would have developed on the sandy bottom of the lake as wave action, aquatic predators, and wading terrestrial scavengers broke apart the remains of naturally dying aquatic vertebrates, which would have been preserved as a transgressive lag deposit at the base of the transgressive systems tract (Fig. 32). Shoreline regressions would eventually transition the lake into a playa lake facies with abundant oxidation and multiple desiccation events.

7.5 Deep lake model

A deep lake model proposes that the Scots Bay Member was deposited in shallow coves of a large, deep rift valley lake. Other outcrops of the McCoy Brook Formation represent strata from the side of the Triassic rift valley system. Large talus slopes and large angular basalt clasts within the fluvial and eolian successions of the McCoy Brook Formation at Wasson Bluff suggest that these outcrops were near cliff scarps (Tanner and Hubert, 1992). This implies that the “fish bed”

represents a nearshore environment. The maximum thickness of lacustrine strata deposited in Scots Bay Lake is unknown since the strata have either been eroded or underlie the Bay of Fundy.

Modern rift valley lakes are deep. Lake Turkana, for instance, has a maximum depth of approximately 109 m, and an average depth of 30.2 m (Johnson and Odada, 1996). An interesting characteristic of deep alkaline lakes is that they have vertical stratification in the water column. Temperature and dissolved substances cause density differences in the water that stratify the lake in chemically distinct zones (Boehrer et al., 2008). The upper layer of the water column, called the epilimnion, is oxygenated, whereas the lower layer of the lake, called the hypolimnion, may be anoxic. The most decisive factor for the thickness of the epilimnion is wind, and high wind events can cause partial homogenization of the water body. This overturning of the lake can cause catastrophic fish kill events. Malenda et al. (2012) proposed that this fish kill mechanism was responsible for prominent fish-part conglomerates of the Triassic Lockatong Formation of the Newark Supergroup (Fig. 41a).

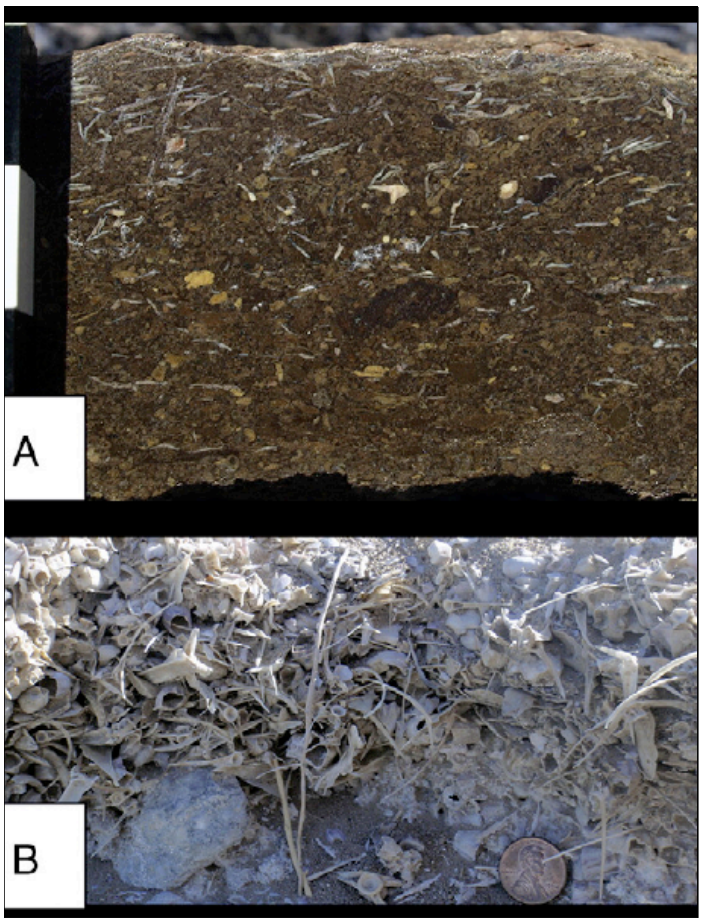

Figure 41: a) Fish-part conglomerate from the Triassic Lockatong Formation of the Newark Supergroup; b) condensed section of fish material along the shoreline of the Salton Sea (modified from Malenda et al., 2012).

The Salton Sea is a modern hypersaline lacustrine environment with a strong association between storm events and mass fish kills. The hypolimnion is supersaturated with respect to calcite, gypsum, celesite, hydroxyapatite, and fluorapatite, and is oxygen-depleted (Malenda et al., 2012). During high wind events the lake overturns and the eplimnion becomes oxygen depleted as well, causing a mass fish kill due to hypoxia. The carcasses of fish bloat with gases and float to the surface. The bodies are driven ashore by wind and wave action, and collect in condensed sections along the high-water mark where they are disarticulated by

birds and terrestrial predators (Fig. 41b). Malenda et al. (2012) linked this taphonomic process to the vertebrate-rich Triassic Lockatong Formation strandline deposits. The fish-part conglomerates of the Lockatong Formation have similar proportions of fish material to the condensed sections of fish material along the shore of the Salton Sea, and phytosaur teeth are found in the Triassic fossil assemblage, indicating the presence of terrestrial predators. Intraformational sandstone and conglomerate facies associated with the fish-part conglomerate bed are evidence of high-energy storm events.

The vertebrate-bearing sandstone of Facies 2 meets the criteria for the taphofacies presented by Malenda et al. (2012). The fish material is in a clast-supported assemblage, teeth of terrestrial predators were found amongst the fish material, and the semi-arid climate (Olsen, 1981; Hubert and Mertz, 1980) implies that the Scots Bay Lake would have been alkaline and likely chemically stratified, if deep enough. However, no sedimentological evidence of high-energy storm events was observed in the Scots Bay Member at Wasson Bluff. Thus, the Scots Bay Member "fish bed" is provisionally interpreted as a transgressive lag at the base of the succession locally, although it may include material derived from fish kills in deeper parts of the lake.

8.0 Conclusion

The exposure of the Scots Bay Member at Wasson Bluff represents a deceptively complex stratigraphic section. Depressions in the surface of the basalt may be over 2.5 m deep and lack predictable geometries. Thus, below the regional baseline datum that represents drowning of an extensive, irregular basalt surface, the thickness and distribution of the Scots Bay Member is unpredictable.

Measured sections of the initial 10 m of strata overlying the North Mountain Basalt reveal nine facies: basal sandstone, vertebrate-bearing sandstone, mottled siltstone, green sandstone, ostracode-bearing biomicrite, nodular limestone, red mudstone, red sandstone, and red siltstone. The basal 1.9 m corresponds to the Scots Bay Member.

Facies associations help define the systems tracts of the lacustrine deposits of the Scots Bay Member. Above the regional baseline datum these tracts define the regional sequence stratigraphy and may be be laterally continuous basinwide. Medium-grained sandstones and mottled siltstone facies are associated with lakeshore transgression. The maximum flooding surface is defined as the top of ostracode-bearing beds, and the subsequent highstand is characterized by beds of red mudstone. Fluvial facies and isolated playa ponds that form a hard cap of nodular limestone are associated with dry periods during the lowstand systems tract. From these associations a lake-level curve may be inferred, which implies an overall first-order transgressive-regressive cycle of the Scots Bay Lake with multiple second-order sequences (Fig. 32).

The taphonomic mechanism that produced the vertebrate-bearing sandstone remains unknown. However it is probable that this bed represents a transgressive lag deposit and not a catastrophic fish kill event such as the one described by Malenda et al. (2012), although fish kills in deeper parts of the lake might have contributed skeletal material to the bed. A transgressive lag deposit is compatible with both the shallow and deep lake models for the regional water budget. The distribution of fish material is associated with basalt clasts that create traps for sediment around the level of the regional baseline datum. This vertebrate-rich deposit may be a laterally continuous strandline or an isolated occurrence associated with the hummocky basalt clasts at the fringe of the isolated playa pond that formed the nodular limestone. The microenvironments formed on top of the North Mountain Basalt during early deposition of the Scots Bay Member distinctly affected taphonomy.

References

Arp, Gernot, F. Bielert, V.E. Hoffmann, and T. Loffler. 2005. Paleoenvironmental significance of lacustrine stromatolites of the Arnstadt Formation ("Steinmergelkeuper", Upper Triassic, N-Germany). Facies, 51: 419-441.

Bell, W.A. 1958. Possibilities for occurrence of petroleum reservoirs in Nova Scotia. Nova Scotia Department of Mines Miscellaneous Publication; 177.

Blackburn, T.J., P.E. Olsen, S.A. Bowring, N.M. McLean, D.V. Kent, J. Puffer, G. McHone, E.T, Rasbury, and M. Et-Touhami. 2013. Zircon U-Pb Geochronology links the end-Triassic extinction with the Central Atlantic Magmatic Province. Science, 340, 6135: 941-945.

Boehrer, B., and M. Schultze. 2008. Stratification of lakes. Reviews of Geophysics, 46; 1-27.

Boggs, S. *Principles of Sedimentology and Stratigraphy – 5th edition*. University of Oregon. Pearson Education Inc: New Jersey, 2012.

Catuneanu, O., V. Abreu, j. Bhattacharya, M. Blum, R. Dalrymple, P. Eriksson, C. Fielding, W. Fisher, W. Galloway, M. Gibling, K. Giles, J. Holbrook, R. Jordon, C. Kendall, B. Marcurda, O. Martinsen, A. Miall, J. Neal, D. Nummedal, L. Pomar, H. Posamentier, B. Pratt, J. Sarg, K. Shanley, R. Steel, A. Strasser, M. Tucker, and C. Winker. 2009. Towards the standardization of sequence stratigraphy. Elsevier: Earth-Science Reviews, 92; 1-33.

Cirilli, S., A. Marzoli, L. Tanner, H. Bertrand, N. Buratti, F. Jourdan, G. Bellieni, D. Kontak, and P.R. Renne. 2009. Latest Triassic onset of the Central Atlantic Magmatic Province (CAMP) volcanism in the Fundy Basin (Nova Scotia): New stratigraphic constraints. Elsevier, Earth and Planetary Science Letters, 286, 3-4; 514-525.

Coleman, J. 1966. Ecological changes in a massive fresh-water clay sequence. Transections – Gulf Coast Association of Geological Societies, 16; 159-174.

Dennar, C.I. 2012. Vegetation influence in strengthening channel banks in the Pennsylvanian Joggins Formation, Nova Scotia. HBsc Thesis, Dept. of Earth Sciences, Dalhousie University.

Dott, R.H. 1964. Wacke, greywacke, and matrix – What approach to immature sandstone classification. Jour. Sed. Petrology, 34; 625-632.

Fedak, T. 2006. Description and evolutionary significance of the sauropodomorph dinosaurs from the Early Jurassic (Hettangian) McCoy Brook Formation. Ph. D. thesis, Dalhousie University, Halifax, N.S.

Fedak, T., Z. Prescott, H.D. Sues. 2014. Identification of new vertebrate diversity within the Scots Bay Member of the Early Jurassic McCoy Brook Formation, Wasson Bluff, Cumberland County, Nova Scotia. Atlantic Geoscience Colloquium abstract.

Ferreira, C., E. Gonçalves, and R. Coutinho. 2001. Community structure of fishes and habitat complexity on a tropical rocky shore. Environmental Biology of Fishes, 61; 353-369.

Folk, Robert. 1959. Practical petrographic classification of limestones. American Association of Petroleum Geologists Bulletin, 43: 1-38.

Garin, Y., D. Melnick, M.R. Strecher, D. Olago, and J. Tiercelin. 2012. East African mid-Holocene wet-dry transition recorded in palaeo-shorelines of Lake Turkana, northern Kenya Rift. Elsevier: Earth and Planetary Science Letters, 331-332; 322-334.

Google Earth. 2014. "Lake Turkana." Web. Retrieved from: http://maps.google.ca/maps?q=lake+turkana&ie=UTF-8&ei=qPclU_P1D7CQyQG7tIG4Bw&ved=0CAoQ_AUoAg.

Government of Canada. 2013. "2013 Tide Tables - Tides, Currents, and Water Levels." Web. Retrieved from tides.gc.ca/eng/data/predictions/2013.

Hassan, S.H. 2000. Sedimentology and paleontology of the Lower Jurassic Scots Bay Formation, Bay of Fundy, Nova Scotia, Canada. MSc thesis, Dept. of Geology, Acadia University; 1-192.

Hubert, J.F., and K.A. Mertz. 1980. Eolian dune field of Late Triassic age, Fundy Basin, Nova Scotia. Geology, 8; 516-519.

Hubert, J.F., and K.A. Mertz. 1984. Eolian sandstones in the Upper Triassic-Lower Jurassic red beds of the Fundy Basin, Nova Scotia. Journal of Sedimentary Petrology, 54, 3; 798-810.

Hurley, I.A., R. Lockridge-Mueller, K.A. Dunne, E. J. Schmidt, M. Friedmas, R.K. Ho, V.E. Prince, Z. Yang, M.G. Thomas, M.I. Coates. 2007. "A new time-scale for ray-finned fish evolution." The Royal Society Proceeding B: Biological Sciences, 274, 1609: 489-498.

Ingersoll, R.V., T.F. Bullard, R.L. Ford, J.P. Grimm, J.D. Pickle, and S.W. Sares. 1984. The effect of grain size on detrital modes: a test of the Gazzi-Dickinson point-counting method. Journal of Sedimentary Petrology, 54, 1; 103-116.

Janvier, P. 1996. *Early Vertebrates*. New York: Oxford Science Publications.

Johnson, I, and Odada, E. 1996. *Limnology, Climatology and Paleoclimatology of the East African Lakes.* Amsterdam: Overseas Publishers Association.

Kotpal, R.L. 2010. *Modern Textbook of Zoology: Vertebrates.* New Dehli, India: Rastogi Publications.

Leleu, S., and A.J. Hartley. 2010. Controls on the stratigraphic development of the Triassic Fundy Basin, Nova Scotia: implications for the tectonostratigraphic evolution of Triassic Atlantic rift basin. Journal of the Geological Society, London, 167; 437-454.

Leleu, S., X.M.T. Van Lanen, and A.J. Hartley. 2010. Controls on the architecture of a Triassic sandy fluvial system, Wolfville Formation, Fundy Basin, Nova Scotia, Canada: Implications for the interpretation and correlation of ancient fluvial successions. Journal of Sedimentary Research, 80; 867-883.

Luttrell, G.W. 1989. Stratigraphic nomenclature of the Newark Supergroup of eastern North America. United States Geological Survey Bulletin 1572, Washington; 27-28.

Maisey, J.G. 1996. *Discovering Fossil Fishes*. New York: Nevraumont Publishing Company.

Malenda, F., E. Simpson, M. Szajna, D. Fillmore, E. Heness, E. Kraal, and J. Wilk. 2012. Taphonomy of lacustrine shoreline fish-part conglomerates in the Lockatong Formation (Collegeville, Penn., USA): Toward the catastrophoc fish kills in the rock record. Paleogeography, Paleoclimatology, Paleoecology 313-314; 234-245.

Mertz, K.A., J.F. Hubert. 1990. Cycles in sand-flat sandstone and playa-lacustrine mudstone in the Triassic-Jurassic Blomidon redbeds, Fundy rift basin, Nova Scotia: implications for tectonic and climatic controls. Canadian Earth Science, 27: 442-451.

Moore, R., C. Lalicker, and A. Fischer. 1952. *Invertebrate Fossils*. New York: McGraw-Hill Book Company.

Morton, Nicol. 2012. Inauguration of the GSSP for the Jurassic System. Episodes, 35, 2; 328-332.

Olsen, P.E. 1981. Comment and reply on 'Eolian dune field of Late Triassic age, Fundy Basin, Nova Scotia.' Geology, 9; 557-562.

Olsen, P.E. 1986. A 40-million-year lake record of Early Mesozoic orbital climatic forcing. Science, New Series, 234, 4778; 842-848.

Olsen, P.E., A.R. McCune, and K.S. Thomson. 1982. "Correlation of the Early Mesozoic Newark Supergroup by vertebrates, principally fishes." *American Journal of Science*, 282; 1-44.

Olsen, P.E., and A.R. McCune. 1991. Morphology of the *Semionotus elegans* species group from the Early Jurassic part of the Newark Supergroup of eastern North America with comments on the family semionotidae (neopterygii). Journal of Vertebrate Paleontology, 11, 3; 269-292.

Olsen, P.E. and P.J.W. Gore. 1989. Tectonic, Depositional, and Paleoecological History of Early Mesozoic Rift Basin, Eastern North America. Field Trip Guidebook T351, 28th International Geological Congress. Gulf, North Carolina, USA to Parrsboro, Nova Scotia, Canada, July 20-30 1989.

Olsen, P.E., J.H. Whiteside, and T. Fedak. 2005. Triassic-Jurassic faunal and floral transition in the Fundy Basin, Nova Scotia. North American Paleontology Conference, Halifax, NS; 1-53.

Olsen, P.E., and R.W. Schlische. 1990. Transtensional arm of the early Mesozoic Fundy rift basin: Penecontemporaneous faulting and sedimentation. Geology, 18; 695-698.

Prescott, Z.M. 2010. Analysis of the vertebrate community represented in the early Mesozoic fish bed of Wasson Bluff. Unpublished B.Sc. honours thesis, Department of Biology, Dalhousie University; 1-48.

Schlische, R.W., and R.V. Ackermann. 1994. Kinematic significance of sediment-filled fissures in the North Mountain Basalt, Fundy rift basin, Nova Scotia, Canada. Journal of Structural Geology, 17, 7; 987-996.

Tanner, L. 1994. Distribution and origin of clay minerals in the Lower Jurassic McCoy Brook Formation, Minas Basin, Nova Scotia. Sediment. Geol., 92; 229-239.

Tanner, L. 1996. Formal definition of the Lower Jurassic McCoy Brook Formation, Fundy rift basin, eastern Canada. Atlantic Geology, 32; 127-135.

Tanner, L.H., and Hubert, J.F. 1992. Depositional environments, palaeogeography and palaeoclimatology of the Lower Jurassic McCoy Brook Formation, Fundy basin, Nova Scotia. Palaeogeogeography, Palaeoclimatology, Palaeoecology, 96: 261-280.

Tunbridge, I. 1984. Facies model for a sandy ephemeral stream and clay playa complex; the Middle Devonian Trentishoe Formation of North Devon, U.K. Sedimentology, 31; 697-715.

Van Drecht, L. 2014. Sedimentology and paleoenvironment of an Early Jurassic dinosaur bone bed at Wasson Bluff, Parrsboro, NS. Unpublished B.Sc. honours thesis, Department of Earth Sciences, Dalhousie University; 1-?.

Wikipedia, the free encyclopedia. 2013. "Portal: Geography of Kenya/selected picture." Web. Accessed February 15, 2014. Retrieved from: http://en.wikipedia.org/wiki/Portal:Geography_of_Kenya/Selected_picture.

Appendix A – Safety and access

Safety concerns must be noted regarding the field area at Wasson Bluff. Visitors to the site must prepare themselves with the proper equipment and knowledge including hard hats, sturdy footwear, first-aid kit, sun-hat, water, and tide chart.

Rock-fall is a serious threat at Wasson Bluff. Due to the relatively unconsolidated nature of the deeply weathered basalt and fissile sediments near the contact, the cliffs are highly unstable. Evidence of recent rock-falls may be observed along the beach in the form of large fans of angular boulders. These boulder fields should be avoided when possible since they represent areas of recent instability. Hard hats should be worn at all times when working within 10 m of the cliff.

Cell reception is poor on the beach. Be prepared to deal with emergencies by bringing a stocked first-aid kit. Always visit Wasson Bluff with a buddy; geology is more fun in groups!

Taking samples is strictly prohibited since Wasson Bluff is a Special Protected area, but you can get a permit for research work. Do not bring a rock hammer lest you be tempted to use it.

Know the tide times; the outcrop is underwater for approximately one hour +/- high stand. Tide charts are available online through the Government of Canada website

or in hard copy at most information and tourism offices around the province (Gov. of Canada, 2013).

There are two points of access to the beach: (1) the gorge, and (2) the beach.

(1) The first is via a small gorge which leads directly to the field area. Take Swan Creek Road past the Fundy Geological Museum and keep left, driving approximately eight kilometers until you see a sign for Two Islands. Slow down and keep your eyes peeled for mailbox #2031 on your right hand side. There is parking for two cars in a gravel pit on the side of the road. Walk through the field towards the coastline, being sure to close the gate behind you, and follow the path through the woods to a small set of stairs that will take you over a barbed wire fence. You will now be at the top of the gorge. Keep right and carefully traverse your way down the slope. The slope is very steep and slick, use extreme caution while walking down. Keep space between people in case of accidental rock-fall. Once down at the beach take a left and you will see the contact with the North Mountain Basalt and the beginning of the section studied by this thesis.

(2) The second approach is via the beach. Follow the same instructions as approach (1) but continue driving until you pass Spring Tide Lane on your left. Take your next right. This road will lead you to parking by the beach. Once on the beach walk west for approximately a kilometer and a half to arrive at the thesis section.

Appendix B – Field notes

Table 9: Table of grain size abbreviations.

Grain size	Abbreviation
Clay	c
Silt	s
Very fine-grained sand	vf
Fine-grained sand	f
Medium-grained sand	m

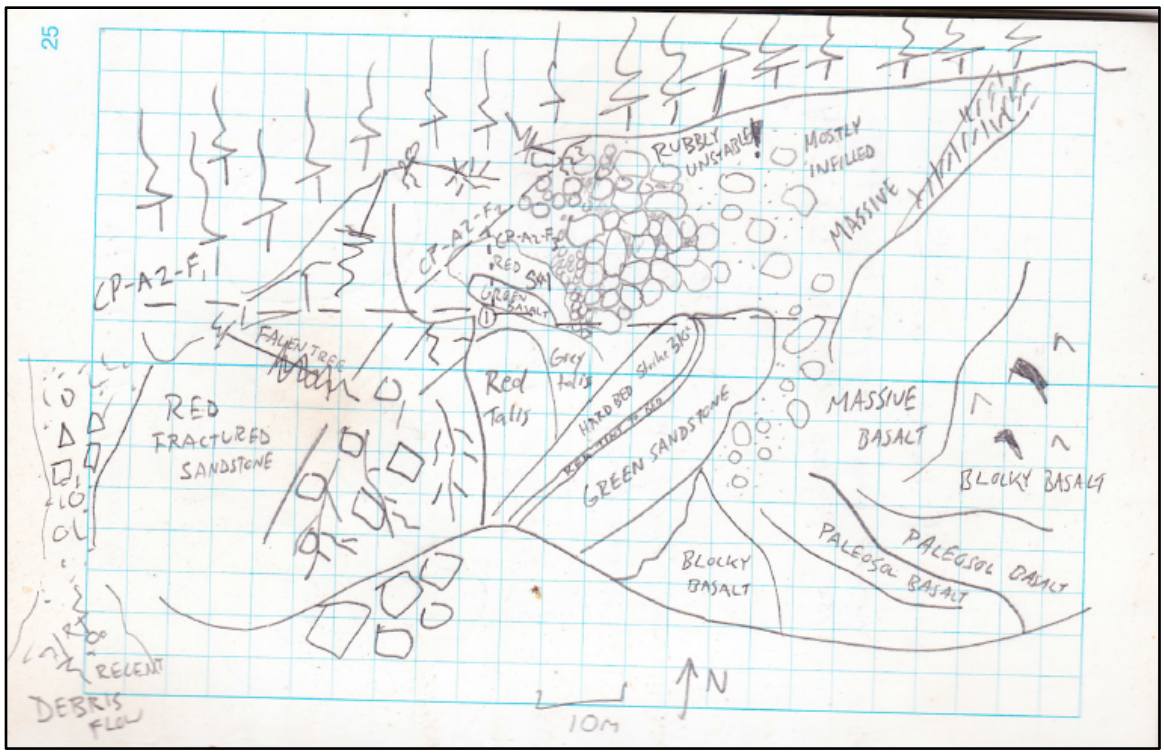

Figure 42: Field sketch of "fish bed" at Wasson Bluff.

Bed #	Field bed #	Unit thickness (m)	Corrected thickness	Fresh colour	Weathered colour
1A	CP-01-01	0.4	0.118547431	-	Brown, green lithic
2A	CP-01-02	0.5	0.148184289	Red-brown	Red-grey
3A	CP-01-03-01	0.5	0.148184289	Grey-blue	-
4A	CP-01-03-02	0.15	0.044455287	Red-brown/grey	-
5A	CP-01-03-03	0.38	0.11262006	Buff green	-
6A	CP-01-03-04	0.17	0.050382658	Green w/ red cracks	-
7A	CP-01-03-05	0.3	0.088910574	Green w/ brown	-
8A	CP-01-03-06	0.65	0.192639576	Red > green	-
9A	CP-01-03-07	0.4	0.118547431	Green w/ diffuse red	-
10A	CP-01-03-08	0.25	0.074092145	Green w/ red cracks	Red-brown
11A	CP-01-03-09	0.3	0.088910574	Red	Red-brown
12A	CP-01-03-10	0.65	0.192639576	Red w/ green mottle	-
13A	CP-01-03-11	1.8	0.533463442	Red w/ green mottle	-
14A	CP-01-04	3.75	1.11138217	Red-orange	Red-brown
15A	CP-01-05	1.4	0.41491601	Red-orange	Red-brown
16A	CP-01-06	1.55	0.459371297	Red-brown	Red-orange
17A	CP-01-07	2.8	0.82983202	Orange-brown	Brown
18A	CP-01-08	1	0.296368579	Orange-brown	Brown
19A	CP-01-09	0.9	0.266731721	Orange-brown	Orange-brown
19A	CP-04-01	0.6	0.177821147	Red-orange	-
20A	CP-04-02	1.35	0.400097581	Red-orange	-
21A	CP-04-03	1.27	0.376388095	Red-orange	-
22A	CP-04-04	0.44	0.130402175	Red-orange	-
23A	CP-04-05	1.19	0.352678609	Red-orange	-
24A	CP-04-06	1.05	0.311187008	Red-orange	-
25A	CP-04-07	2.5	0.740921447	Red-orange	-
26A	CP-04-08	2.3	0.681647731	Red-orange	Red-brown-grey
27A	CP-04-09	0.65	0.192639576	Red w/ green mottle	-
28A	CP-04-10	0.65	0.192639576	Red w/ green mottle	-
29A	CP-04-11	0.4	0.118547431	Red w/ green mottle	-
30A	CP-04-12	0.5	0.148184289	Red w/ green mottle	-
31A	CP-04-13	0.1	0.029636858	Grey-green	-
32A	CP-04-14	1.3	0.385279152	Red-orange	-
33A	CP-04-15	0.8	0.237094863	Red-orange	-
34A	CP-04-16	2.3	0.681647731	Red-orange	Dull red-brown
1B	CP-02-01	0.4	-	-	Pale purple/blue-grey
2B	CP-02-02	1.4	-	Green (wet)	Pale green
3B	CP-02-03	0.12	-	Purple-grey	Pale red-grey

Bed #	Field bed #	Grains			
		Size	Types	Sorting	Roundness
1A	CP-01-01	f-m	Qtz, basalt lithics	Moderate - Well	Well rounded
2A	CP-01-02	f-m	Qz, mica	Well sorted	Well rounded
3A	CP-01-03-01	vf	-	-	-
4A	CP-01-03-02	s	-	-	-
5A	CP-01-03-03	vf	-	-	-
6A	CP-01-03-04	Carbonate	Cabonate cement?	-	-
7A	CP-01-03-05	vf	-	-	-
8A	CP-01-03-06	s	-	-	-
9A	CP-01-03-07	Carbonate	Carbonate cement?	-	-
10A	CP-01-03-08	s (m)	-	-	-
11A	CP-01-03-09	s	-	-	-
12A	CP-01-03-10	s	-	-	-
13A	CP-01-03-11	s	-	-	-
14A	CP-01-04	m, m, f	Qtz, mica, black grains	Well sorted	Well rounded
15A	CP-01-05	f, m, f	Qtz, mica, minor lithic	Well sorted	Well rounded
16A	CP-01-06	f	Qtz, mica, lithics	Well sorted	Well rounded
17A	CP-01-07	m	Qtz, lithics	Well sorted	Well rounded
18A	CP-01-08	f	Qtz	Well sorted	Well rounded
19A	CP-01-09	f	Qtz	Well sorted	Well rounded
19A	CP-04-01	f	Qtz, mica, black lithics	Well sorted	Well rounded
20A	CP-04-02	vf, vf, s	Qtz, mica	Well sorted	Well rounded
21A	CP-04-03	vf, f, f	Qtz, mica, green lithic	Well sorted	Well rounded
22A	CP-04-04	f-m, f-vf	Qtz, mica, black lithics	Well sorted	Well rounded
23A	CP-04-05	vf	Qtz, lithics	Well sorted	Well rounded
24A	CP-04-06	m	Qtz, lithics	Well sorted	Well rounded
25A	CP-04-07	f-m	Qtz, lithics, mica	Well sorted	Well rounded
26A	CP-04-08	f-m	Qtz, lithics, mica	Well sorted	Well rounded
27A	CP-04-09	c	-	Well? too fine	Well? too fine
28A	CP-04-10	vf	Qtz, mica	Well sorted	Well rounded
29A	CP-04-11	c	-	-	-
30A	CP-04-12	c	-	-	-
31A	CP-04-13	f	Qtz (no mica)	Well sorted	Well rounded
32A	CP-04-14	c	-	-	-
33A	CP-04-15	c (vf)	-	-	-
34A	CP-04-16	m	Qtz, mica (<5%)	Well sorted	Well rounded
1B	CP-02-01	f	Mica, qtz, lithics	Well sorted	Round
2B	CP-02-02	m	Qtz, black lithics, mica	Well sorted	Subround
3B	CP-02-03	vf	Qtz, calcite, mica	Well sorted	-

Bed #	Field bed #	Basal bed contact		Sedimentary structures
		Abrupt/Gradational	Style	-
1A	CP-01-01	Abrupt	Erosional	Trough crossbeds?
2A	CP-01-02	Abrupt, planar	Erosional	-
3A	CP-01-03-01	Abrupt	Planar	-
4A	CP-01-03-02	Abrupt	Planar	-
5A	CP-01-03-03	Abrupt	Planar	Diffuse laminae
6A	CP-01-03-04	Abrupt	Planar	Diffuse laminae, cracks
7A	CP-01-03-05	Abrupt	Planar	-
8A	CP-01-03-06	Gradational	-	-
9A	CP-01-03-07	Abrupt	Planar	-
10A	CP-01-03-08	Abrupt	Planar	-
11A	CP-01-03-09	Gradational	Planar	-
12A	CP-01-03-10	Gradational	-	-
13A	CP-01-03-11			
14A	CP-01-04	Not seen	Not seen	Fining upwards scour fill
15A	CP-01-05	Abrupt	Planar (scours?)	Scours, concave up
16A	CP-01-06	Abrupt	Erosional, scour	Cross bedding, scours
17A	CP-01-07	Abrupt	Erosional, scour	
18A	CP-01-08	Abrupt	Erosional, scour	Cross bedding
19A	CP-01-09	Abrupt	Erosional	10-15cm cross sets
19A	CP-04-01	-	-	31cm x 5cm cross sets
20A	CP-04-02	Abrupt: fault trace 080°	Fault plane	
21A	CP-04-03	Gradational	Scour	20cm deep scour
22A	CP-04-04	Abrupt	-	Scour
23A	CP-04-05	Abrupt	Planar	
24A	CP-04-06	Gradational	Planar	Large scour perhaps?
25A	CP-04-07	Abrupt	Planar	
26A	CP-04-08	Abrupt	Planar	Stacked scours
27A	CP-04-09	Abrupt	Planar	
28A	CP-04-10	Gradational	Planar	Mottles taper at base
29A	CP-04-11	Gradational	Planar	
30A	CP-04-12	Gradational	Planar	Discontinuous bedding
31A	CP-04-13	Abrupt	Planar	Relatively thicker mottle
32A	CP-04-14	Abrupt	Planar	
33A	CP-04-15	Gradational	Planar	
34A	CP-04-16	Abrupt	Planar	Abundant scours
1B	CP-02-01	Abrupt	Erosional	Discontinuous layering
2B	CP-02-02	Abrupt	Planar	
3B	CP-02-03	Abrupt	Planar	Diffuse, planar bedding

Bed #	Field bed #	Bedding		Cement fizz?
		Thickness	Style	Minor fizz
1A	CP-01-01	None visible	-	No
2A	CP-01-02	10-15cm	Wavy, concave up surfaces	-
3A	CP-01-03-01	Thin laminations	Planar	-
4A	CP-01-03-02	Thin laminations	Planar	-
5A	CP-01-03-03	Thin, diffuse laminae	-	-
6A	CP-01-03-04	Discontinuous	-	-
7A	CP-01-03-05	Discontinuous laminae	Diffuse	-
8A	CP-01-03-06	Discontinuous laminae	Diffuse	Yes, strong
9A	CP-01-03-07	-	-	-
10A	CP-01-03-08	-	-	-
11A	CP-01-03-09	-	-	-
12A	CP-01-03-10	-	-	-
13A	CP-01-03-11	-	-	-
14A	CP-01-04	Discontinuous laminae	-	No
15A	CP-01-05	-	Wavy, cross stratified	No
16A	CP-01-06	-	Wavy	No
17A	CP-01-07	-	-	-
18A	CP-01-08	~10cm	Planar	-
19A	CP-01-09	2-10cm	Planar	-
19A	CP-04-01	1cm	Planar	-
20A	CP-04-02	1mm, some <0.5mm	Planar	-
21A	CP-04-03	Massive scour	-	-
22A	CP-04-04	2mm laminae, scour	-	-
23A	CP-04-05	Thin laminations, fissile	Planar	-
24A	CP-04-06	Massive	-	-
25A	CP-04-07	1cm grading to massive	Planar	-
26A	CP-04-08	2-5cm grading to massive	Planar	-
27A	CP-04-09	Discontinuous 2mm	-	-
28A	CP-04-10	2mm w/ massive mottle	Planar	-
29A	CP-04-11	2mm	-	-
30A	CP-04-12	2mm	Planar	-
31A	CP-04-13	Massive	Planar	-
32A	CP-04-14	Fissile	Planar, discontinuous	-
33A	CP-04-15	Fissile	Discontinuous	-
34A	CP-04-16	2-10cm w/ larger scour fill	-	-
1B	CP-02-01	0.5cm	Discontinuous	-
2B	CP-02-02	20-30cm	-	Yes, strong
3B	CP-02-03	0.5-2cm (diffuse)	Wavy	

Bed #	Field bed #	Fossils	Concretions	Other features
1A	CP-01-01	-	-	-
2A	CP-01-02	-	-	-
3A	CP-01-03-01	Teeth	-	-
4A	CP-01-03-02	-	-	-
5A	CP-01-03-03	-	-	-
6A	CP-01-03-04	-	-	-
7A	CP-01-03-05	-	-	-
8A	CP-01-03-06	-	-	-
9A	CP-01-03-07	Bone?	-	-
10A	CP-01-03-08	Bone	-	-
11A	CP-01-03-09	-	-	-
12A	CP-01-03-10	-	-	-
13A	CP-01-03-11	-	Nodules?	-
14A	CP-01-04	-	-	-
15A	CP-01-05	-	-	-
16A	CP-01-06	-	-	-
17A	CP-01-07	-	-	-
18A	CP-01-08	-	-	-
19A	CP-01-09	-	-	-
19A	CP-04-01	-	-	Fault striking 80˚
20A	CP-04-02	-	-	Fault at base
21A	CP-04-03	-	-	-
22A	CP-04-04	-	-	-
23A	CP-04-05	-	-	-
24A	CP-04-06	-	-	-
25A	CP-04-07	-	-	-
26A	CP-04-08	-	-	-
27A	CP-04-09	-	-	-
28A	CP-04-10	-	-	-
29A	CP-04-11	-	-	-
30A	CP-04-12	-	-	-
31A	CP-04-13	-	-	-
32A	CP-04-14	-	-	-
33A	CP-04-15	-	-	-
34A	CP-04-16	-	-	-
1B	CP-02-01	-	-	Slickenlines
2B	CP-02-02	-	-	-
3B	CP-02-03	Bone, teeth, and scales	Nodules	Faulted upslope

Bed #	Field bed #	Comments
1A	CP-01-01	-
2A	CP-01-02	Interesting there is no fizz. Micas present. Planar surface at top.
3A	CP-01-03-01	Grey fissile siltstone, breaks into thin laminated sections
4A	CP-01-03-02	Slightly more soft than CP-01-03-01 but still very fissile
5A	CP-01-03-03	Fairly fissile
6A	CP-01-03-04	Good sample taken for thin section, possible carbonate cement
7A	CP-01-03-05	Fractures badly, breaking along brown cracks of mottle
8A	CP-01-03-06	Much the same but more oxidation
9A	CP-01-03-07	Hard bed, good sample for thin section and slab
10A	CP-01-03-08	Check for shiny bone/scale fragments
11A	CP-01-03-09	Very friable
12A	CP-01-03-10	More red than previous beds
13A	CP-01-03-11	Harder than CP-01-03-10, but still fissile
14A	CP-01-04	Exposed as wide, flat, horizontal surface
15A	CP-01-05	Series of scour successions. Base is concave up similar feature@ top.
16A	CP-01-06	Late day light very good for seeing scour features
17A	CP-01-07	Tide rising, light going, rushing. Poor outcrop.
18A	CP-01-08	Apparent siltstone lenses result of erosion and tide on exterior rind.
19A	CP-01-09	Sealing w/ channels good so far
19A	CP-04-01	Overlys basalt, could not dig for contact due to time restriction, good surfaces, fault trace is muddy (clays) and slick, angular discontinuity
20A	CP-04-02	Fines upwards, fine laminations have micas settling parallel to bedding
21A	CP-04-03	-
22A	CP-04-04	-
23A	CP-04-05	-
24A	CP-04-06	-
25A	CP-04-07	-
26A	CP-04-08	Thickness of scour set same as previous bed; cycle?
27A	CP-04-09	-
28A	CP-04-10	-
29A	CP-04-11	Same as last few beds but less grey-green mottle content
30A	CP-04-12	-
31A	CP-04-13	-
32A	CP-04-14	-
33A	CP-04-15	Could be lumped with CP-04-14
34A	CP-04-16	Note: all scour abundant features have been ~2.3m thick
1B	CP-02-01	Sits right on top of basalt, infills cracks and hummocks
2B	CP-02-02	Buff Green Sst unit, many vertical fractures causing spawling
3B	CP-02-03	Very competent, blocky debris on beach, carbonate content

Appendix C – Sample inventory

Wasson Bluff Field Sample Inventory, Colin Price 2013			
Permit#	P2013NS01		
Sample #	Lithology	Fossils (Y/N)	Thin Section (Y/N)
CP-01-00	Basalt	N	Y
CP-01-01	Basal sandstone	N	N
CP-01-02	Basal sandstone	N	Y
CP-01-03-01	Vertebrate-bearing sandstone	Y	N
CP-01-03-02	Red mudstone	N	N
CP-01-03-03	Mottled siltstone	N	N
CP-01-03-04	Ostracode-rich biomicrite	N	Y
CP-01-03-05	Mottled siltstone	N	N
CP-01-03-06	Mottled siltstone	N	N
CP-01-03-07	Ostracode-rich biomicrite	Y	Y
CP-01-03-08	Red mudstone	Y	Y
CP-01-03-09	Red mudstone	N	N
CP-01-03-10	Red mudstone	N	N
CP-01-03-11	Red mudstone	N	N
CP-01-04	Red sandstone	N	N
CP-01-06	Red sandstone	N	Y
CP-01-07	Red sandstone	N	N
CP-01-08	Red sandstone	N	N
CP-01-09	Red sandstone	N	N
CP-02-01	Basal sandstone	N	Y
CP-02-02	Green sandstone	N	Y
CP-02-03	Nodular limestone	Y	Y
CP-03-01	Basal sandstone	N	Y
CP-03-02	Mottled siltstone	Y	Y
CP-03-03	Vertebrate-bearing sandstone	N	Y
Total samples = 25			Total thin sections = 12

Appendix D – Point counting data

PETROG: Report Name = Colin (p.1/4)				
Sample	CP-01-02	CP-02-02	CP-01-03-07	CP-01-03-04
Well Name	Section A	Section B	Section A	Section A
Sample Code	CP-01-02	CP-02-02	CP-01-03-07	CP-01-03-04
Facies #	1	4	5	5
Facies Name	Basal Sst	Green Sst	Biomicrite	Biomicrite
Authigenic Mineral, Calcite	0.5			
Bioclastic Grain, Animalia		0.25		
Bioclastic Grain, Ostracoda			7.5	6.25
Carbonate Grain, Undifferentiated		0.75		
Detrital Grain, Feldspar Group	1.5	1.25		
Detrital Grain, Alkali Feldspars		0.25		
Detrital Grain, Plagioclase	1.25	0.75		
Detrital Grain, Microcline	0.25	0.25		
Detrital Grain, Quartz - Undifferentiated	51.25	47.75	2.5	3.25
Detrital Grain, Quartz - Monocrystalline	47.5	44		
Detrital Grain, Quartz - Polycrystalline	3.75	3.75		
Detrital Grain, Mica Group	1	1.25	1.375	0.375
Detrital Grain, Biotite		0.25	0.125	
Detrital Grain, Muscovite	1	1	0.25	0.375
Detrital Grain, Heavy Minerals	1.25	1		
Detrital Grain, Augite				
Detrital Grain, Garnet Group				
Detrital Grain, Zircon	1.25	1		
Detrital Grain,	5.75	0.5		0.25
Detrital Grain, Intrabasinal – Claystone*	2	0.25		
Detrital Grain, Intrabasinal – Mudstone*	3	0.25		0.25
Detrital Grain, Extrabasinal - Mudstone	0.5			
Detrital Grain, Intrabasinal - Sandstone				
Detrital Grain, Extrabasinal - Igneous	0.25			
*Altered detrital igenous lithics misinterpreted as claystone/mudstone lithics				

PETROG: Report Name = Colin (p.2/4)				
Sample	CP-01-02	CP-02-02	CP-01-03-07	CP-01-03-04
Well Name	Section A	Section B	Section A	Section A
Sample Code	CP-01-02	CP-02-02	CP-01-03-07	CP-01-03-04
Facies #	1	4	5	5
Facies Name	Basal Sst	Green Sst	Biomicrite	Biomicrite
Matrix	38.25	44.75	89.625	89.875
Matrix, Undifferentiated	4.25			
Matrix, Carbonate	0.75	7.25	3.5	
Matrix, Calcareous	0.25	0.25	0.5	17.75
Matrix, Pseudo-Carbonate	0.5	2.5	84.625	68.5
Matrix, Illitic-Smectitic	4.5	15.75		
Matrix, Pseudo-Terrigenous		5		
Matrix, Terrigenous	23.25	9.25		
Matrix, Oxides	4.75	4.75	1	3.625
Porosity, Intergranular	0.5	2.5		

PETROG: Report Name = Colin (p.3/4)			
Sample	CP-03-01	CP-03-03	CP-01-06
Well Name	Section C	Section C	Section A
Sample Code	CP-03-01	CP-03-03	CP-01-06
Facies #	1	2	8
Facies Name	Basal Sst	Vertebrate-bearing Sst	Red Sst
Authigenic Mineral, Calcite		0.5	
Bioclastic Grain, Animalia		19	
Bioclastic Grain, Ostracoda		0.5	
Carbonate Grain, Undifferentiated			
Detrital Grain, Feldspar Group	3	2	10.25
Detrital Grain, Alkali Feldspars	1.25		0.5
Detrital Grain, Plagioclase	1.25	0.75	2.75
Detrital Grain, Microcline	0.5	0.25	4
Detrital Grain, Quartz - Undifferentiated	31	21	48
Detrital Grain, Quartz - Monocrystalline	26	19	38.75
Detrital Grain, Quartz - Polycrystalline	5	2	9.25
Detrital Grain, Mica Group	4.75	1.5	0.5
Detrital Grain, Biotite	0.5	0.5	0.25
Detrital Grain, Muscovite	2.75	1	0.25
Detrital Grain, Heavy Minerals	1.5	0.5	0.75
Detrital Grain, Augite	0.75	0.25	0.5
Detrital Grain, Garnet Group	0.25		0.25
Detrital Grain, Zircon	0.5	0.25	
Detrital Grain,	2.25	1	9.25
Detrital Grain, Intrabasinal – Claystone*	1.5	0.5	4
Detrital Grain, Intrabasinal – Mudstone*	0.5	0.25	4
Detrital Grain, Extrabasinal - Mudstone			
Detrital Grain, Intrabasinal - Sandstone	0.25		1.25
Detrital Grain, Extrabasinal - Igneous		0.25	
*Altered detrital igenous lithics misinterpreted as claystone/mudstone lithics			

PETROG: Report Name = Colin (p.4/4)			
Sample	CP-03-01	CP-03-03	CP-01-06
Well Name	Section C	Section C	Section A
Sample Code	CP-03-01	CP-03-03	CP-01-06
Facies #	1	2	8
Facies Name	Basal Sst	Vertebrate-bearing Sst	Red Sst
Matrix	59	54	9.75
Matrix, Undifferentiated			
Matrix, Carbonate			
Matrix, Calcareous			
Matrix, Pseudo-Carbonate			
Matrix, Illitic-Smectitic	1	36	0.5
Matrix, Pseudo-Terrigenous			
Matrix, Terrigenous	32	5.5	5.25
Matrix, Oxides	26	12.5	4
Porosity, Intergranular			21.5

Summary:						
PETROG: Report Name = Colin; Study name = colin						
Sample	Well Name	Sample Code	Sum of Detrital Grains	Sum of Authigenic Minerals	Sum of Matrix	Sum of Porosity
CP-01-02	Section A	CP-01-02	65.5	0.5	33.5	0.5
CP-02-02	Section B	CP-02-02	56.5	0	40	2.5
CP-01-03-07	Section A	CP-01-03-07	3.875	0	88.625	0
CP-01-03-04	Section A	CP-01-03-04	7.5	0	86.25	0
CP-03-01	Section C	CP-03-01	67	0	33	0
CP-03-03	Section C	CP-03-03	38.5	0.5	41.5	0
CP-01-06	Section A	CP-01-06	72.75	0	5.75	21.5